GENERAL ELECTRIC REVIEW

A MONTHLY MAGAZINE FOR ENGINEERS

Manager, M. P. RICE   Editor, JOHN R. HEWETT   Associate Editor, E. C. SANDERS

Subscription Rates: United States and Mexico, $3.00 per year; Canada, $3.25 per year; Foreign, $3.50 per year; payable in advance. *Library and Student Rates:* United States and Mexico, $2.00 per year; Canada, $2.25 per year; Foreign, $2.50 per year; payable in advance.

Remit by post-office or express money order, bank check, or draft, made payable to the *General Electric Review*, Schenectady, N. Y.

Advertising forms close on the first day of the month preceding date of issue.

Entered as second-class matter, March 26, 1912, at the post office at Schenectady, N. Y., under the Act of March, 1879.

Vol. XXVII, No. 8   AUGUST, 1924

Copyright 1924
by General Electric Company

CONTENTS

PAGE

Frontispiece: A Radio Equipped Air Mail Plane of the DeHaviland Type 490

Editorial: An Important Contribution to the Power Industry 491

Air Mail Radio Equipment 492
By I. F. BYRNES

A Six-ton Induction Furnace Installation 498
By M. UNGER

Studies in the Projection of Light: Part XI 504
By FRANK BENFORD

The Protection of Steam Turbine Disk Wheels From Axial Vibration: Part III . . 511
By WILFRED CAMPBELL

1500-volt Direct-current Electric Railway Installation of the Kobe-Himeji Railway Co., Kobe, Japan 536
By M. TAKAGI

Studies of Electric Discharges in Gases at Low Pressures: Part II 538
By DR. IRVING LANGMUIR and HAROLD MOTT-SMITH, JR.

House Service Generators; Their Types and Field of Application 549
By W. R. HEROD

An Example of Metallic-arc Welding in Bridge Repair 555

The Effect of a Horn on the Pitch of a Loud Speaking Telephone 556
By E. W. KELLOGG

Radicalism That Means Real Progress 563
By C. M. RIPLEY

In Memoriam: Wilfred Campbell 564

Library Section 565

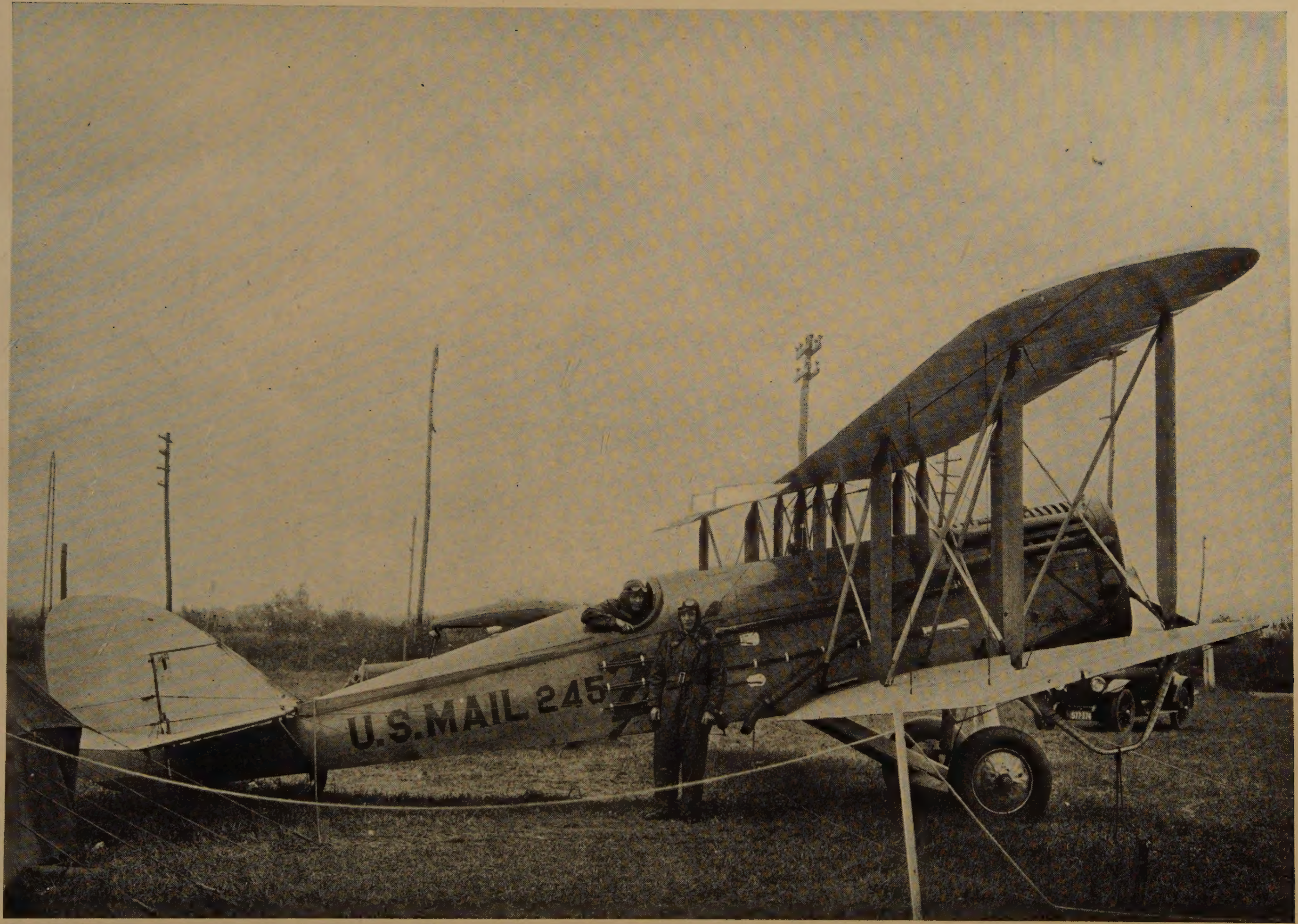

Radio Equipped Mail Plane of the Air Mail Division of the U. S. Post Office Department, at Schenectady, N. Y., where the radio equipment was installed and tested in flight. (See article: "Air Mail Radio Equipment," page 492)

GENERAL ELECTRIC REVIEW

An Important Contribution to the Power Industry

There is concluded in this issue of the REVIEW an article on "The Protection of Steam Turbine Disk Wheels from Axial Vibration," prepared by Wilfred Campbell* and other engineers of the General Electric Company. This article is all too brief to describe adequately the magnitude of the investigation which has been made to determine the real causes of axial vibration in turbine wheels and to develop an effective means of protection against it. This work, lasting over a period of several years, is of immense value to the power industry for it has finally yielded the true explanation of this type of vibration and has resulted in that surety of control over the factory product which guards against this vibration taking place.

An early phase of the investigation was the devising of special apparatus and the undertaking of a vibration survey of all machines already in operation for the protection of the operating companies. The statistical records of these data later proved to be of great assistance in solving the problem.

It is noteworthy that the analysis was however not confined solely to the type of vibration found to be most serious. By a curious prank of fortune, several forms of wave motion more difficult of understanding were discovered first. For instance, the earliest waves detected in model wheels were caused by windage and they appeared to the observer to progress around the wheel in the direction of rotation, whereas in reality they were driven backward in the wheel by the windage encountered but, of course, travelled backward in the wheel at a lower rate than the wheel revolved forward.

The first waves that were recorded in real turbines under operating conditions were similar travelling waves with all the characteristics of those in the model wheels only they could not be explained by windage because they travelled backward in space as well as relative to the wheel, and thus progressed in the wheel at a speed greater than the wind which had been supposed to drive them.

In the midst of these complex discoveries, a wave stationary in space appeared to be but a special case among many types. Only the most thorough statistical examination finally demonstrated the seriousness of the stationary wave and caused the condition for its resonance to be named the wheel critical speed.

Throughout these investigations the classic theories of the mathematical physicists enabled the prediction of resonant speeds. But such writings were entirely devoid of any hint as to which types of resonance, or whether travelling wave trains, were serious in turbine wheels. When the wheel critical speeds had been defined a great contribution to turbine design was made.

To verify the application of this conclusion to the manufactured product, a special turbine wheel testing machine was built (see page 511). Then followed a long struggle in which the elastic theory was assumed satisfactory for the prediction of resonant speeds. The article describes how careful experiments in the turbine laboratory verified the theories of vibration; and also, on the other hand, how the cumulative experience in checking actual designs in the wheel testing machine finally showed that the most careful methods of manufacture are not uniform enough to permit complete reliance on calculations.

Accordingly a second and larger testing machine was built and both put in regular service as necessary tools in the building of wheels. Thus the process of manufacture under the supervision of experts assures the successful operation of new turbines.

—E. L. ROBINSON

**With the greatest regret we announce on page 564 the recent death of this accomplished engineer to whom we are indebted for the article on which this editorial is based.—*EDITOR.*

Air Mail Radio Equipment

By I. F. Byrnes

Radio Engineering Department, General Electric Company

With the inauguration of night flying as a regular feature of the trans-continental air mail service, which took place last month, it is *increasingly* important that the pilot be able at any time to communicate with the landing stations. The difficulties attending the design of suitable radio transmitting and receiving equipment for this service are described in detail by the author. Not the least of these were the space limitations and the necessity for apparatus capable of easy adjustment and operation so as to prevent interference with the pilot's most important duty, the control of the plane. Reliable radio transmitting and receiving equipment will undoubtedly play an important part in making possible the Post Office Department's expectation of delivering mail in San Francisco thirty-three hours after it has started from New York City.—Editor.

In the Air Mail Division of the U.S. Post Office Department continuity of service is an important requirement. This means that daily flights must be made between the various assigned points throughout the country. Radio communication between plane and ground or from plane to plane has long been recognized as a great asset to safety and reliability in aviation. The average non-stop flight of a mail plane is from 400 to 500 miles. It frequently happens that weather conditions change while a pilot is covering his route and it is of considerable assistance if he can be given advance information before coming into a stormy section. The advantage of radio communication in case of a forced landing is obvious.

The radio transmitting and receiving equipment described in this article was built for the Air Mail Service in order to secure operating data under field conditions and to familiarize the pilots with radio apparatus. Most mail carrying planes are of a modified DeHaviland type as shown in Fig. 1 and also the frontispiece of this issue. A compartment that will hold about 600 lb. of mail is built in directly behind the 400-h.p. Liberty engine. The pilot's cockpit is located a considerable distance back of the engine. Under average conditions a speed of about 100 miles an hour is maintained.

A study of the radio requirements of the Air Mail Service brought out a number of interesting points. The apparatus should be easy to adjust and operate by the pilot without interfering with his more important duty of controlling the plane. Telephony only was required since personnel with code training ordinarily is not available. A normal range between plane and ground of 100 miles was considered satisfactory. With land stations 200 miles apart, a pilot would always be in communication with at least one base station. It was decided to use a battery driven dynamotor for the transmitter plate supply. While in the air the regular charging generator on the Liberty engine would help keep the battery charged. In case of a forced landing, the pilot could rig up a temporary antenna and operate his transmitter a considerable time from the battery. The weight and size of the whole radio equipment had to be kept at a minimum in order not to greatly reduce the mail load of the plane.

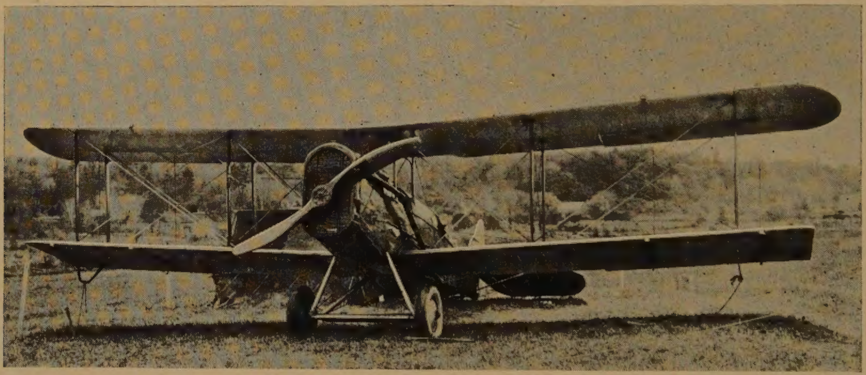

Fig. 1. U. S. Mail Plane, of a Modified DeHaviland Type, Used in Making Radio Tests at Schenectady

The complete equipment as finally built consisted of the following principal units:

Transmitter
Receiver
Control Box
Dynamotor
Fairlead
Antenna reel and fish.

Views of the radio transmitter are shown in Figs. 2, 3, and 4. Both mechanically and electrically this transmitter differs considerably from those heretofore used in aircraft service. All the vacuum tubes are rigidly mounted on the transmitter frame proper and spiral springs with leather holding straps furnish the necessary cushioning effect.

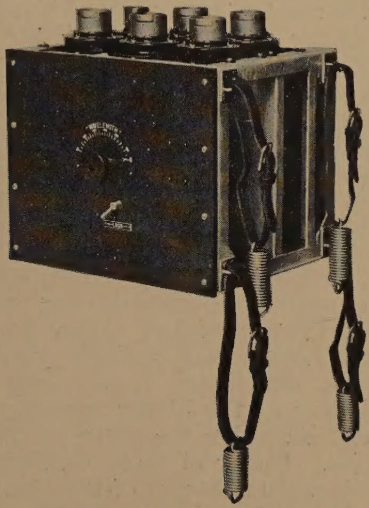

Fig. 2. Front View of the Radio Transmitter for Air Mail Plane Service

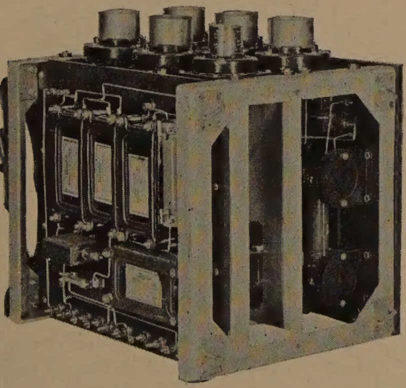

Fig. 3. Side View of the Radio Transmitter

Only one adjustment, a variometer that may be locked in any position, is provided on the panel.

Two important electrical characteristics must be maintained for a satisfactory aircraft transmitter. The transmitted wavelength or frequency should remain constant even through the trailing antenna changes in capacity due to swinging. The tuning of the transmitter should be simple and not require vigilance on the part of the pilot in order to prevent overloading of the vacuum tubes.

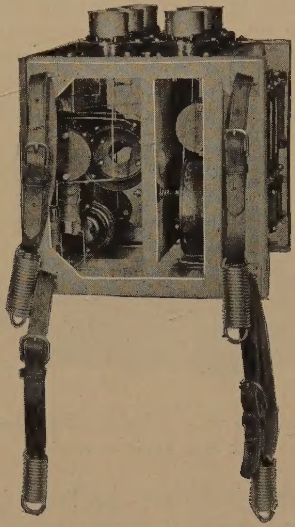

Fig. 4. Rear View of the Radio Transmitter

Reference will be made to the schematic diagram shown in Fig. 5 in describing the transmitter circuits. All tubes with the exception of the speech amplifier are model UV-211. This tube operates at a normal plate potential of 1000 volts and will conservatively deliver 75 watts output as a

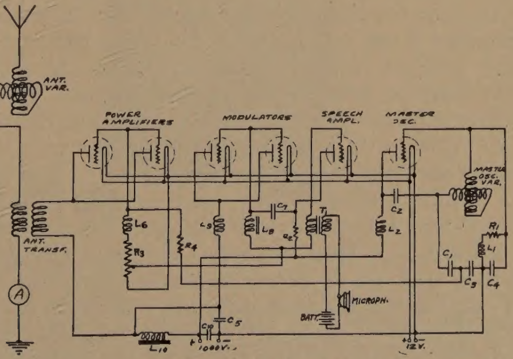

Fig. 5. Schematic Diagram of Connections for Aircraft Telephone Transmitter Unit

power amplifier or oscillator. The filament consumption is 3.25 amp. at 10 volts. A UV-210 or "7½-watt" tube is used as the speech amplifier. This tube operates at 400 volts plate potential and requires 1.2 amp. at 7.5 volts for filament heating.

A wavelength range of approximately 190 to 290 meters is covered by the transmitter. This range is controlled by means of the calibrated master oscillator variometer shown on the panel in Fig. 2. Referring to Fig. 5, it will be seen that the master-oscillator frequency-determining circuit is made up of the variometer and condensers *C1*, *C3*, and *C4* in series. The direct-current input to the plate of the master oscillator is fed through the choke *L2*. Condenser *C2* is the usual low-reactance plate-blocking condenser. The alternating-current plate voltage of the master oscillator is determined by the reactive drop across condensers *C1* and *C3*. The alternating-current grid voltage is built up across condenser *C4*. Grid excitation for the two-power amplifier tubes is obtained from condenser *C3* with a current-limit resistor *R4* in series with the circuit. This resistor prevents excessive current flow in the amplifier grid circuit when the amplifier plate voltage falls to momentary low values during modulation.

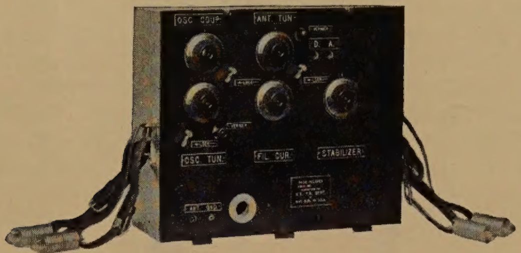

Fig. 6. Front View of the Radio Receiver for Air Mail Plane Service

Coupling between the power-amplifier plate circuit and the antenna is obtained by means of an antenna transformer. This is a simple transformer made up of a single-layer plate coil and a single-layer antenna coil with the correct ratio of turns to efficiently match the plate impedance of the tubes to the antenna resistance. The coils are arranged to provide close coupling between the circuits. Protection of the amplifier tubes against overload is secured in the following manner. Assume the master-oscillator variometer has been set at any arbitrary position and that the antenna circuit is not in resonance to the particular frequency of the master. Radio-frequency excitation is therefore being applied to the power-amplifier grids, and, in the usual circuits, a large alternating-current plate current would flow with corresponding large plate losses. In this transmitter, however, the plate winding offers a very high reactance to the flow of plate current as long as the master frequency and the antenna frequency are not the same. Plate loss is thus held at a safe value. Upon tuning the antenna circuit, by means of the antenna variometer, to the master frequency, the high reactance of the plate winding is in effect reduced when resonance is secured and the power-amplifier tubes take up their normal load. An antenna transformer of this type can be built to cover frequency ranges of about three-to-one with good efficiency and no adjustments are necessary over the entire range. Greater frequency ranges are rather difficult to obtain with a single transformer due to the distributed capacitance of the plate winding at the higher frequencies and insufficient inductive reactance at the lower frequencies. Either of these conditions will destroy the safety feature of the transformer under detuned operation.

The modulation circuits of the transmitter were designed to give a reasonable percentage of modulation and good quality under the severe conditions existing for aircraft telephony. The microphone must be designed with "anti-noise" characteristics so that engine noises and air rush do not cause an undesirable background in the speech, and as a result the microphone output is low. The plate circuit of the speech amplifier has connected in series with it a resistor *R2* which serves the double purpose of reducing the plate potential on the tube to a safe value and of acting as a coupling resistor. Sound waves on the microphone set up

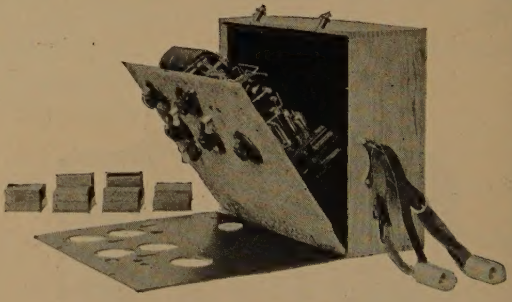

Fig. 7. The Radio Receiver in Open Position

potential variations between grid and filament of the speech amplifier, and these in turn cause an audio voltage to be built up around resistor *R2*. This voltage is transferred to the grid circuit of the two modulator tubes through condenser *C7*. A fixed negative bias is maintained on the modulator and speech amplifier grids by utilizing part of the IR drop in the power amplifier grid leak. An iron core reactor *L8* in the modulator grid circuit prevents the audio voltage from being short circuited to the filament. Plate modulation of the power-amplifier tube is secured by the familiar constant-current method. The plate current drawn by the modulator tubes must flow through the audio reactor *L10*. Variations in modulation plate current build up an audio voltage around the reactor that either aids or opposes the normal direct potential on the radio amplifiers. Since the antenna current is almost directly proportional to the power-amplifier plate potential, the radio output is modulated whenever the microphone is actuated.

The radio receiver is shown in Figs. 6, 7, and 8. A total of seven UV-199 tubes are used in a superheterodyne circuit in this receiver. Special flexible mountings for the tubes and a felt lining for the box are provided in order to eliminate microphone noises. A wavelength range of 190 to 290 meters is covered by the receiver, corresponding to the transmitter range. A schematic diagram of the receiver circuits is shown in Fig. 9. Referring to this diagram and the panel view in Fig. 6, the receiver action is explained as follows:

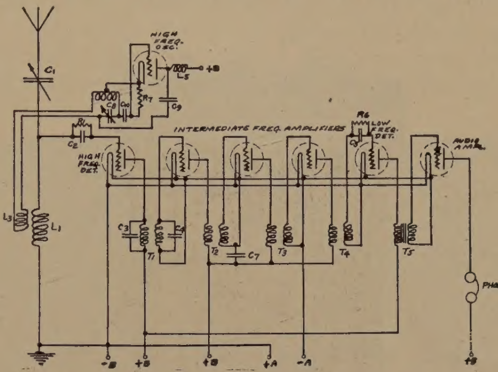

Fig. 9. Schematic Diagram of Connections for Aircraft Telephone Receiver Unit

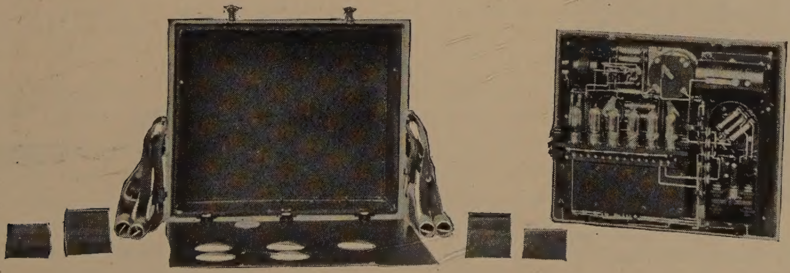

Fig. 8. The Radio Receiver Disassembled

The incoming signal is tuned by means of a series condenser marked "Ant. Tun." on the panel. Voltage is applied to the grid of the high-frequency detector through a grid condenser and leak the same as in a single-circuit tuner. At the same time a local signal (non-modulated) is also impressed on the grid by means of a coupling coil that is connected in the high-frequency oscillator circuit. The frequency of this local signal may be controlled by the condenser marked "Osc. Tun." Connected in the plate circuit of the high-frequency detector are an inductance and a condenser marked *C3*, these being tuned to a frequency of 50,000 cycles (6000 meters). This circuit is coupled to a similarly tuned circuit in the grid of the first intermediate amplifier. When the local oscillator is tuned so that its frequency is 50,000 cycles above or below the incoming signal, maximum current at 50,000 cycles will flow in the detector plate circuit and no alternating voltage will be applied to the intermediate amplifier grids if the frequency differs appreciably from this value. Three stages of radio-frequency amplification, adjusted for best operation at 50,000 cycles, are used. Finally the signal is reduced to audibility by the low-frequency detector and further amplified by one stage of audio amplification. It is evident that in a superheterodyne receiver of this type the incoming signal must be a modulated wave.

A number of controls were placed on the receiver panel in order to secure test data. The dial marked "Stabilizer" permitted amplification control by bias adjustment on the intermediate amplifiers and also prevented oscillation in these stages. In flight the pilot merely had to turn on the filament current and then tune the antenna condenser and oscillator condenser for maximum signal. It is interesting to note that this receiver was the first to use UV-199 tubes in commercial aircraft service.

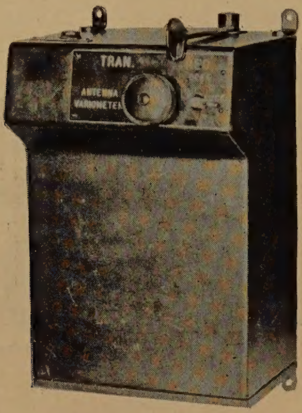

Fig. 10. Radio Control Box for Air Mail Plane Service

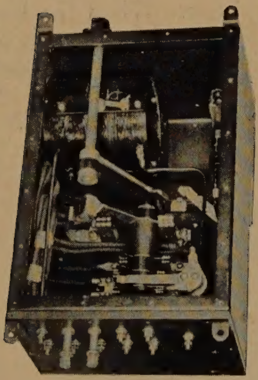

Fig. 11. The Radio Control Box with Bottom Removed

The control box is shown in Figs. 10 and 11. The antenna variometer is mounted inside the box together with a multiple-pole send-receive switch. This switch performs the usual functions of transferring the antenna, starting the dynamotor, and controlling the filament circuits.

A view of the dynamotor used for plate supply is shown in Fig. 12. This machine requires an input of 78 amp. at 12 volts and delivers 0.65 amp. at 1000 volts. It may be thrown directly across the line and comes up to speed in less than two seconds.

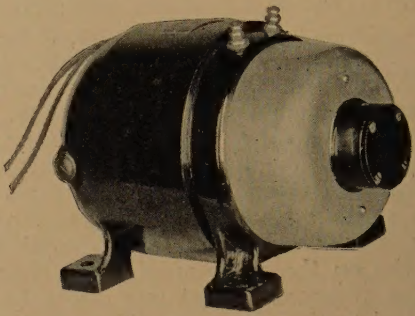

Fig. 12. Radio Dynamotor Set for Air Mail Plane Service

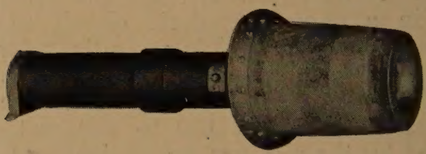

Fig. 13. Fairlead or Lead-out Insulator for the Trailing Antenna

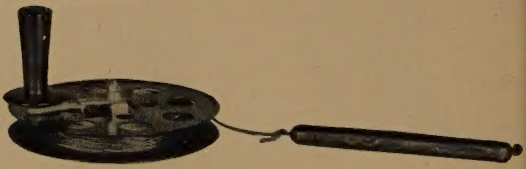

Fig. 14. Antenna, Reel, and Fish Mail for Air Service

The fairlead or lead-out insulator for the trailing antenna is shown in Fig. 13. The lower end is bell shaped to permit the wire to feed out smoothly. A metal lining makes good contact to the outgoing wire and is used for connecting the antenna to the radio equipment.

In previous aircraft installations much trouble has been experienced with the reel and weight. If the pilot should take his hand off the reel the antenna was liable to unreel quickly and finally snap off. It was also impossible to reel up inside the cockpit the lead weight or fish ordinarily used. Both difficulties are overcome in the units shown in Fig. 14. An automatic toggle locks the reel unless a slight pressure is applied to the handle, while the lead weight is so shaped that when the operator is through using the antenna the whole assembly may be brought inside the cockpit. This also makes it possible to replace a weight in flight if necessary.

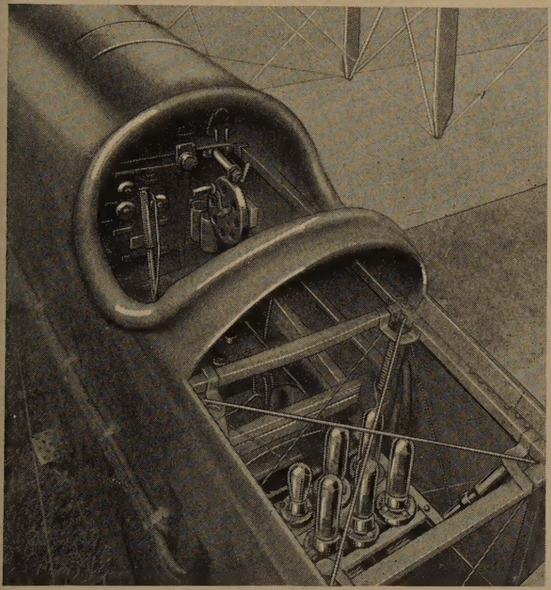

Fig. 15. Radio Installation in Air Mail Plane, Showing Transmitter, Receiver, Reel, and Control Box

When the equipment was ready for service tests, the Post Office Department sent a plane to Schenectady. The manner in which the actual installation was made is shown in Figs. 15 and 16. The transmitter was mounted in the rear of the pilot and the receiver was placed directly in front of him under the control panel of the plane. The control box was located underneath the pilot's seat with the handle of the send-receive switch in a convenient position. The antenna reel was placed on the right-hand side of the cockpit, and directly below it the fairlead. The small space available for an aircraft installation is clearly shown by the photographs. Leads from the dynamotor and battery, that were located in the mail compartment forward, were run along the outside of the fuselage into the pilot's cockpit.

A one-kilowatt telephone transmitter was used as the base transmitter during the tests.

During all the tests duplex operation was carried on from the land station, as the one-kilowatt transmitter operated continuously.

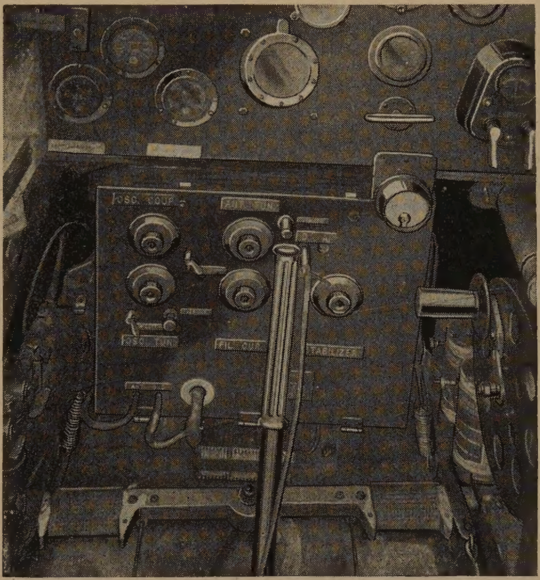

Fig. 16. A Close-up View of the Receiver and Antenna Reel in the Mail Airplane

Transmitting and receiving wavelengths were spaced about 20 meters apart.

Tests made at Schenectady during the early trials of the equipment and subsequent tests under actual service conditions have proved that the range of the set is well over 100 miles from plane to ground station. The range from ground to plane is largely determined by the power of the land transmitter, as it is necessary to limit the receiver amplification in the plane due to engine noises and generally unfavorable receiving conditions.

A Six-ton Induction Furnace Installation

By M. Unger

Transformer Engineering Department, General Electric Company

The electric furnace, while of comparatively recent origin, has assumed a position of considerable importance in metallurgy. Following the satisfactory results which attended the installation and operation of a two-ton induction furnace at its Pittsfield Works, the General Electric Company has placed in operation a furnace of similar design but of three times the capacity. The author describes the new furnace and its auxiliary apparatus, and explains how its principle of operation results in a high-grade melt of extreme uniformity.—Editor.

Several years ago a new type of induction furnace of two-ton capacity was placed in commercial operation for the melting of steel. The experience with this furnace was so satisfactory that it was decided to build a larger unit. This later furnace, which is of six-ton capacity, has recently been placed in successful operation, and a general description of the furnace and its installation may be of interest.

Principle of the Induction Furnace

The induction furnace is based on the principle of the transformer, i.e., it contains a magnetic iron core and primary and secondary circuits. Through magnetic lines of force, the alternating-current energy supplied to the primary circuit is transmitted to the secondary circuit which consists of a single loop or ring, i.e., the metallic bath as illustrated in Fig. 1.

The power input and hence the temperature of the bath is controlled readily by changing the voltage supplied to the primary winding.

Due to the comparatively large distance between the primary and secondary circuits, the reactance becomes quite high; and this means that unless the power supplied is of low frequency, the furnace will operate at low power-factor. Furnaces of this type are therefore generally designed for frequencies lower than those standard among central stations, so that it becomes necessary to install a frequency changer. Furthermore, in order to gain simplicity in design, the furnaces are made single-phase. Therefore, by using a motor-generator, power can be taken from standard polyphase power systems and by using a motor of the synchronous type, a high power-factor load, perfectly balanced, and free from undesirable fluctuations, will be taken from the system. This therefore becomes a very desirable load for central stations.

In the furnace illustrated in Fig. 1, the primary winding is located above the secondary or bath, where it is entirely out of danger in case of a metal leak in the crucible.

The electro-magnetic forces acting upon the bath are of special interest and will be briefly discussed.

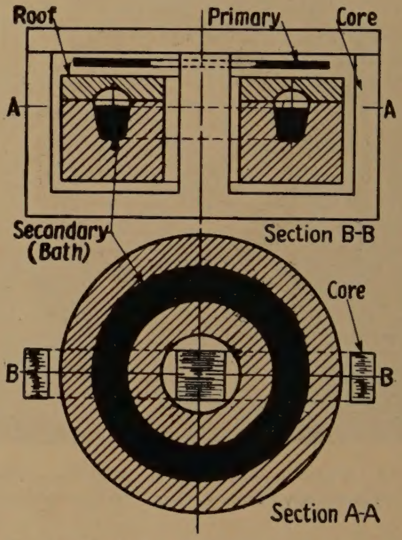

Fig. 1. General Design of Induction Furnace

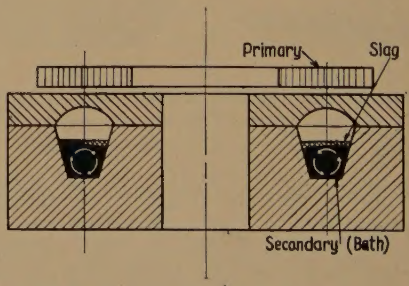

Fig. 2. Diagram of the Furnace Showing Circulation of the Molten Metal in Vertical Planes

Electro-magnetic Forces

These forces are of a two-fold nature, viz., an attracting or pinch force and a repelling force, both of considerable magnitude.

Parallel conductors, free to move and carrying currents in the same direction, will pull together until the surrounding lines of magnetic force form the shortest loop possible. This attracting force is called the pinch force when applied to a liquid conductor, which may be considered as a bundle of an infinite number of strands of current-carrying elements. The tendency is to form a circular cross-section of the conductor, and in case of a rectangular section the corners will be curved or rounded off.

This attracting force acts only on particles carrying current so that particles less conducting, such as oxides, slag, and gases, are forced out to the circumference, i.e., a separation takes place and this is of course a very desirable feature.

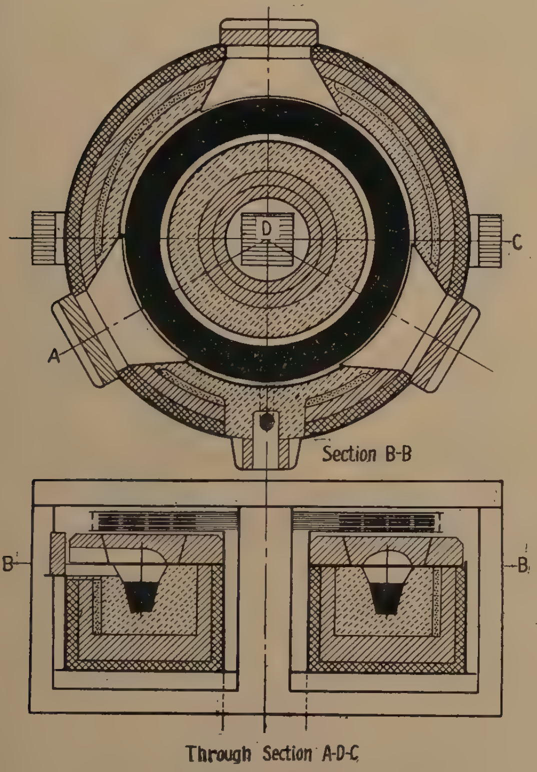

Fig. 3. Sectional Views of the Six-ton Induction Furnace

In case the cross-section of the conductor is non-uniform or in case the current is raised excessively, the pinch force may become great enough actually to interrupt or pinch off the circuits momentarily. This is undesirable from an operating standpoint, but the difficulty is not present in this new type of furnace except under very abnormal conditions.

Parallel conductors free to move and carrying currents in opposite directions repel each other. In the induction furnace, the primary and the secondary circuits present this condition, and the current carrying elements of the bath are repelled towards the bottom of the crucible, thus forcing impurities to the surface.

In addition to forcing out the impurities, the combined forces give rise to circulation of the bath, one circulation in vertical planes perpendicular to the direction of the electric current and another, much less pronounced, in horizontal planes in the direction of the current. Due to greater concentration of magnetic flux along the inner side of the bath than along the outer side, the forces predominate on the inside so that the bath surface becomes sloped inwards and the edges rounded as shown in Fig. 2. This diagram also shows by arrows the circulation of metal in vertical planes.

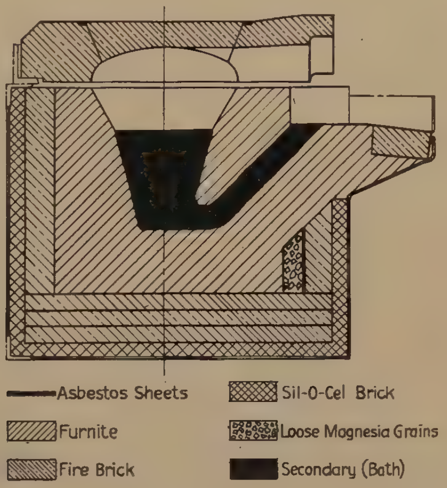

Fig. 4. Sectional View of the Furnace Through the Pouring Spout and a Legend Showing Some of the Materials Used in the Construction of the Furnace

From a metallurgical standpoint, the tendency for impurities to be forced out of the bath together with the gentle circulation is of considerable value when refining and uniformity of temperature and composition are considered.

Furnace Design

The furnace is rated 800 kw. at 2200 volts, single-phase, 8.5 cycles, with a hearth capacity of 12,000 lb. The general design of the furnace is shown in Figs. 3 to 9 inclusive.

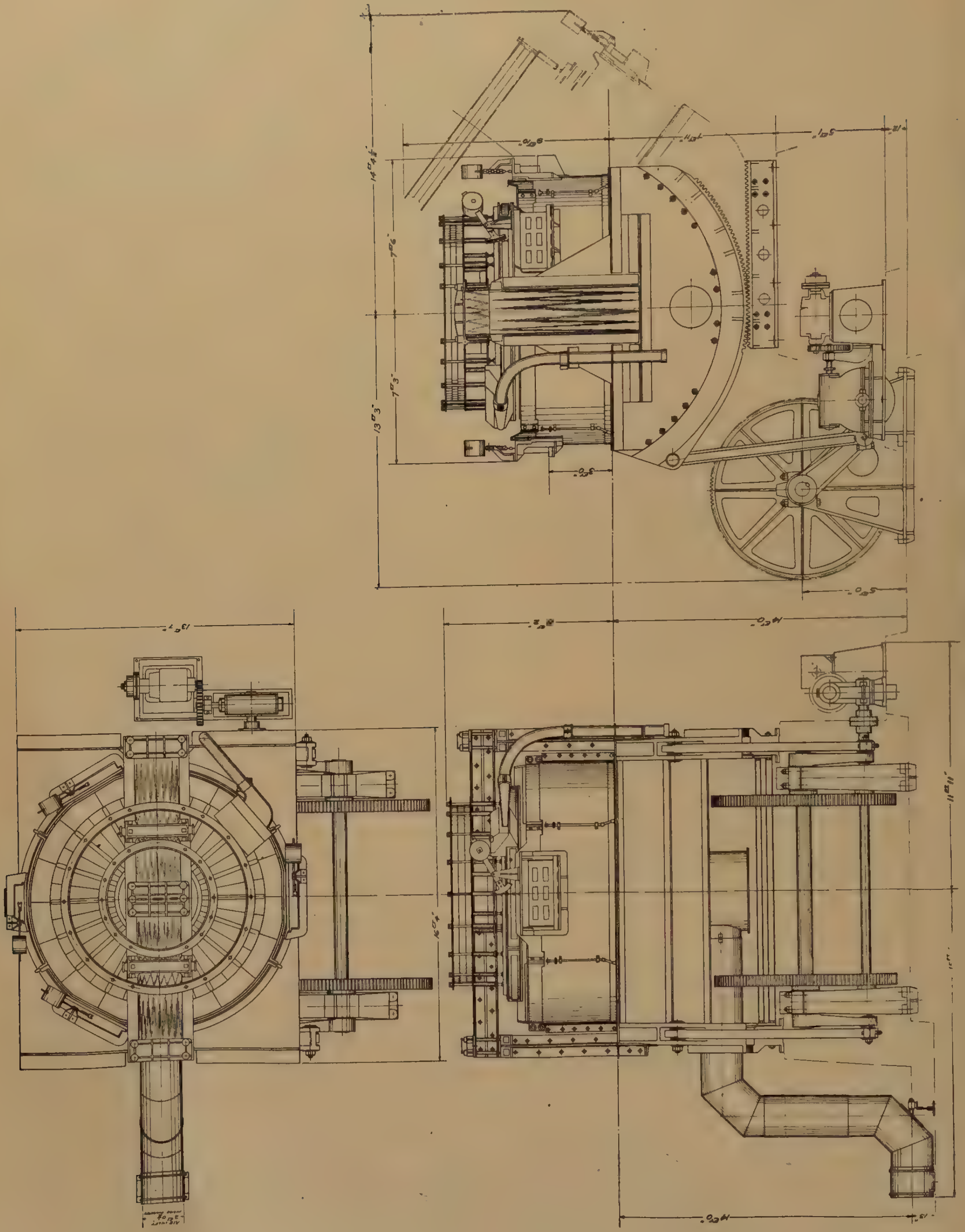

Fig. 5. Plan and Elevations of the Six-ton Induction Furnace Showing Its Principal Dimensions and Details of Construction

The core which is of the three-legged type is made up of non-ageing transformer steel clamped by insulated bolts. It weighs approximately 35 tons.

The winding consists of sixteen circular disk type coils, the conductor being of rectangular copper with mica as turn-insulation. The coils are covered by several layers of mica and asbestos tape impregnated with a heat resisting compound. The coils are of very strong electrical as well as mechanical construction and will stand a temperature up to 200 deg. C. Surrounding the coils is a non-magnetic casing of brass which communicates with the inside cylinder of the crucible up through which cooling air is forced. Power is delivered to the winding through two 600,000-cir. mil. cables brought up alongside the furnace in a 6-in. iron pipe.

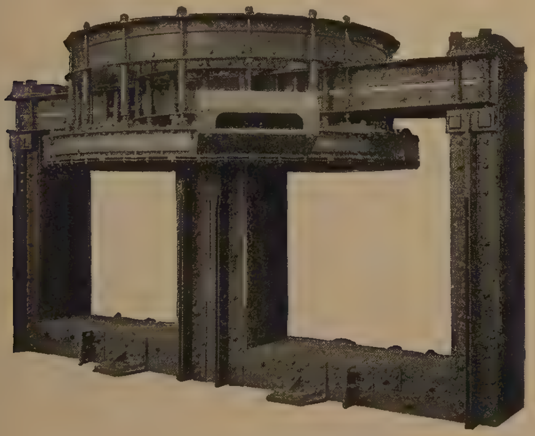

Fig. 6. Core and Coils for the Six-ton 800-kw. Induction Furnace

The development of a suitable refractory lining material has been a difficult problem. It was solved by the use of calcined and electrically fused magnesia known under the trademark "Furnite" and developed by the General Electric Company, after many expensive experiments. This material is mixed with hot pitch and rammed into place around suitable forms. The roof is made of firebrick of special shapes built up as a unit between two steel rings.

The furnace is provided with four doors, one of which is used exclusively in pouring. A so-called "tea-pot" pouring spout as shown in Fig. 4 is used successfully for pouring the metal from below the slag line.

The casing surrounding the crucible is made of heavy iron plate. The inner cylindrical casing is connected at the bottom to a sheet iron pipe which conducts the air from a blower to the furnace winding. No water cooling of any description is used in connection with this furnace, and in the absence of electrodes there is no need for automatic control equipment.

The furnace is tilted on a straight track through a pair of rods connected to bell cranks as shown in Fig. 5. The tilting mechanism is driven by a 25-h.p., direct-current motor equipped with a solenoid brake. The furnace occupies a floor space of about 16 ft. by 16 ft.

Auxiliary Apparatus

The power is supplied at 25,000 volts, 60 cycles, 3-phase, This is first stepped down to 2200 volts and is then converted into 2200-volt, 8.5-cycle, single-phase power by means of a motor-generator.

Three single-phase, 475-kv-a. transformers connected delta/delta are used, and one reserve transformer is provided. The motor is of the synchronous type and is designed so that it may be operated with a leading power-factor as high as 80 per cent. An automatic power-factor regulator has been provided so that the load may be taken at the most advantageous leading power-factor. The generator, which is rated 2000 kv-a., 8.5 cycles, single-phase, although of quite large dimensions, is cooled entirely by natural ventilation. The exciter, 125 volts, is mounted on the same shaft with the motor-generator. The motor and the generator have motor-operated rheostats, the generator rheostat being such that with normal exciter voltage the generator voltage can be held anywhere from 25 per cent of normal to 10 per cent above normal.

The switchboard and instruments are of conventional design. A small control board is mounted near the furnace, and from this the operators perform all necessary control of the furnace power.

For cooling the furnace winding, two blower sets, one a spare, have been provided. Each blower is rated 10,000 cu. ft. of air per minute at 4-oz. pressure and is driven by a 30-h.p. motor. For cleaning and cooling the air, an air washer of Sturtevant design is used.

Plant Layout

The entire equipment is installed in a modern steel building and the various pieces of apparatus are located as shown in Fig. 10. The main electrical connections are shown in Fig. 11.

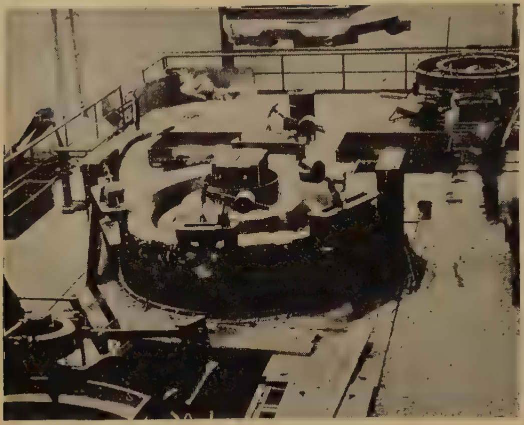

Fig. 7. Six-ton Induction Furnace with Rammed Lining in Place

Operation

In order to operate the furnace, the secondary must be a closed ring or circuit as otherwise no induced current can flow and consequently there will be no heating. The first charge must consist therefore of a ring of steel or iron. This ring is heated by supplying energy to the primary winding of the furnace, the heat being applied gradually so as to first dry and bake out the lining. As soon as the ring has melted, the furnace may be charged up to full capacity and metallurgical processes started.

A certain amount of metal must be left in the furnace after each pouring so as to hold the electric circuit complete. This of course does not apply in case liquid charges are used, i.e., in case of duplexing.

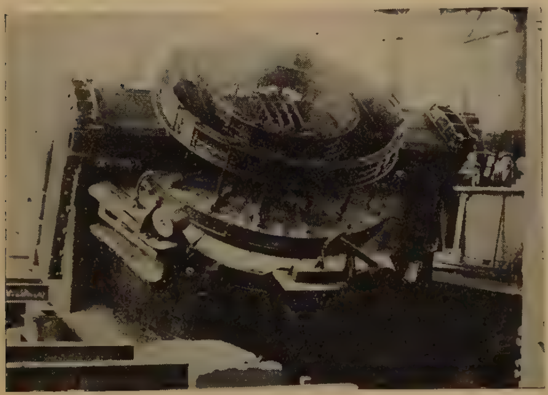

Fig. 8. The Induction Furnace in the Tilted Position

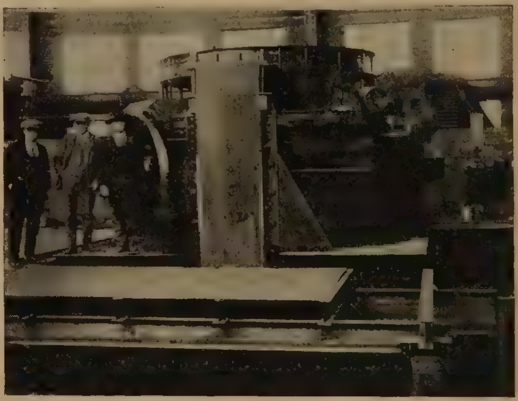

Fig. 9. The Induction Furnace in the Upright Position

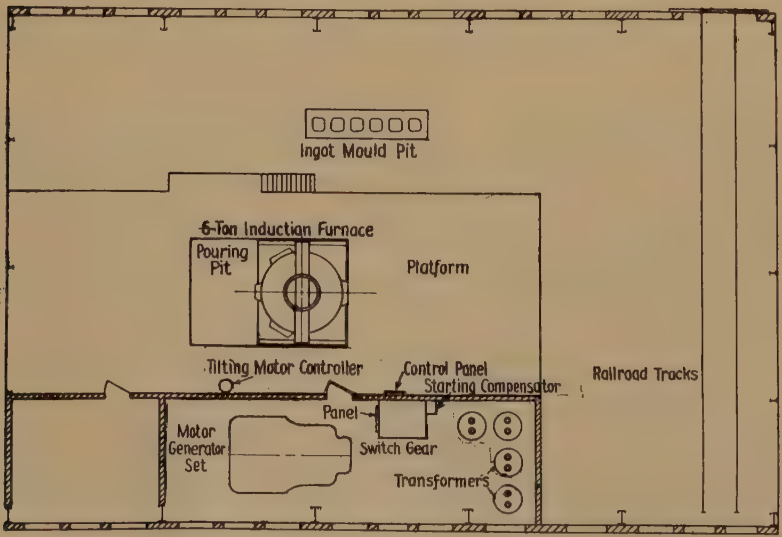

Fig. 10. The Floor Layout of the Six-ton Induction Furnace

Instead of using only one ring for starting, which sometimes may cause trouble from rupture, it is standard practice to use two rings of different melting points, in this case, a cast-steel and a cast-iron ring. These rings are generally melted in 60 to 72 hours giving the lining ample time to set. The combined weight of these rings which form the initial charge is about 5000 lb. Either cold scrap or liquid metal may then be added to bring the charge up to the full amount, namely 12,000 lb. Refining and alloying is now done according to well established metallurgical practice. When the heat is ready, it is regular practice to pour 7000 lb. in a ladle which is transferred to a truck over the pouring pit. Generally two ingots of 3500 lb. each are poured from each heat.

The average time for melting, refining, and alloying a charge of 7000 lb. of scrap is four hours with a total overall energy consumption, as measured at the 25,000-volt bus, of about 800 kw-hr. Much better records have been obtained for individual heats and, as more experience is gained, conditions are bound to improve still further. The furnace is operated by one melter and two helpers in 8-hour shifts, the operation being continuous 24 hours a day, seven days a week. The product is of high grade and of extreme uniformity which latter feature is of particular value for certain materials.

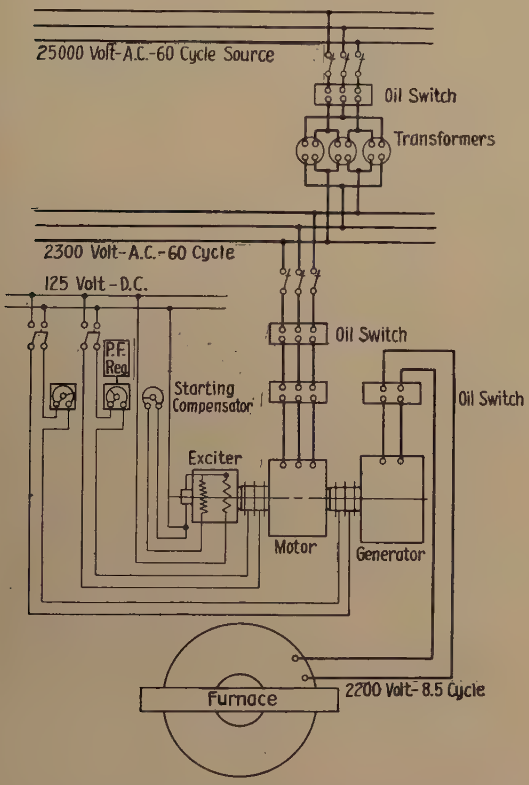

Fig. 11. Diagram of the Electric Circuits and Motor-generator Set for Supplying the Six-ton Induction Furnace with Energy

As to the life of the lining, the furnace has not been in operation long enough to give a representative figure.

From the central station standpoint, this furnace makes a very desirable load. Fig. 12 gives a representative record of power requirements for a two-ton furnace and the absence of fluctuations combined with the high or leading power-factor should be appreciated.

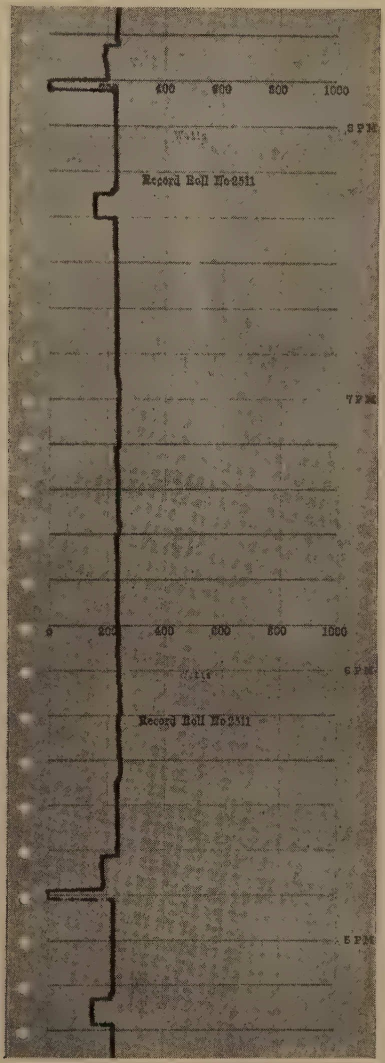

Fig. 12. A Typical Section of the Power Curve of a Two-ton Induction Furnace

Studies in the Projection of Light

PART XI

ENERGY AND LIGHT ANALYSIS OF ARC AND INCANDESCENT SEARCHLIGHTS

By Frank Benford

Physicist, Illuminating Engineering Laboratory, General Electric Company

Concerning the useful output of a lighting unit it has been said that: "Every advantage in appearance, distribution of light, or adaptation to some particular purpose is paid for ultimately in light." Applied to the searchlight but little sacrifice is made for the sake of appearance. However, the adaptation of the light source, and the addition of necessary auxiliaries, to deliver light in a concentrated beam requires exceptional care in design and workmanship in order to convert as much as possible of the total light into useful light. A very interesting analysis of high-intensity, plain-carbon, and incandescent searchlights is presented below in terms of energy and light at various stages of projection. —Editor.

Absolute Efficiency of Projection

An engineer studying for the first time the relation between the electrical input of a searchlight and its output in energy and light will probably have one of two strong reactions, depending on whether, in things professional, he is an optimist or a pessimist. He may take the view that because so little has been accomplished there is still ample opportunity for the enterprising investigator and inventor, or he may say to himself that with all the work that has been done the present status shows the hopelessness of efforts to produce light economically. The holder of the latter view is automatically put out of the game, and at worst he can act only as a temporary drag on the coat tails of the optimist, who is going somewhere, and knows it. For the sake of keeping the optimist on the right track it is often wise for him to have definite and itemized data about the condition of the art, and on the following pages the energy of the high-intensity, the plain-carbon, and the incandescent searchlight is therefore considered in some of its more important details.

To take the most unfavorable comparison first, let us consider what would be the output of light from a radiator that emits all its energy in the form of green light of wavelength 0.556 microns. According to Ives, one watt converted into such radiation would give 666 lumens, and 18,000 watts received by a searchlight would be converted into 12,000,000 lumens or units of light. The photometric data discussed later will show the useful output for the most effective searchlight to be 140,000 lumens or a net efficiency of 1.2 per cent of the perfect spectrum-line radiator.

For reasons which will be gone into more fully in another place, pure green light of wavelength 0.556 microns would not be suitable for the detection of an enemy plane or ship which will endeavor to avoid being seen by deceptive coloration and by maneuvering, and a full spectrum from violet to red is required of the searchlight. The output of light for energy so distributed is about 220 lumens per watt or 4,000,000 lumens for the 18,000-watt input. The actual searchlight, therefore, has on this new basis an efficiency of 3.5 per cent.

A radiator with the foregoing characteristics is as yet an unknown thing, and the nearest to perfection is the light of day which corresponds roughly to a radiator at 5500 deg. A. At this temperature 40 per cent of the energy is within the bounds of the visible spectrum and the best lumen output is 1,650,000 for 18,000 watts input. Using this as our basis of comparison the present high-intensity searchlight, which is the peak of engineering achievement, has an efficiency of 8.5 per cent. This 5500 deg. A radiator is an ultimate goal which we may reasonably strive to approach, because the crater of the 150-amp. arc does actually give radiation indicative of a temperature of about that value; and the problem at once becomes that of finding ways to identify and conserve the lost 90 per cent. It is not the intention to attempt a solution here, or even to speculate on possible ways, but merely to record such facts as have been found in practical and experimental work done with this important and interesting arc since its invention by Mr. Beck some ten years ago.

High-intensity Arc

Energy and Light at Various Stages of Projection

The high-intensity arc, like the plain-carbon arc, requires stabilizing resistance when on a constant-potential line; and so in Tables VIIIa and VIIIb 40 volts has been allowed for rheostat drop although this is in excess of the actual needs.

Item (9) of Table VIIIa shows a thermal efficiency of 11.3 per cent for the most effective searchlight yet devised, and an efficiency of 25.2 per cent in projecting such light as is generated into the beam where it may be effective. The last item, light and energy received on a distant target, is added mainly to point out that the thermal transmission for the total energy in the beam is slightly better than for the luminous energy. The reasons for this distinction will be given in detail when the discussion of atmospheric effects is taken up.

TABLE VIIIa

ENERGY AND LIGHT AT VARIOUS STAGES OF PROJECTION

150-AMP. HIGH-INTENSITY SEARCHLIGHT

	ENERGY			LIGHT		
	Factor	Watts	Per Cent	Factor	Lumens	Per Cent
(1) Input 150 x 120		18,000	100.0			
(2) At lamp terminals	0.667	12,000	66.7			
(3) At arc	0.950	11,400	63.4		555,000	100.0
(4) In direction of mirror	0.520	5,870	33.0	0.600	333,300*	60.0
(5) Incident on mirror	0.930	5,458	30.7	0.935	311,000	56.1
(6) Reflected from mirror	0.750	4,130	23.0	0.850	265,000	47.7
(7) Beyond positive head	0.960	3,910	22.1	0.960	254,000	45.8
(8) Transmitted through door	0,850	3,370	18.8	0.880	224,000	40.3
(9) Excluding stray light	0.600	2,020	11.3	0.625	140,000*	25.2
(10) At distant target	0.880	1,780	9.9	0.850	119,000	21.4

*Direct test; others from various sources.

TABLE VIIIb

ANALYSIS OF LOSSES IN ENERGY AND LIGHT

150-AMP. HIGH-INTENSITY SEARCHLIGHT

	ENERGY		LIGHT	
	Watts	Per Cent	Lumens	Per Cent
(1) Resistance loss in rheostat	6,000	33.3		
(2) Losses in lamp coils, etc.	600	3.3		
(3) Radiated outside of mirror angle	5,530	30.8	221,700	40.0
(4) Loss on negative head	390	2.2	22,300	3.9
(5) Absorbed by mirror	1,350	7.5	46,000	8.4
(6) Absorbed by heads	220	1.2	11,000	1.9
(7) Absorbed and reflected by door	540	3.0	30,000	5.5
(8) Stray outside of beam	1,350	7.5	84,000	15.1
(9) Scattered by atmosphere	240	1.3	21,000	3.8
Total of losses	16,220	90.1	436,000	78.6
Projected to plane of target	1,780	9.9	119,000	21.4
Total input	18,000	100.0	555,000	100.0

The high-intensity searchlight is ranked first, not because of any pronounced advantage in total light output, for it will be shown later that some incandescent units turn out as many lumens per watt of input, but because the crater brilliancy and the beam strength of its arc are separated by a wide gulf from its nearest competitor, the plain-carbon arc.

Table VIIIb presents the previous data in a form somewhat better for study of the individual losses and their effects upon the component parts of the searchlight.

The greatest single waste of energy occurs in the rheostat. This loss might conceivably be eliminated by the use of a constant-current source of supply. However, the problem is not that of saving energy but rather that of obtaining the greatest amount of useful light for a given current. We may divide the sources of the losses into three groups as follows:

(1) Generation at incorrect temperature.
(2) Generation at incorrect location.
(3) Waste due to optical design and optical materials.

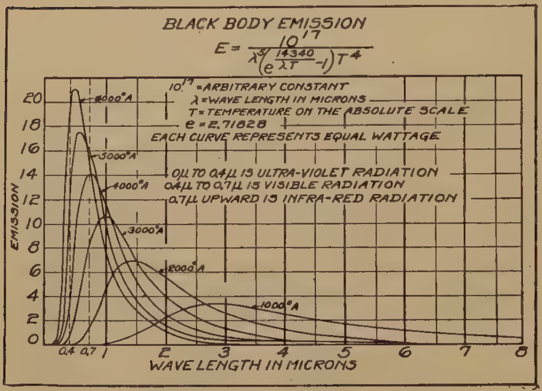

Fig. 131. A non-selective, or "black body," radiates energy when at different temperatures as shown by these curves. The energy that becomes visible radiation is confined within the narrow limits of 0.4 to 0.7 microns, shown by the dotted ordinates, and energy outside of these limits is wasted insofar as the production of light is concerned

Under group (1) we have the light and energy from the sides of the positive electrode, and from the arc stream and flame. Parts of all these sources come within useful bounds, but the temperature is not correct for the best output.

Group (2) includes the rheostat and all other parts heated by the current except those parts actually radiating useful light. This group is responsible for more than half the wasted energy.

Group (3) is concerned with the materials and proportions of the mirror and door, and the disposition of the lamp heads so as to form a minimum obstruction.

Carbon Arc

Energy and Light at Various Stages of Projection

The plain-carbon arc is at a disadvantage in several ways as compared with the gaseous type. Slightly more rheostat drop is required to stabilize the arc, and the carbon itself is limited to an upper temperature of less than 4000 deg. A. This is in itself a serious disability, but there are several advantages tending to even the score. Thus the loss on the lamp heads is often much less, the wasteful flame of the high-intensity arc is almost wholly missing, and in general the direction of radiation is much more favorable for the best results. The transmission through the atmosphere is nearly always higher and there is a gain of one per cent or so in the reflecting factor of the mirror. This latter feature is often of some importance particularly when the wattage per square inch is high. For equal wattage the heating effect of the plain-carbon arc is less and overheating of the mirror is therefore not so common.

In the generation of light the negative electrode, through the shadow it throws, is a controlling factor. The manipulation of this arc calls for some skill on the part of the operator, who must exercise great care to avoid forming an uneven crater with a long extension on one side. In Fig. 132 is shown some typical craters formed at various arc voltages. The 60-volt crater is most nearly ideal.

The distribution curves in Fig. 133 show the effects of the negative shadow. The close grouping of five of the curves at 60 deg. indicates that for a range of 25 volts the actual output from the crater is nearly constant and all the variation is in the shadow.

The effective range in arc volts and amperes for a particular electrode is plotted in Fig. 134, where the working range is indicated by full lines and the unstable range by dotted lines. The lower limit, line *A-A*, is largely determined by arc hissing; and the upper limit, line *B-B*, is set by the breaking of the arc when it

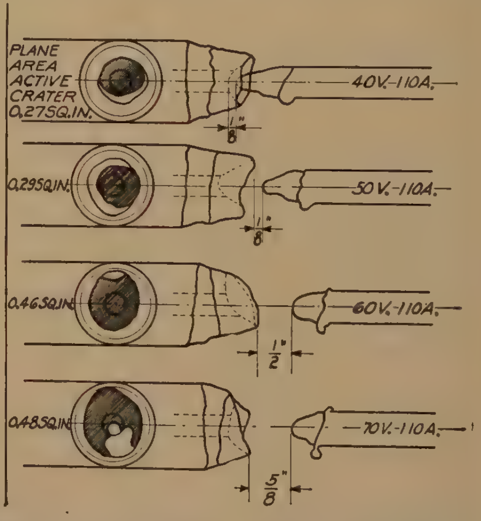

Fig. 132. The end views of the craters, on the left, show how the crater of the plain carbon arc is only partly covered by active surface (shaded). This active area moves about and requires the personal attention of an operator to prevent the crater from being badly misformed

becomes too long. The line *C-C* marks the ideal photometric condition.

A comparison of items (10) in Tables VIIIa and IXa shows the plain-carbon arc to be inherently more economical of such light as is generated, and thus the wide gap between the arcs is somewhat closed in the performance of the beams. The plain arc is some 15 per cent more economical in directing light to the mirror and has some 36 per cent advantage in keeping the reflected light within the beam. The effects of the two factors are plainly visible in the beams themselves. The plain-carbon arc beam is clear cut, with a fringe from the flame that is just visible, and there is but little direct light scattered in the immediate vicinity of the searchlight. The high-intensity beam is soft-edged with a pronounced "tail" of light from the flame, and unless the lamp is provided with a special shield the direct light from the flame will flood the foreground with yellow light.

In Table IXb the losses for the plain arc are given individually. The values of watts and lumens in the two tables of losses cannot be directly compared because the electrical inputs are not the same, but the percentage values allow of a direct comparison.

Incandescent Searchlights

Energy and Light at Various Stages of Projection

The mirrors used in incandescent searchlights vary greatly in their angular proportions and also in their reflectivity. The better grade of mirrors are identical with those used with arc lamps, but the cheaper form fall far short of the degree of perfection that represents the best present practice. To a certain extent the optical imperfections in certain wide-angle floodlights are intentional because a sharp definition of the filament image is to be avoided. It usually happens that along with these optical aberrations there occur further losses that are not useful and are not intentional. In metal mirrors there are two prolific sources of loss. These are a low reflectivity as compared with a high-grade glass mirror, and scattering of light from minute surface scratches left by the polishing process. It thus happens that a 60-deg. high-grade glass mirror gives practically the same projection efficiency as a 110-deg. metal mirror. The beam from the glass mirror is narrow whereas the metal mirror gives a

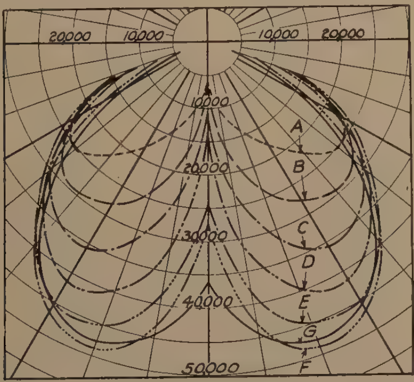

Fig. 133. The photometric influence of the shadow of the negative electrode of a plain carbon arc is shown by these curves. The current was constant at 110 amp.

A—45 volts at arc.	*D*—60 volts at arc.
B—50 " " "	*E*—65 " " "
C—55 " " "	*F*—70 " " "

G—75 volts at arc.

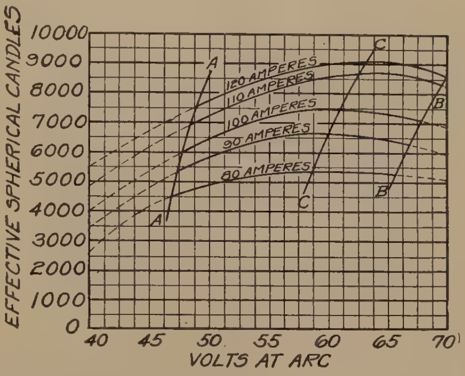

Fig. 134. The effective output of a plain carbon arc is here analyzed for variations in both current and arc voltage. The dotted sections of the curves indicate an unstable or noisy arc. The line *C–C* passes through the region of greatest efficiency

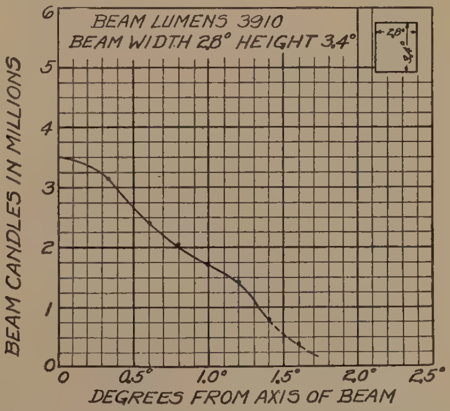

Fig. 135. A typical distribution of light when using an incandescent lamp of the monoplane type and an 18-in. diameter mirror of high optical accuracy

TABLE IXa

ENERGY AND LIGHT AT VARIOUS STAGES OF PROJECTION

200-AMP. PLAIN-CARBON SEARCHLIGHT

	ENERGY			LIGHT		
	Factor	Watts	Per Cent	Factor	Lumens	Per Cent
(1) Input 200 x 120..........		24,000	100.0			
(2) At lamp terminals.......	0.500	12,000	50.0			
(3) At arc..................	0.950	11,400	47.5		165,000*	100.0
(4) In direction of mirror.....	0.700	7,980	33.2	0.750	124,000	75.0
(5) Incident upon mirror.....	0.930	7,420	30.9	0.930	115,000	69.8
(6) Reflected from mirror....	0.770	5,710	23.8	0.860	99,000	60.0
(7) Beyond positive head.....	0.980	5,600	23.3	0.980	97,000*	58.8
(8) Transmitted through door	0.850	4,750	19.8	0.880	85,400	51.7
(9) Excluding stray light....	0.920	4,380	18.2	0.960	82,000	49.7
(10) At distant target.........	0.900	3,940	16.4	0.880	72,200	43.7

*Direct test; others from various sources.

TABLE IXb

ANALYSIS OF LOSSES IN ENERGY AND LIGHT

200-AMP. PLAIN-CARBON SEARCHLIGHT

	ENERGY		LIGHT	
	Watts	Per Cent	Lumens	Per Cent
(1) Resistance loss in rheostat........................	1,2000	50.0		
(2) Losses in lamp coils, etc...........................	600	2.5		
(3) Radiated outside of mirror angle....................	3,420	14.3	41,000	25.0
(4) Loss on negative head and electrode................	560	2.3	9,000	5.2
(5) Absorbed by mirror................................	1,710	7.1	16,000	9.8
(6) Absorbed by heads..................................	110	0.5	2,000	1.2
(7) Absorbed and reflected by door.....................	850	3.5	11,600	7.1
(8) Stray outside of beam..............................	370	1.6	3,400	2.0
(9) Scattered by atmosphere............................	440	1.8	9,800	6.0
Total of losses..................................	20,060	83.6	92,800	56.3
Projected to plane of target....................	3,940	16.4	72,200	43.7
Total input....................................	24,000	100.0	165,000	100.0

TABLE Xa

ENERGY AND LIGHT AT VARIOUS STAGES OF PROJECTION

500-WATT, 4.35-AMP., 115-VOLT FILAMENT FLOODLIGHTING BEAM FROM 110-DEG. METAL MIRROR

	ENERGY			LIGHT		
	Factor	Watts	Per Cent	Factor	Lumens	Per Cent
(1) At lamp terminals........		500	100.0			
(2) At filament..............	0.980	490	98.0		7850*	100.0
(3) In direction of mirror......	0.580	284	56.8	0.580	4550	58.0
(4) Incident upon mirror......	0.950	269	53.9	0.950	4320	55.0
(5) Reflected from mirror.....	0.750	202	40.4	0.700	3020	38.5
(6) Beyond lamp bulb........	0.950	192	38.4	0.960	2900	36.9
(7) Transmitted through door.	0.800	154	30.7	0.830	2405	30.6
(8) Excluding stray light......	0.750	115	23.1	0.800	1930*	24.5
(9) At distant target..........	0.910	105	21.0	0.890	1710	21.8

*Direct test; others from various sources.

TABLE Xb

ANALYSIS OF LOSSES IN ENERGY AND LIGHT

500-WATT, 4.35-AMP., 115-VOLT MONOPLANE FILAMENT FLOODLIGHTING BEAM FROM 110-DEG. METAL MIRROR

	ENERGY		LIGHT	
	Watts	Per Cent	Lumens	Per Cent
(1) Loss in base, etc.	10	2.0		
(2) Radiated outside of mirror angle	206	41.2	3300	42.0
(3) Loss at lamp socket	15	2.9	230	3.0
(4) Absorbed by mirror	67	13.5	1300	16.5
(5) Absorbed by bulb, etc.	10	2.0	120	1.6
(6) Absorbed and reflected by door	38	7.7	495	6.3
(7) Stray outside of beam	39	7.6	475	6.1
(8) Scattered by atmosphere	10	2.1	220	2.7
Total of losses	395	79.0	6140	78.2
Projected to plane of target	105	21.0	1710	21.8
Total	500	100.0	7850	100.0

TABLE XIa

ENERGY AND LIGHT AT VARIOUS STAGES OF PROJECTION

600-WATT, 20-AMP., 30-VOLT, 4-COIL MONOPLANE FILAMENT CONCENTRATED INCANDESCENT BEAM 60-DEG. GLASS MIRROR

	ENERGY			LIGHT		
	Factor	Watts	Per Cent	Factor	Lumens	Per Cent
(1) At transformer terminals		630	1.000			
(2) At lamp terminals	0.950	600	0.950			
(3) At filament	0.980	588	0.931		15,600*	100.0
(4) In direction of mirror	0.341	201	0.318	0.341	5,320	34.1
(5) Incident upon mirror	1.000	201	0.318	1.000	5,320	34.1
(6) Reflected from mirror	0.750	150	0.238	0.860	4,570	29.3
(7) Beyond lamp bulb	0.970	146	0.231	0.980	4,480	28.7
(8) Transmitted through door	0.850	124	0.196	0.880	3,940	25.3
(9) Excluding stray light	0.950	118	0.187	0.990	3,910*	25.0
(10) At distant target	0.910	107	0.170	0.890	3,480	22.3

* Direct test; others from various sources.

TABLE XIb

ANALYSIS OF LOSSES IN ENERGY AND LIGHT

600-WATT, 20-AMP., 30-VOLT, 4-COIL MONOPLANE FILAMENT CONCENTRATED BEAM FROM 60-DEG. GLASS MIRROR

	ENERGY		LIGHT	
	Watts	Per Cent	Lumens	Per Cent
(1) Loss in transformer	30	5.0		
(2) Loss in base	12	1.9		
(3) Radiated outside of mirror angle	387	61.3	10,280	65.9
(4) Loss by obstructions	0	0.0	0	0.0
(5) Absorbed by mirror	51	8.0	750	4.8
(6) Absorbed and scattered by bulb	4	0.7	90	0.6
(7) Absorbed and reflected by door	22	3.5	540	3.4
(8) Stray outside of beam	6	0.9	30	0.3
(9) Scattered by atmosphere	11	1.7	430	2.7
Total of losses	523	83.0	12,120	77.7
Projected to plane of target	107	17.0	3,480	22.3
Total	630	100.0	15,600	100.0

wide beam, and the beam intensities often vary in the ratio of thirty to one.

Tables Xa, Xb, XIa, and XIb go into the details of two typical incandescent units and the final results would almost seem to indicate that there is a "constant" somewhere in the process that requires a uniform result. This is not the case, however, for it is optically possible to make a wide-angle mirror of almost identical efficiency with the narrow-angle one, and the results therefore represent current practice rather than physical limitations.

Summary

The efficiency of the high-intensity arc as a light generator is far above any other light source, but the projection efficiency is low. The plain-carbon arc reverses matters and has a low generation efficiency, but a high projection efficiency. The incandescent seems to suffer by comparison in both respects, but on account of a better balancing of factors the incandescent at its best approaches the high-intensity in efficiency but is far behind in intensity. The output in lumens per watt is 7.8 for the high-intensity arc, 3.9 for the plain-carbon arc, while the incandescent varies between these two values, and is thus a worthy competitor in many cases where high beam intensities are not required.

Viewing these searchlights merely as optical devices, the figures for the utilization of generated light show a remarkable relation. We have for the high-efficiency arc 25.2 per cent, concentrated incandescent beam 25.0 per cent, spread incandescent beam 24.5 per cent, and plain-carbon arc 49.7 per cent, or exactly double the other values.

In central beam intensities, all units with equal diameter of mirror would compare by actual test as follows:

High-intensity beam = 100.0.
Plain-carbon beam = 21.0.
Monoplane filament and glass mirror = 8.0.
Concentrated filament and metal mirror = 0.5.

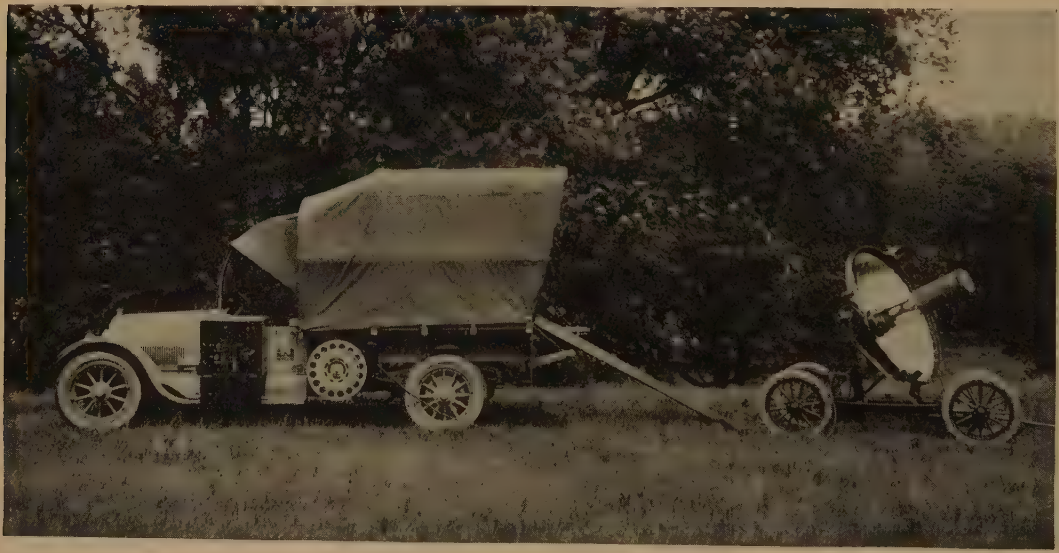

Fig. 136. One of the notable developments of the war was a high-speed truck that acted as carrier and power plant for an anti-aircraft searchlight of the open type. The efficiency of projection of this unit was good when using plain carbons, but the high-efficiency arc suffered when exposed to the wind

(To be continued)

The Protection of Steam Turbine Disk Wheels From Axial Vibration

PART III

METHODS OF DESIGN AND TESTING FOR THE PROTECTION OF TURBINE BUCKET WHEELS FROM AXIAL VIBRATION

By WILFRED CAMPBELL
TURBINE ENGINEERING DEPARTMENT, GENERAL ELECTRIC COMPANY

Prepared with the co-operation of A. L. Kimball, Jr., Research Laboratory, and E. L. Robinson, Turbine Engineering Department; both of General Electric Company

We regret to announce that this concluding section of the article has become a posthumous work of Mr. Campbell. Under this unhappy circumstance, we recall with satisfaction that Mr. Campbell lived to receive distinguished credit for his accomplishment. This came in the form of a Charles A. Coffin Award, and in the delivery of a remarkable paper on the subject before the A.S.M.E., of which this article is a reprint. A further appreciation of Mr. Campbell's work appears on page 564.

The purpose of making a thorough investigation of axial vibration in turbine wheels, and an outline of the early work which led to the discovery of the real cause of this type of vibration, appeared as Part I of this article in our June issue. In the second part, included in the July issue, the theory of the phenomenon was discussed and reasons given for the necessity of placing reliance on actual tests as well as on mathematical analyses. The methods of conducting such tests, the testing equipment developed, and the procedure which has eliminated such vibrations under operating conditions are described below in the concluding part of the record of this investigation.—EDITOR.

The data obtained in the previous building and testing of wheels are utilized in the design of wheels having similar dimensions and forms. In the case of wheels already in service the speed coefficient may be used with considerable confidence in calculating critical speeds when the frequency of vibration of the wheel at rest is known. It is highly desirable, however, to check results whenever possible by rotating the wheel in a wheel-testing machine.

Turbine Wheel-testing Machine

Fig. 59 is a photograph of the testing laboratory showing two complete wheel-testing machines. The smaller machine in the foreground has the cover removed. Fig. 60 is a photograph of the smaller machine with the cover in place ready for test. This machine comprises a sort of bombproof chamber within which the wheel to be tested is operated. The upper half of the casing of this testing chamber is semi-circular in shape, to constitute a hood over the wheel under test. This member is made of cast steel 8 in. thick for protection in case of accident to the test wheel.

The machine consists of a steam chamber in which the test wheel is mounted on the shaft alongside a heavy disk or wheel as appears more clearly in Fig. 61. This shaft carrying the two wheels may be rotated at any required speed by means of a steam turbine. One pipe supplies steam to the casing when necessary while another pipe is utilized to convey the exhaust steam to the vacuum pump and condenser. An absolute pressure of about 4 lb. per sq. in. is maintained in the casing during standard tests.

The purpose of the steam in the wheel chamber circulating during the test is to keep the wheel relatively cool. If turbine wheels are rotated at high speed while surrounded by air at atmospheric pressure, so much heat is generated by the windage that the temperature of the wheel rises unduly. By circulating steam through the casting to the vacuum pump and condenser, the heating energy caused by rotation of the wheel is removed and the temperature of the wheel is maintained at the desired value.

Use of the Oscillograph

In order to observe or record wave motions or vibrations which may occur in the wheel under test, a standard oscillograph is used, together with two sets of exploring coils suitably located within the wheel-testing machine. One set is stationary while the other rotates with the wheel. These exploring coils transmit to the oscillograph, which records them, electrical indications of the movement of the turbine wheel. The stationary coils indicate the movements of the wheel rim toward and away from the exploring coil as the wheel passes by the coil. The movable coil which rotates with the wheel, on the other hand, records only the lateral motion of one given point in the wheel circumference. The records from these two coils disclose the nature of the wave phenomena developed in the wheel.

Exploring coils, located within the casing of the wheel-testing machine, are made steamproof by complete enclosure in a metal casing. Metal-cased wire is used for the electrical connections to the coils.

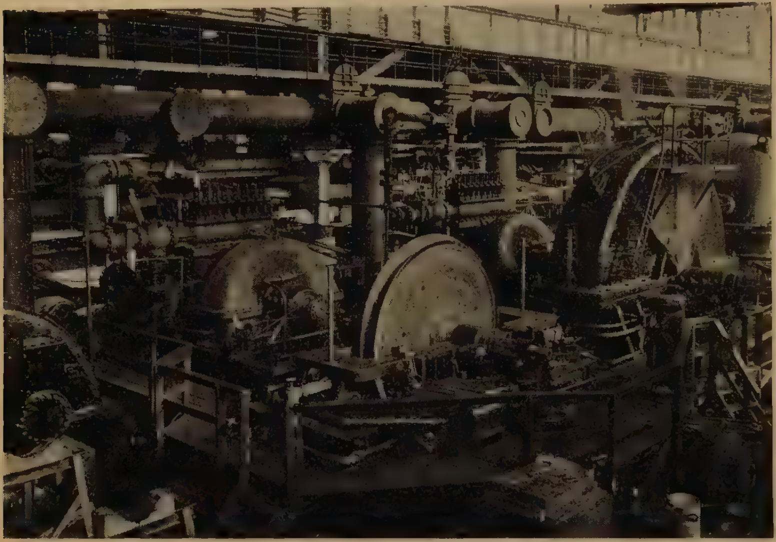

Fig. 59. Testing Machines for Determining the Vibration Characteristics of Turbine Wheels Under Running Conditions

(The cover is removed from No. 1 machine to show test wheel within.)

The rotating coils are carried in a tubular member fastened on the periphery of the relatively stiff coil-carrying wheel, always used in testing, whose vibration characteristics are so well known as not to be confused with those of the wheel under test. The tubular member is held parallel to the shaft and is adjusted in order to obtain the desired air gap between the coil and the test wheel. The metal-cased conductor from this coil is carried down the side of the coil-carrying wheel, brought out through the end of the hollow shaft, and connected to a collector ring. Another coil is placed 180 deg. away. This is used as a reserve and it serves also to maintain balance.

In some cases the wheel to be tested is of such dimensions that the vibration data are obtained from a point in the bucket region. In this case it is customary to silver-solder a small armature between two buckets in front of the rotating coil. Ordinarily, the air gap is between 1/8 and 3/8 in. on the large wheels and sometimes less on very small wheels.

The fixed exploring coil, already referred to, is suitably supported within the casing adjacent to the wheel rim, the metal-cased wire connection from this coil being brought outside the casing where electrical connection is made with the oscillograph.

Electrical Connections

The electrical connections of the various exploring coils, the electrical circuits of the amplifiers used, and of the oscillograph, and of the exciting magnet used in test are shown diagrammatically in Fig. 62. The wires from the rotating coils lead out through the shaft and are connected to slip rings, the brushes from which lead to the primary of a transformer, a suitable source of direct current being connected in series. The development of brushes and rings which

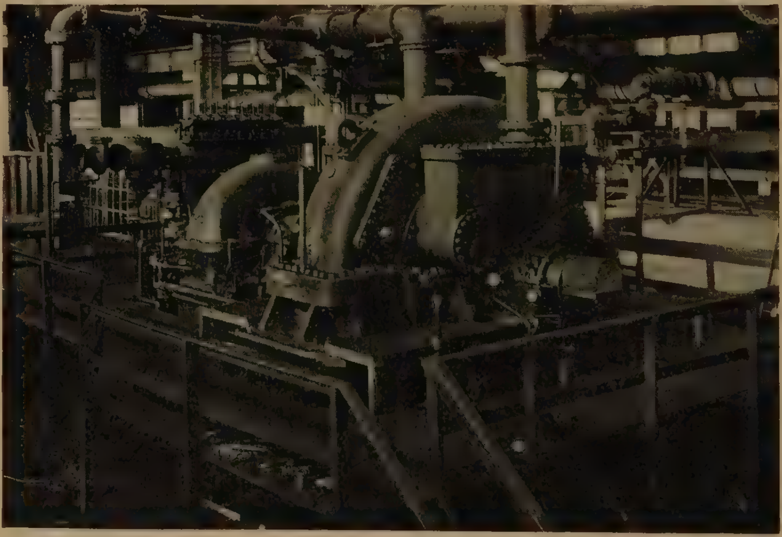

Fig. 60. No. 1 Wheel-testing Machine Assembled with Cover in Place Ready for Test

would satisfactorily collect the minute currents for the oscillograph was one of the many lesser achievements in the construction of this apparatus.

The stationary coil is connected through a switch to the primary of another transformer. The secondary windings from these transformers are connected respectively to suitable amplifying devices for magnifying the current fluctuation produced through the action of the test wheel on the exploring coils.

It will be understood that the current in one of these exploring coils, coming from the battery, develops a magnetic field whose magnitude varies in accordance with the variation in the air gap between the adjacent parts of the wheel and the magnetic coil. In the case of the rotating coil the lateral vibration of the adjacent part of the wheel produces a change in magnetic reluctance. In the case of the stationary coil the change in magnetic reluctance is produced by variations in the distance of the wheel rim as it sweeps by the stationary coil. These variations in distance are due partly to irregularities in the structure of the wheel itself, and in case of wave phenomena, to lateral deflections of the wheel.

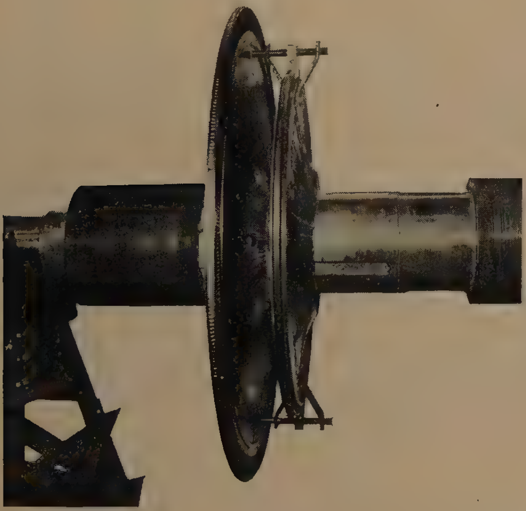

Fig. 61. **Testing-machine Shaft Showing Exploring Coils Carried on an Adjacent and Relatively Stiff Wheel**

The current induced in the transformer secondary windings is amplified by vacuum tubes. This amplified fluctuating current is then led through another transformer, the secondaries of which lead to the oscillograph vibrators.

The oscillographs, indicated diagrammatically in the upper portion of Fig. 62, are standard instruments for producing and for recording images representing the fluctuations from instant to instant of electric currents. These images may be produced by the trace of a point of light upon a ground glass or in a mirror, or images may be recorded permanently on a photographic film.

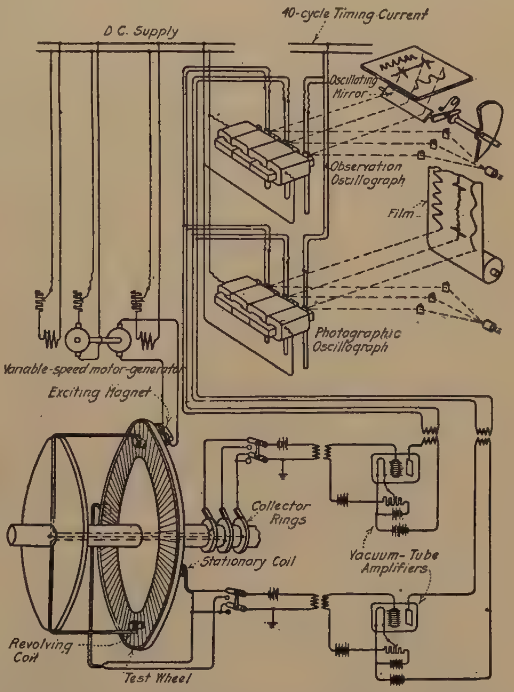

Fig. 62. **Electrical Connections for Wheel-testing Machine**

(Both revolving and stationary exploring coils are connected through vacuum-tube amplifiers to the observation and photographic oscillograph instruments. The exciting magnet receives current from a variable speed motor-generator set.)

The fluctuating current is led to the bifilar suspension armature which carries a small mirror. This armature, which is located in a strong magnetic field, oscillates in proportion to the fluctuations in the current. Light from an arc lamp is transmitted through a lens and prisms to the mirror, and is reflected in turn to a suitable receiving surface. As used at present, this consists of an oscillating mirror which is arranged to oscillate about a horizontal axis. The frequency of these oscillations is directly proportional to the speed of rotation of the test wheel. When this mirror is oscillated the wave forms are rendered visible by reflection on a ground-glass receiving screen. The pivoted mirror is caused to oscillate by means of an arm which is held by a spring in contact with a cam. This cam is driven by a synchronous motor connected with the cam shaft. The synchronous motor receives the current from a small alternator driven directly by the shaft carrying the test wheel, the result being that the wave motions appear to be stationary instead of progressing across the field of vision.

The illumination of the screen is interrupted periodically by a shutter attached to the camshaft. During this dark period the cam returns the mirror to its initial position, and the light is then allowed to illuminate the screen again. Actually, only a spot of light is reflected on the screen, but owing to the rapid rotation of the camshaft and the phenomenon known as the "persistence of vision" the spot appears as a complete, more or less wavy line.

Three bifilar circuits carrying oscillating mirrors are used in the oscillograph, and are connected respectively to the coil circuits whose wave forms it is desired either to observe or record. For reasons which will be explained, the oscillograph just referred to is used only for purposes of observation. One circuit receives its current indirectly from the rotating coil, another from the stationary coil, and the third circuit receives its current from a source of 40-cycle alternating current, so that the indications produced from the operation of this latter member of the oscillograph serve as a time standard for the waves produced by the other two circuits.

A similar oscillograph, provided for the taking of photograph films, has all its circuits connected in multiple with those of the observation oscillograph just described, so that both receive currents of the same character. Inasmuch as the wave phenomena in the turbine wheel are transitory, the presence or absence of these wave phenomena is observed by inspection of the reflections from the oscillating mirror. When, however, the operator observes in the mirror of the observation oscillograph the occurrence of any particular wave phenomenon which it is desired to record, then at the desired instant he signals an assistant. The latter thereupon operates the shutter of the recording oscillograph, causing an exposure to be made upon the film, which is immediately developed in the usual manner.

For the purpose of causing at will a vibration of the test wheel, a well-insulated electromagnet is located opposite the periphery of the wheel. This is usually located at the wheel rim in such a manner that the magnetic attraction will be in a direction parallel to the shaft. Electrical connections for this magnet are brought out from the shell and the alternating current is supplied from a variable-speed motor-generator set. Suitable rheostats enable frequencies varying through wide limits to be obtained. An electrical tachometer is used for measuring the speed of the motor-generator set. This is graduated in terms of frequency of the alternating current generated.

For the efficient use of the apparatus and the best organization of the work it has been found desirable to have two complete testing machines in use. While one is connected to the instrument chamber for the taking of records, the other machine is open or being assembled with the next wheel. All of the instruments for observation and control are grouped in the instrument room, including both the observation oscillograph and the photographic oscillograph. The necessary tachometers, control switches, rheostats, and the speaking tube to the turbine operator are within reach of the man in charge whose post is at the observation oscillograph. The developing room is immediately adjacent and equipped with all facilities for the quick development of records so that the operator can see, while the wheel remains at speed, whether his films successfully record the desired phenomena.

In testing a turbine wheel it is convenient first to determine the natural periods of vibration of the wheel when at rest, or standing still. This is often done with the wheel placed in the wheel-testing machine, previous to making the rotation test. The electromagnet already described, placed close to the rim of the wheel, receives the alternating current, thereby producing a pulsating magnetic pull on the wheel rim. Inasmuch as the magnet exerts a pull for each half wave of the alternating current the pulsating attraction exerted upon the wheel is numerically double that of the frequency of the alternating current. The nodal points on the wheel circumference are determined by observation and touch. Oscillograph records also corresponding to each particular number of nodes are taken and recorded.

Oscillograph Films

Fig. 63 gives reproductions of oscillograph records of a wheel tested in the wheel-testing machine. Film *A* is the record taken to determine the standing frequency. The sine curve T is the timing wave corresponding to the alternating current from supply mains. The curve S is the record of the stationary exploring coil. The vibration of the wheel as disclosed by this curve is caused by the action of the alternating-current magnet. When the frequency of the current in this magnet has been brought up to a value corresponding to one of the nodal frequencies of the wheel, a relatively large vibration of the wheel ensues, as is recorded on the film at S.

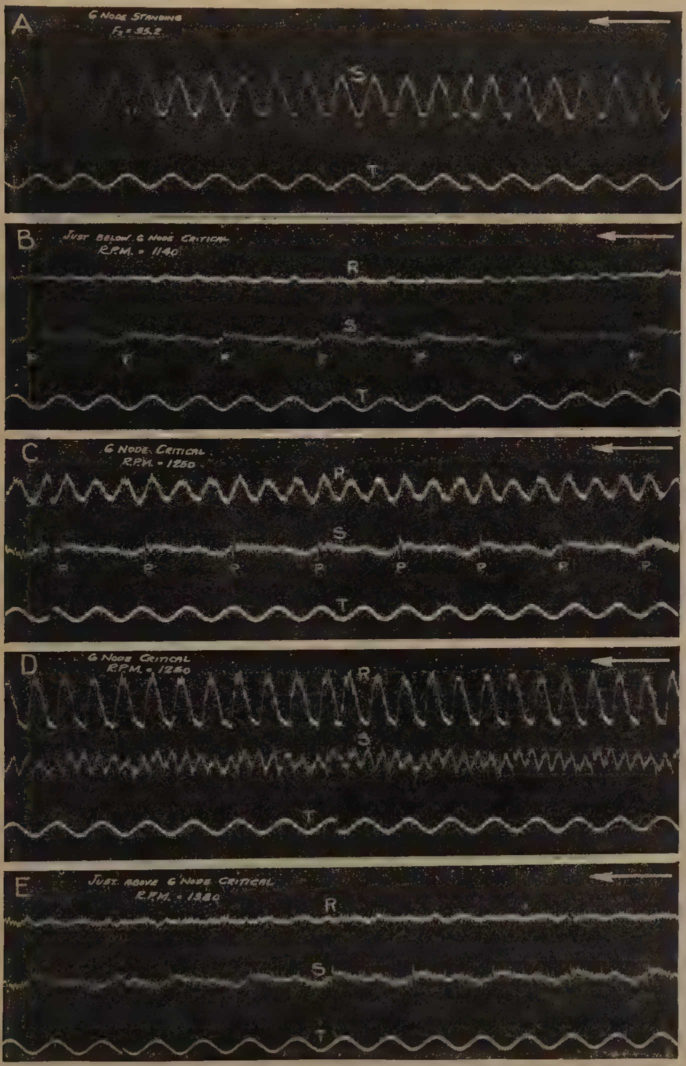

Fig. 63. Typical Oscillograph Records

T is a 40-cycle timing wave.
S is the record made by the stationary coil.
R is the record made by the revolving coil.
A—Wheel stationary, 6-node vibration, 55.2 cycles per sec.
B—1140 r.p.m. The stationary coil S gives the wheel "autograph." No vibration is indicated.
C—1250 r.p.m., 6-node critical speed. The revolving coil R shows the backward wave in the wheel. The stationary coil S still shows the wheel "autograph" since the wave is stationary in space.
D—1250 r.p.m., 6-node critical speed. A moment later than C. The stationary coil S shows the development of the forward wave train at double the frequency shown by the backward wave train in the revolving coil record R.
E—1380 r.p.m. Wave phenomena have vanished. Compare with B.

If now the test wheel be set in rotation, the current in the alternating-current magnet having been discontinued, the stationary exploring coil produces indications in the oscillograph even though no critical speed be obtained at which wave phenomena can develop.

Indications of this character are shown in the record reproduced as film B. Here, as before, T is a timing wave. The irregular line S is the record of the stationary coil. This represents the wheel running rigidly and entirely free from wave phenomena. It will be noted that various peculiarities in the line repeat themselves at regular intervals, as for example, at the points P. The distance between like points P represents the time of one revolution of the wheel. By comparison of the timing wave T, which in this case was that of an alternating current of 40 cycles, the speed of rotation of the wheel can be accurately determined from the film, and may be checked up with the speed of the turbine driving the test wheel. Thus the line S, when its irregularities regularly repeat themselves, may well be referred to as the autograph of the wheel because it is different for every wheel tested.

The record at R on the oscillograph film B is that of the rotating coil. It will be noted that this record shows numerous fluctuations of very small amplitude. These are so small as to be negligible and show that there are no wave phenomena now present in the wheel.

Upon increasing the speed of the rotation of the wheel a point is finally reached where a wave train is markedly developed. This is clearly shown in film C. It will be observed that the record of the revolving coil is now in the form of a very marked wave, while the record of the stationary coil is substantially unchanged. This indicates the presence of a traveling wave of considerable magnitude in the turbine wheel. As the wave travels past the rotating coil the adjacent portion of the wheel oscillates backward and forward so as to produce the wave record *R*. It will now be noted that in the space of one revolution, as indicated by the distance between the points *P*, there occur three wave crests on each side of the zero line in the record of the rotating coil. Since there are three wave crests on each side of the wheel, making a total of six, this record indicates the presence of a 6-node wave train. Furthermore, the fact that the stationary coil gave the same record as in *B* indicates that the wave train in the wheel had no apparent effect on the stationary coil. It follows, therefore, that the waves were stationary in space, and that the test wheel was running at a critical speed corresponding to a 6-node wave train.

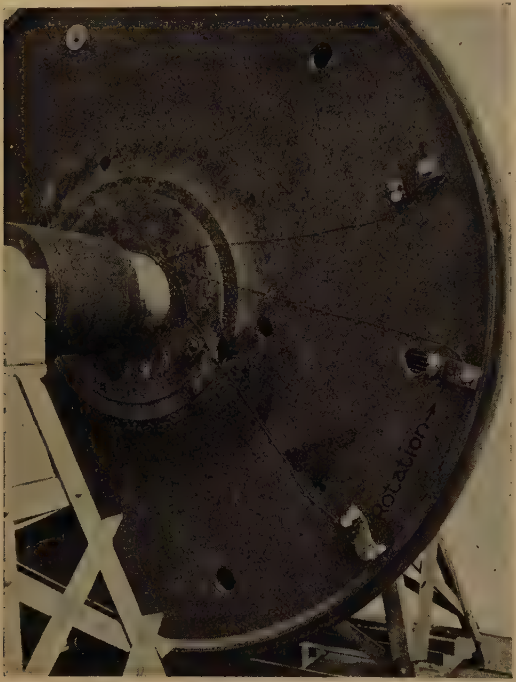

Fig. 64. Coil-carrying Wheel Equipped with Three Coils Spaced 30 Degrees Apart for Detailed Analysis of Wave Motion

The wheel was then permitted to run at this speed for a short time whereupon the oscillograph disclosed certain changes taking place in the wave phenomena, as shown in film *D*. It will be noted here that the wave motion, as shown by the rotating coil record *R*, has become much more marked, and furthermore, that the stationary coil *S* has lost its original character and shows a series of waves, which upon examination will be found to be just twice as many in number as those now appearing in the rotating coil record *R*. This double frequency wave *S* represents a wave traveling forward in the wheel. The fact that the frequency shown on curve *S* is exactly twice the frequency of the curve *R*, confirms the fact that we are here dealing with a critical-speed phenomenon in which the backward-traveling wave is stationary in space and which has a forward wave superposed upon it.

These speeds have been given the name "critical speeds" because nearly all vibration accidents have been associated with this condition, and also to distinguish them from other known resonant conditions.

In film *E* is illustrated what happens upon slightly raising the speed of the turbine wheel over that corresponding to the record produced in *D*. It will be noted that the fixed coil record *S*, and the rotating coil *R* have returned practically to the condition exhibited in *B*, wherein the speed of the wheel was slightly below the critical speed.

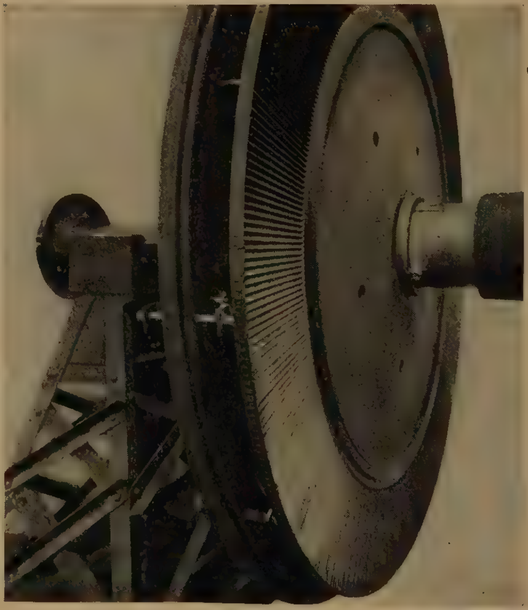

Fig. 65. Assembly of Test Wheel with Three Revolving Exploring Coils

One of the principal reasons for making rotation tests on the turbine wheel itself is that the various frequencies corresponding to vibration with radial nodes depend on the speed of rotation. It has been explained that the natural periods of vibration of the wheels increase as the wheel is set in rotation. This is readily shown by setting a wheel in resonant vibration with a definite number of nodes, by the use of the alternating-current magnet with the wheel at rest, and then, while the wheel is in violent vibration, setting it in rotation. When the speed is sufficiently increased, vibration dies out. Upon decreasing the frequency of the magnet a sufficient amount, the wheel will again vibrate and a backward-traveling wave will develop having the same number of nodes as before. Furthermore, a similar but forward-traveling wave may be produced by sufficiently increasing the frequency of the magnet. When, therefore, for a given speed of rotation a certain frequency of impulse is applied to the wheel, less than that which would set the wheel into vibration if the wheel were at rest, a backward-traveling wave in the wheel may be induced, while if a certain higher frequency were applied, a wave traveling forward in the wheel at the same speed in the wheel as the backward-traveling wave may be induced. These relationships have been explained in connection with the frequency-speed diagrams, Figs. 32 and 35, and the unprovoked occurrence together with the recording of such waves has been noted.

Demonstration of a Single Wave in the Testing Machine

The definite excitation of traveling waves under other than critical conditions is accomplished in the wheel-testing machine by means of the alternating-current magnet placed within the shell opposite the periphery of the wheel. The existence and direction of motion of such traveling waves in response to artificial excitation have been demonstrated further by a special series of tests using three oscillograph coils placed at intervals of 30 deg. on the carrier wheel as shown in Figs. 64 and 65.

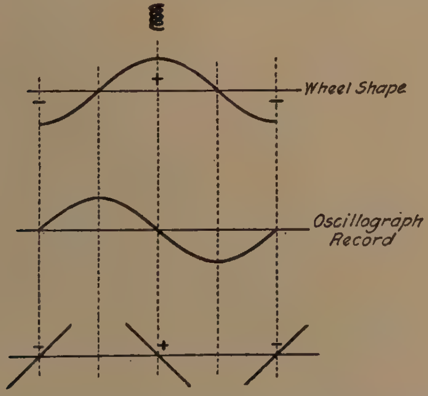

Fig. 66. The Oscillograph Record Differs 90 Degrees from the Wheel Motion. The Convention Indicated Enables the Films to be Analyzed

In order to interpret the films properly it is necessary to note that the wave crest of the oscillograph record is normally displaced one-quarter cycle from the crest of the wave in the wheel. Although each cycle on the film represents one vibration cycle, the actual motion of the wheel is recorded only indirectly by the film. The oscillograph records the induced voltage (with a negligible electrical lag) and the voltage reaches its maximum when the change of air gap is occurring most rapidly, that is, when the wheel is in its neutral position. Similarly, when the wheel pauses at its extreme position there is an instant of zero voltage during which the motion and induced voltage reverse their directions. Fig. 66 illustrates these relations. In all three coils the polarity was the same and also in each case the convention shown in Fig. 66 applies, namely, when the oscillograph record slopes downward to the right the wheel has a plus deformation and when it slopes upward to the right the deflection is minus.

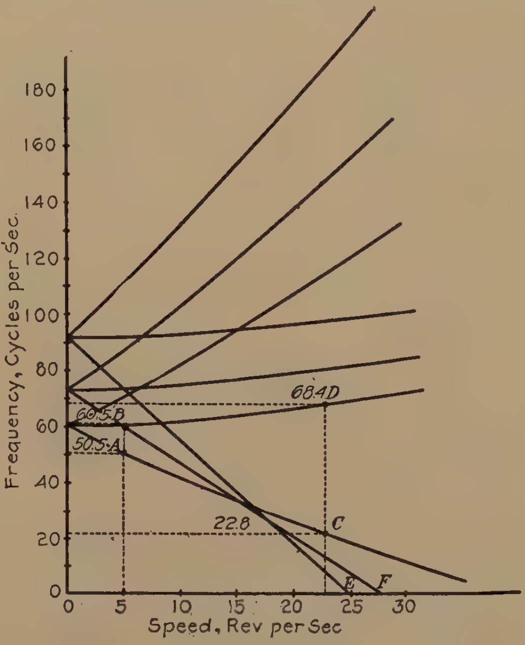

Fig. 67. Frequency-speed Diagram for 3-coil Test

The frequency-speed diagram for the wheel shown in Fig. 65 is given in Fig. 67. The curves for revolving coil frequencies and forward and backward wave frequencies as measured by a fixed coil are given for 4, 6 and 8 nodes.

At a speed of 5 r.p.s. a backward wave would register on a fixed coil a frequency of

50.5 cycles per second as shown at *A*, Fig. 67. The test shows the development of such a wave. The wheel was brought up to a speed of 5 r.p.s. and the alternating-current magnet frequency was made 50.5. A record represented by *B*, Fig. 68, was taken. The numbering of the coils is shown at *A*, No. 1 being the leading coil in every case. On the records of the coils, numbered 1, 2 and 3 to correspond with the diagram at *A*, is shown a deformity of the sine wave caused by the stationary alternating-current exciting magnet as each coil in turn passed it. This deformity serves to indicate the velocity of the wheel relative to that of the wave. The projections of the deformity on the zero axis are joined by a line marked "wheel slope." The horizontal projection of this line represents the time taken by the wheel to rotate the 60 deg. separating coil No. 1 from coil No. 3. The actual speed of rotation given by the electric tachometer thus permits the calibration of the horizontal or time scale of the film and gives the frequency of the disk as recorded by the revolving coils as 60.5 as shown at *B*, Fig. 67.

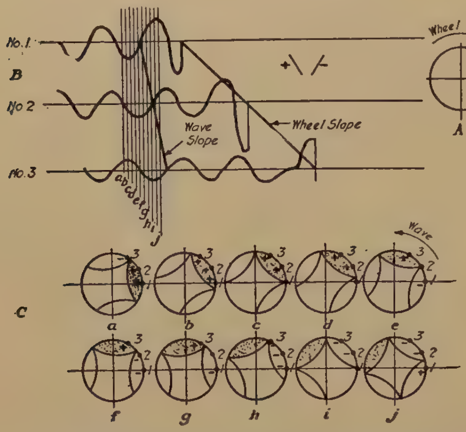

Fig. 68. 4-node Backward Wave at 300 R.P.M. Maintained by a Stationary A-c. Magnet, Frequency 50.5 (See A, Fig. 67)

(The disk frequency is 60.5. The wave velocity exceeds the wheel velocity and therefore the wave travels backward in space as well as in the wheel.)

The determinations of the direction and speed of the wave travel and the shape of the wave are made as follows: Since the coils are 30 deg. apart, the three traces on the record at *B*, Fig. 68, represent the motion of the edge of the wheel from its neutral position due to the wave motion at those three points on the circumference at any particular instant of time. Utilizing the convention explained in Fig. 66, the shape of the wheel at any instant is shown by the intersection of any vertical line with the three wave records. A series of vertical lines are drawn representing successive instants of time *a* to *j*. For each instant, a separate diagram is made at *C* and the corresponding deformation at each coil is noted.

An examination of Fig. 68, *a* to *j*, shows that a 4-node figure is definitely determined and at the same time the direction of rotation of the wave with respect to the three rotating coils is indicated. In this case it will be seen to be in a direction opposite to the rotation of the wheel itself. In order to determine the velocity of the wave, the points corresponding to the intersections of the zero line by the wave records of the three coils may be joined with a straight line as was done in the case of the wheel. This line is marked "wave slope" and the horizontal projection indicates the time taken for the wave to traverse 60 deg. or $\frac{1}{6}$ of a revolution. It is plain from Fig. 68 that the wave, which is traveling backward in the wheel, moves 60 deg. in a much shorter time than the wheel itself and hence the wave must actually be progressing backward in space.

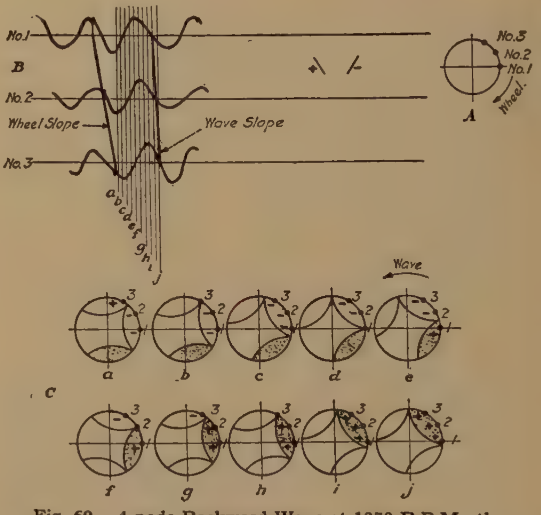

Fig. 69. 4-node Backward Wave at 1370 R.P.M., the First Minor Resonance (See C, Fig. 67)

(The wave velocity exceeds the wheel velocity and therefore the wave travels backward in space as well as in the wheel.)

A second test is illustrated in Fig. 69. The speed was brought up to 22.8 r.p.s. as shown in Fig. 67 at *C*. At this condition it will be noted that the frequency of the 4-node backward wave relative to a fixed point is exactly equal to the speed of rotation in r.p.s. This is called a minor resonant speed for 4 nodes, a condition which will be discussed presently. An examination of the records in the same way as described for Fig. 68 shows a 4-node backward wave with a speed of rotation greater than the wheel speed so that the wave is progressing backward in space. The frequency of the wheel relative to the rotating coils is 68.4 as shown at *D*, Fig. 67.

Fig. 70 represents the condition observed with the wheel rotating at 24.7 r.p.s. The phenomenon recorded corresponds to the point *E*, Fig. 67. In this case the wheel and the wave slopes have exactly the same angle so that the velocity of the wave equals that of the wheel. The analysis shows the wave to be backward relative to the wheel, and therefore in this case the wave was stationary in space. This is an 8-node critical speed. Each particle of the wheel circumference traversing this wave passes through four high spots on each side of the wheel and would thus, in case of contact with the diaphragm, result in rubbing at four equidistant spots. Should rubbing occur on the opposite side of the wheel, it would result in four equidistant spots intermediate to the spots on the first side of the wheel.

Fig. 71 illustrates a 6-node critical speed occurring at 27.7 r.p.s. as shown at *F*, Fig. 67. In this case if rubbing should occur it would take place at three equidistant spots on each side, with alternate spacing.

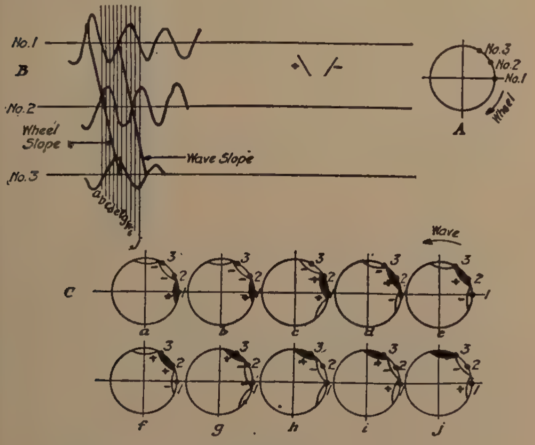

Fig. 70. 8-node Critical Speed at 1480 R.P.M. (See E, Fig. 67)

(The backward wave velocity in the wheel equals the forward wheel velocity, so that the wave is stationary in space.)

Confirmation of Breakages

It has been the custom, since the first vibration troubles were successfully explained, to make tests in all the cases of serious wheel or bucket trouble. Either a duplicate wheel is made or, if in a suitable condition, the wheel that suffered the injury is itself used. The first test made in this manner was of the 17th stage wheel of a 20,000-kw., 1500-r.p.m., 23-stage turbine which developed a traveling wave, as determined by oscillograph record, while under load in the operating turbine.

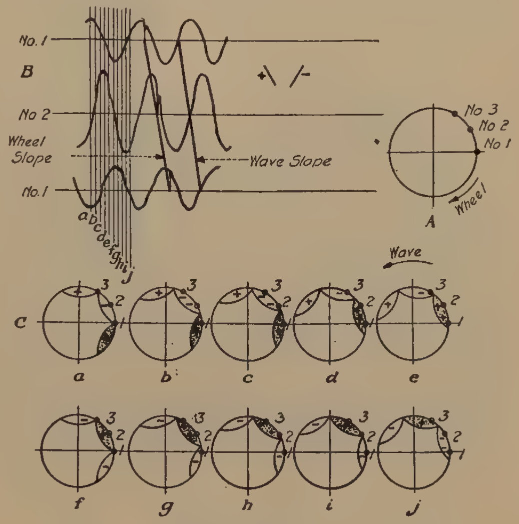

Fig. 71. 6-node Critical Speed at 1660 R.P.M. (See F, Fig. 67)

(The backward wave velocity in the wheel equals the forward wheel velocity, so that the wave is stationary in space.)

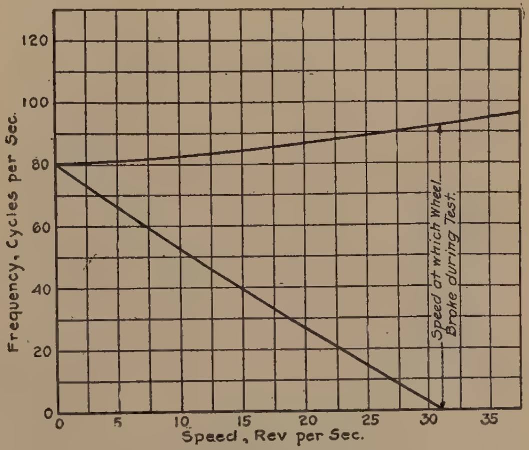

Fig. 72. Frequency-speed Diagram for Six Nodes for Wheel Shown in Fig. 73

By revolving this wheel in the wheel-testing machine and applying the alternating-current magnet at its rim, the fundamental relations between the applied force and the corresponding vibration were determined. Using this information together with that obtained from the oscillograms taken under load conditions it was possible to construct

Fig. 72. From this diagram a prediction could be made that at a speed of about 31 r.p.s. a continuous force applied at a fixed point in space should throw the wheel into vibration with a 6-node stationary wave.

This prediction was tested as follows: With no current on the magnet the wheel speed was brought up through the predicted danger point and nothing was observed. The wheel was then slowed down somewhat below that point and the electromagnet was energized by direct current furnishing a fixed force. The speed was then raised almost to the predicted point, when the wheel developed a violent lateral vibration, rubbing off the pole piece of the exciting magnet and very soon tearing out the buckets from the wheel rim as shown in Fig. 73, a striking corroboration of the prediction and an indication of the seriousness of operating at a critical speed.

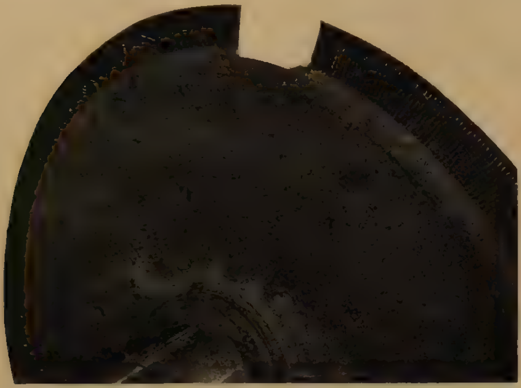

Fig. 73. Turbine Wheel Broken in Testing Machine by Rotation at 6-node Critical Speed. 17th Stage of 20,000-kw. 1500-r.p.m. 23-stage Turbine

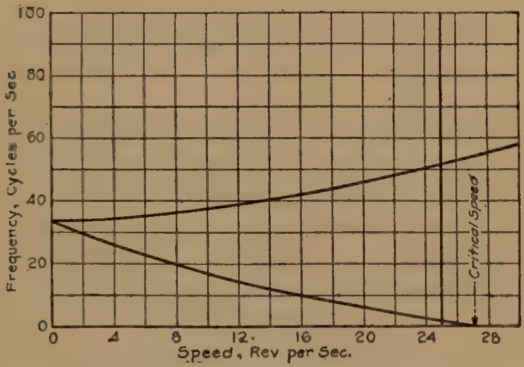

Fig. 74. Frequency-speed Diagram for Four Nodes. 11th Stage of 30,000-kw. 1500-r.p.m. 12-stage Turbine

The 11th-stage wheel of a 12-stage double-flow turbine in a 30,000-kw., 1500-r.p.m. machine had failed in a manner illustrated in Fig. 5. A duplicate wheel in the same turbine was used for the purpose of making rotation tests. Both wheels had been in service and operated several years. Fig. 74 was made from data obtained from a test of the duplicate wheel. A 4-node critical speed due to a wave stationary in space is indicated at 27 r.p.s. just above the running speed of 25 r.p.s. It is not unlikely that the wheel that failed differed slightly, due to minor variations in machining, from the duplicate which was tested. Such a variation might very probably bring its actual wave speed equal to running speed.

The wheel in the testing machine, when operated at the speed of the 4-node wave stationary in space, developed heavy vibration and threw off a piece of shroud band which previously had been slightly damaged in the accident to the broken wheel. It was observed that the diaphragm, opposite the wheel in service which had failed, had been deeply cut by the shroud band of the wheel whereas the wheel used in test had no such contact with the diaphragm.

The natural frequencies taken on another pair of duplicate wheels and also of the same dimensions as the former wheel yielded results from which Fig. 75 is plotted. Here, close coincidence with the operating speed is indicated. That trouble had not occurred with these wheels is attributed to the absence of sufficient exciting force.

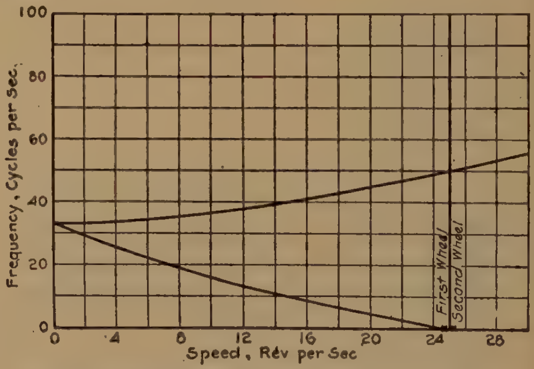

Fig. 75. Frequency-speed Diagram for Four Nodes. 11th Stage of 30,000-kw. 1500-r.p.m. 12-stage Turbine

Still another duplicate wheel in another station had been known repeatedly to rub the diaphragm. All wheels of this type were immediately replaced as soon as the cause of the accident to the broken wheel became known.

Another typical case was that of a third-stage wheel of a 6000-h.p. turbine used for ship propulsion. Fig. 7 is a portion of the broken wheel showing two breaks which occurred through steam pressure equalizing holes. Figs. 8 and 9 show the development of fatigue fractures which originated, in each case, at each side of a hole. Previous to the failure of the wheel under investigation, the ship had been continuously cruising with a propeller speed of 84 r.p.m. owing to foggy weather. At the time of the accident the tachometer showed 84 r.p.m. of the propeller, corresponding to a turbine speed of 48 r.p.s.

The vibration tests were carried out on a duplicate wheel made from the same drawing as the broken one. This wheel was placed upon its own shaft in order to determine the standing frequencies. It was afterward run in the wheel-testing machine to determine the effect of the centrifugal force. These results are plotted in Fig. 76 which shows the 4- and 6-node frequencies. The 6-node critical speed occurred at 48 r.p.s., which was just the speed at which failure actually took place, namely, 84 r.p.m. of the propeller and 48 r.p.s. of the turbine.

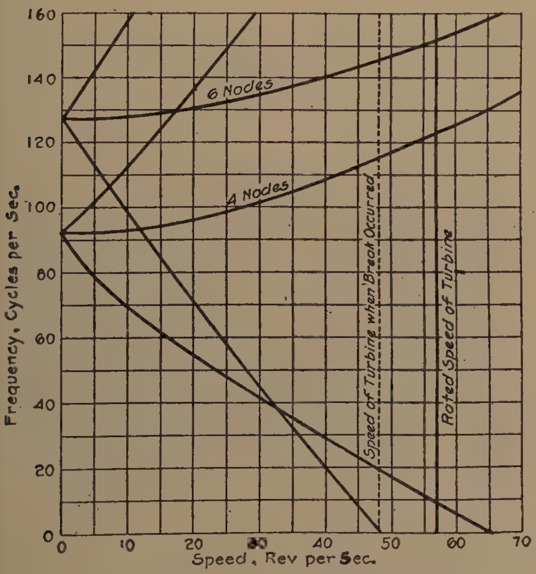

Fig. 76. Frequency-speed Diagram for 3rd Stage of 6000-h.p. Marine Turbine

At this speed, corresponding to the 6-node critical speed of the wheel, the stationary wave could be maintained so that, if this speed were held constant for a considerable time, the wave could develop a large amplitude of vibration and the wheel undergo a series of repeated, or fatigue, stresses which would eventually cause failure. A substitute wheel, designed to replace the broken wheel, was increased in thickness 100 per cent, so that the 4-node critical speed was raised to a point 92 per cent and the 6-node speed to a point approximately 50 per cent above the normal running speed.

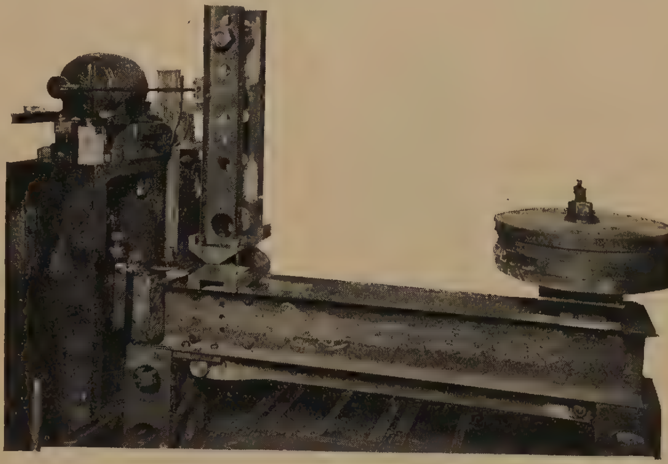

Fig. 77. Turbine-bucket Vibration Machine

Fatigue Cracks in Bucket Dovetails

The breaking of bucket dovetails on the last stage of a 30,000-kw., 1800-r.p.m., 17-stage turbine was attributed to wave phenomena, in which the speed of the backward wave was equal to the speed of rotation. The nature of the break indicated that axial motion of the bucket system had been occurring for a considerable time before rupture took place.

The break occurred at the dovetail and since the vibrational stresses were superposed upon the centrifugal stresses, it was realized that a bucket, to be broken in a similar manner, should be subjected to both kinds of stress. In order to accomplish this, a special machine shown in Fig. 77 was devised, in which it was possible to apply the tension load to the bucket dovetail which it would have in a wheel running at normal speed. The vertical member shown at the left-hand end is allowed to rock around the metal ribbons at its base. The heavy weights together with the lever shown below the base create the necessary tension force on the specimen. The upper end of the bucket is secured to the top end of the vertical member and the section of the wheel at the lower end is secured to the block sliding in the base. This block is then pulled down by the lever already referred to. Fig. 78 illustrates the bucket and wheel section assembled in the vertical rocking member. This arrangement allows lateral motion of the bucket and wheel with a minimum variation of tension during the swing. The vertical rocking member is vibrated by means of a motor-driven eccentric to which a revolution counter is attached.

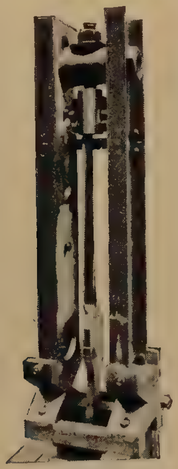

Fig. 78. Detailed View of Bucket in Vibration Machine

Fig. 79 shows at *B* and *C* breakages at the lower tangs of two buckets that occurred in service after two months' operation. The specimen shown at *A* was a duplicate bucket fitted together with a cross-section of the wheel machined to the same width as the bucket. A smooth crack developed in the lower left-hand tang of the bucket. This was produced by means of the apparatus explained, after six million repetitions of the stress.

In the case of the wheel breaking in service no rubbing had been encountered. The amplitude of motion used in the test machine was equal to one-half the clearance between the shroud band and diaphragm.

Upon separating the pieces shown at *A* the surface conditions of the fracture were found to be of the same nature as in the case of the service wheel.

Effect of Forced Rubbing on Vibration at Speeds Other Than Wheel Critical Speed

Since the efficiency of a steam turbine depends to a certain extent upon the clearance between the discharge edges of the nozzles and the entrance edges of the buckets, a test was made to show the effect of rubbing of the wheels on the diaphragm in producing vibration in the wheels.

The object was to determine the possibility of causing and maintaining lateral vibration in a steam-turbine wheel by exerting pressure at the rim by means of a rubbing block and also with a steam nozzle. The tests were made on a large-diameter wheel, shown in Fig. 80, of unusual flexibility. The wheel had been in service (3d stage) in a 20,000-kw., 1200-r.p.m., 9-stage turbine.

The wheel-testing machine was used and a brake shoe was arranged for the purpose of causing contact. This method of applying pressure would be somewhat similar to the worst condition that could occur in a turbine, namely, rubbing at one place. The brake shoe and method of applying pressure is illustrated in Fig. 81. A rope was attached to the external lever and extended to the instrument room. Rubbing pressure could be brought about at will during observation of wheel vibration. Visual observation was made on the ground-glass screen of the oscillograph. When the revolving recording coil showed either vibration or erratic scratching the shoe was quickly released and the wheel permitted to run free. This was repeated for various speeds of the wheel. Fig. 82 is a diagram of the complete information obtained from this test. Standing frequencies were obtained in the usual manner, films recording critical and minor resonant speeds (which will be discussed presently) are indicated by stars. As an alternative to the rubbing shoe a steam nozzle projecting high-pressure steam in an axial direction could be substituted.

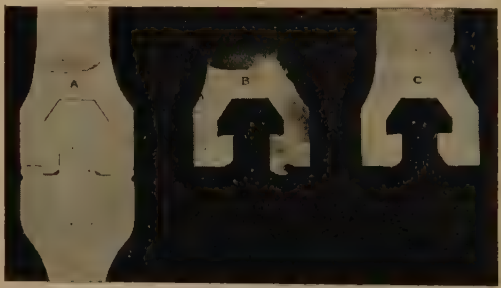

Fig. 79. Broken Turbine-bucket Dovetails. 17th Stage of 30,000-kw. 1800-r.p.m. 17-stage Turbine

(The break in *A* was produced in the vibrating machine, Fig. 77. Breaks *B* and *C* occurred in service.)

It was noticed that when running at a minor resonant speed the wheel forms a definite wave due to the shoe contact but when not at such a speed the record is very erratic, showing that no definite form of vibration took place. Fig. 83 shows the record made during the rubbing period at other than a critical speed. It was impossible to push the wheel into a definite state of vibration even though a large pressure was exerted.

When the shoe was released the wheel usually assumed a 4-node vibration even though it previously had been vibrating in a more complex type. The 4-node type is the one most frequently assumed when a standing wheel is struck a single blow. After the 4-node vibration died out the wheel always ran true again except when running at some critical or minor resonant speed. Figs. 83, 84, and 85, show the wheel in the three states previously referred to at other than a critical or resonant speed, Fig. 83 being made with the shoe in contact, Fig. 84 just after release, and Fig. 85 about a minute later.

No tests were made with the rubbing bar at critical speeds, the steam jet showing that amplitudes could be built up to a large amount at these speeds. The wheel when examined after test had the rim blued by heat developed from friction.

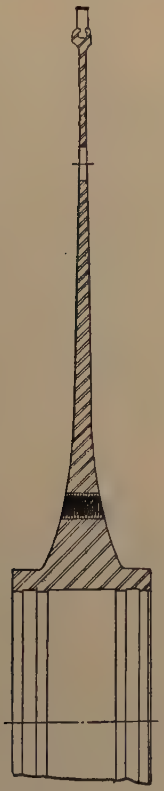

Fig. 80. **Turbine Wheel Used in Rubbing Test. 3rd-stage of 20,000-kw., 1200-r.p.m., 9-stage Turbine**

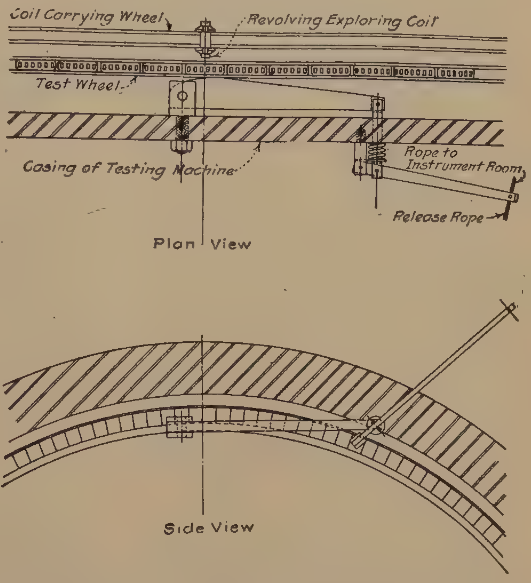

Fig. 81. **Detail of Rubbing Bar Used in Rubbing Test**

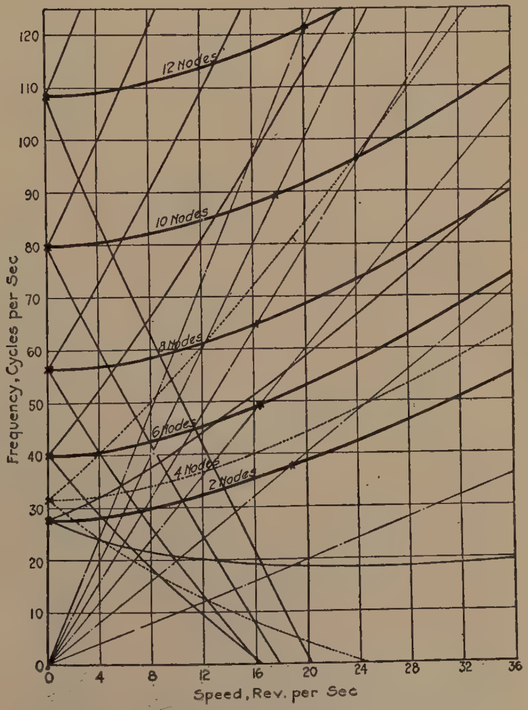

Fig. 82. **Frequency-speed Diagram for Wheel Used in Rubbing Test**

Effect of Temperature on Frequency of Turbine Wheels

Fig. 86 shows the lowering of frequency due to differential temperature. These tests were made in the wheel-testing machine, a gas flame being projected on the rim of the wheel during slow rotation. Thermocouples placed at the rim and the hub, and connected to the collector rings at the end of the shaft, were used for the purpose of measuring the temperature at these two points. It is seen that there are only slight changes in the 2- and 4-node frequencies, due to a temperature difference of 200 deg. F., but greater differences are noticeable with six and eight nodes. These temperature differences are only possible momentarily in service and wheels at the hottest end of the turbine are usually the only ones affected in this way.

Actual measurements of temperature differences in operating turbines between the inner and outer diameters of the diaphragm have not shown anything like these temperature differences. However, it is believed that sufficient margins of variations of this character have been allowed for in the safety limits adopted which prescribe appropriate margins from normal operating speeds for each of the critical speeds.

Effect of Bucket Tightness on Frequency and Critical Speed

The method of fastening buckets to turbine wheels has a very important bearing on frequencies obtained under running conditions. This effect has been very definitely shown from many tests of which a few typical examples are given.

Several wheels were built with bucket dovetails of the type to be inserted in a grooved rim. An attempt was made to obtain a tight fit by initial tension in the neck of the bucket instead of forcing the dovetail head into the groove, which is the common practice. Extra precautions were taken in an attempt to have an initial stress in the narrow neck section of the bucket sufficient to keep this fit tight under running conditions. Fig. 87 shows the various standing frequencies. Test 1 was made on the wheel as originally assembled. Test 2 gives the standing frequencies after light calking of the bucket and Test 3 after heavy calking at the same point.

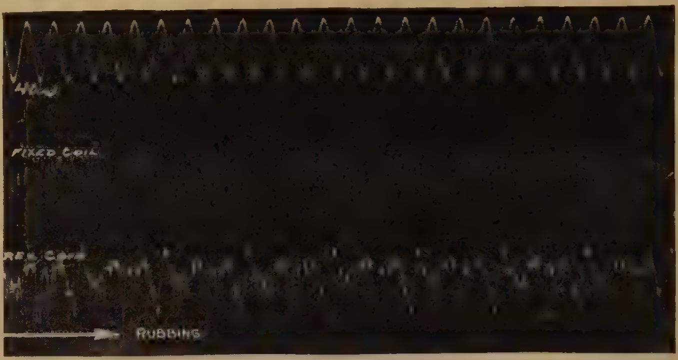

Fig. 83. Oscillograph Record Made During Rubbing Test. Rubbing Bar in Contact

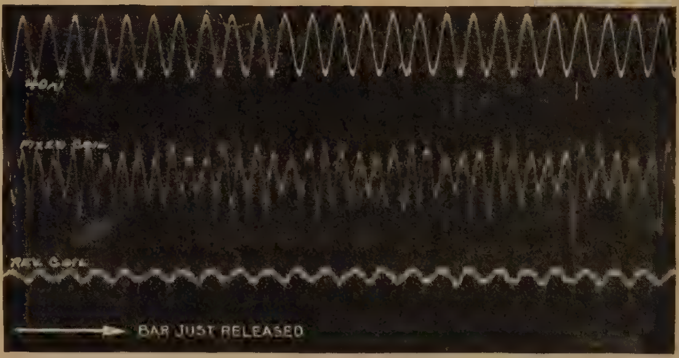

Fig. 84. Oscillograph Record Made During Rubbing Test. Rubbing Bar Just Released

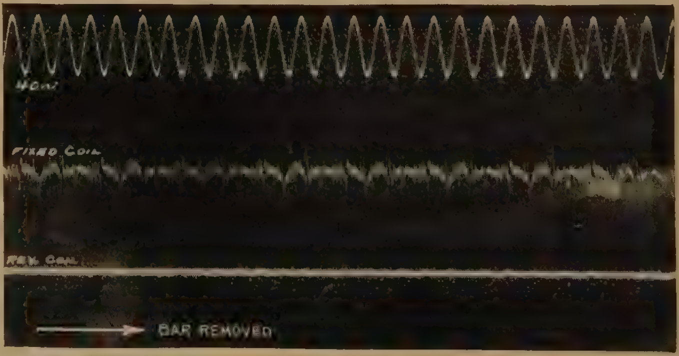

Fig. 85. Oscillograph Record Made During Rubbing Test. A Moment After Release of the Rubbing Bar

It will be noted that between Test 1 and Test 2 a considerable change in the 2-node frequency occurred, much smaller differences occurring with the other types of vibration. Fig. 88 gives the critical speeds for 8, 10, and

12 nodes measured by running Tests 1, 2, and 3 of the wheel under the same conditions, respectively, as shown in Fig. 87. It will be noted that the calking caused very large changes in these critical speeds.

Apparently, in spite of the attempts to insure tightness of the dovetail under running conditions, this was not obtained without the calking operation. The usual type of dovetail, in which the fit is obtained by forcing the dovetail in the groove, is much more consistent in this respect, the first type being unreliable in use because there is no assurance that a tight fit can be maintained.

Tests on the standard-type dovetail, which is forced into the groove, revealed the fact that, while a very considerable change in the standing frequency was brought about by removing the buckets and replacing them loosely, the running tests showed very little change in the critical speeds in the two cases. In the standing condition the stiffness due to the dovetail fit had been changed but in both cases during running conditions the centrifugal forces insured a tight fit regardless of whether or not the buckets had been assembled loosely in the dovetail.

A somewhat similar case occurred with the type of dovetail in which the bucket straddles the rim. In this type of fastening calking is resorted to along the wheel rim for the purpose of insuring tightness. Table III gives the effect on the frequency and critical speed of changes in the tightness of the dovetail. Columns 1, 2, and 3 give the standing frequencies, while columns A, B, and C give the critical speeds recorded during running tests. Columns 1 and A represent the original assembly after the buckets had been assembled with relatively heavy calking. Columns 2 and B give the results after the buckets had been removed and replaced without recalking. Columns 3 and C give the same kind of information after the wheel had been recalked.

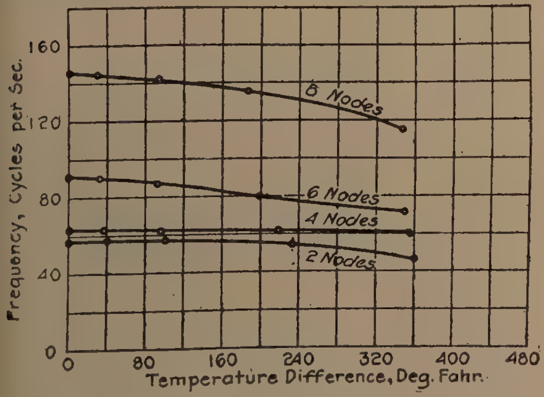

Fig. 86. Effect of Differential Temperature on Frequency (Hot Rim and Cold Hub)

$$f_r = \tfrac{1}{2} n N_s$$

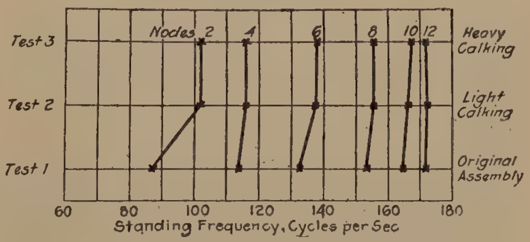

Fig. 87. Effect of Dovetail Tightness Upon Standing Frequency

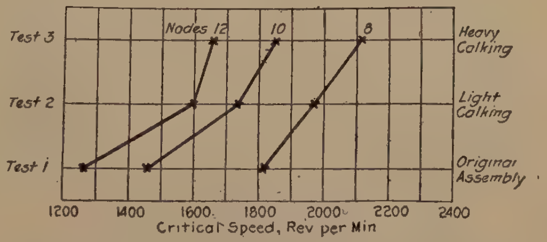

Fig. 88. Effect of Dovetail Tightness upon Critical Speed

It will be noted that both the frequencies and the critical speeds were lowered by removing the buckets from the wheel and reassembling, but both the standing frequencies and the critical speeds were raised to practically the normal conditions upon recalking.

TABLE III

EFFECT OF BUCKET TIGHTNESS ON FREQUENCY AND CRITICAL SPEED

Nodes	STANDING FREQUENCIES			RUNNING CRITICAL SPEEDS		
	Original Assembly 1	Loose Buckets 2	Buckets Recalked 3	Original Assembly *A*	Loose Buckets *B*	Buckets Recalked *C*
4	48	45.2	47.4	34.5	33.7	34.4
6	56	52.4	55.2	21.6	20.8	21.6
8	68	63.2	67.0	18.4	17.9	18.3
10	78	72.8	77.0	16.6	16.0	16.6
12	87	80.8	86.8	15.0	14.3	15.2

Condition for Two-node Resonance

Little has been said so far with regard to the 2-node resonant speed. One reason is that it has rarely been found to have caused trouble. A second reason is that a 2-node wave in a rotating turbine wheel has never been known to be stationary in space. Therefore the same identical causes that produce standing waves with a larger number of nodes cannot be expected to act in the case of the 2-node wave trains.

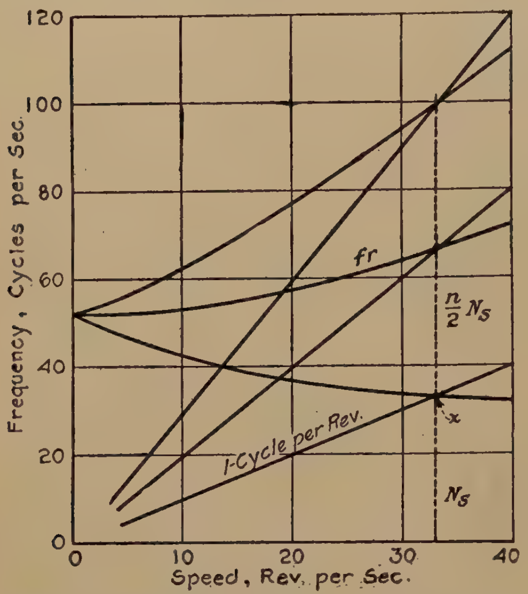

Fig. 89. Frequency-speed Diagram for Two Nodes. The Point x Locates the First Minor Resonant Speed

Two-node vibrations differ from all other radial nodal vibrations in that the forces involved form a couple that is opposed by a corresponding couple in the shaft, whereas in the case of 4, 6, 8, etc., nodes all forces are balanced within the disk. Thus an oscillating motion of one end of the shaft would be expected to cause a 2-node vibration if the frequency of the applied force were equal to the resonant frequency of the disk. This is found to be actually the case when a small unbalanced motor is bolted to the end of the shaft with the armature at right angles to the wheel shaft.

The 2-node frequency is affected by the centrifugal force in a manner similar to that of other types of vibration. Thus the frequency when running, according to equation (5) is

$$f_r=\sqrt{f_s^2+BN_s^2}.$$

If it were possible for the 2-node wave to be stationary in space, this would occur when

$$f_r=\tfrac{1}{2}n\,N_s$$

Substituting this in the above formula the critical speed would be

$$N_s=\sqrt{\frac{f_s^2}{(\frac{1}{2}n)^2-B}} \qquad (15)$$

When B is greater than unity, and n equals 2, it can be seen that N_s, the critical speed, would be imaginary. Since B is always found to be above unity except under very unusual conditions, it is therefore believed that 2-node wave trains stationary in space do not occur.

However, in the wheel-testing machine 2-node records have been made at what is called a 2-node minor resonant speed. Referring to Fig. 89, which is a frequency-speed diagram for two nodes, it will be seen that there is a diagonal line drawn from the zero corner and passing through all points where the frequency is equal to the speed of rotation. This intersects at point x the backward-wave frequency line which, it will be recalled, is also the resonant frequency line for an applied impulse, fixed in space, such as the exciting magnet would give. It is at this speed that the periodic effects of shaft unbalance may excite a 2-node wheel vibration.

It will also be seen that a turbine wheel is in a resonant condition when the natural 2-node frequency for a particular speed, as recorded by a revolving coil, is just twice the revolutions per second of the wheel itself, so that it results in a wave being set up with a wave velocity equal to twice that of the wheel itself. It is possible that a simple vibration shape (i.e., fixed nodes in the disk) could be maintained if the wheel were run in a perfect vacuum, but under other conditions the high-velocity component wave would receive a great amount of damping, probably greatly reducing the amplitude, while not so affecting the backward-traveling wave. The high-velocity wave alone would travel with three times the wheel velocity while the backward wave would have a velocity in space equal to that of the wheel but in an opposite direction.

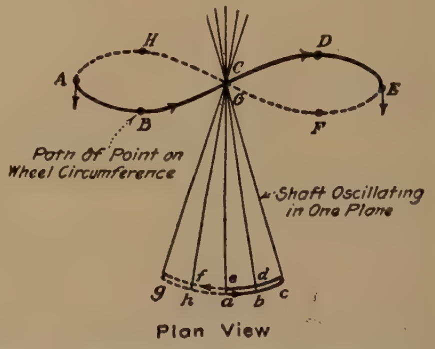
H
D
A
C
E
G
B
F
Path of Point on Wheel Circumference
Shaft Oscillating in One Plane
g
h
f
e
a
d
b
c
Plan View

Fig. 90. Diagram Showing Relation Between Dynamic Unbalance and Two-node Vibration

The path of a bucket during shaft vibration maintained by dynamic unbalance, which might excite a 2-node resonant vibration, is shown in Fig. 90. Dynamic unbalance tends to make the shaft oscillate mostly in one plane, the horizontal stiffness of the bearing supports usually being less than the vertical stiffness. In the neutral position it exerts no force on the bucket. When it swings from *a* to *c* as indicated, it pulls the bucket on the path *ABC*. Swinging back along *c*, *d*, *e*, *f*, *g*, the shaft causes the bucket to travel along *C*, *D*, *E*, *F*, *G*, and on the return swing *g*, *h*, *a*, the bucket travels along *G*, *H*, *A*. It is evident therefore that during one oscillation, i.e., one revolution, of the shaft the bucket goes through two complete cycles. Thus the transverse frequency of the bucket due to unbalance is twice that of the revolutions per second of the wheel itself, which checks with the revolving coil frequency for a 2-node resonant condition discussed in the previous paragraph.

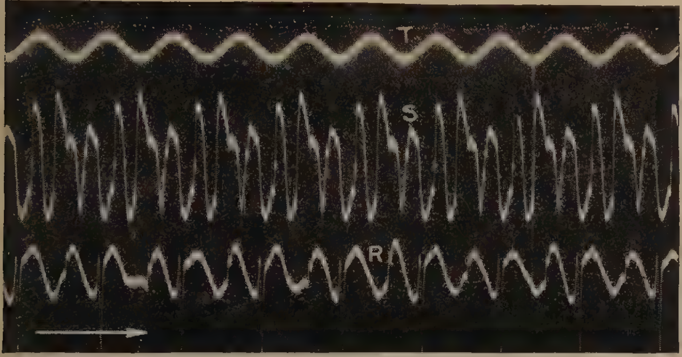

Fig. 91. Oscillograph Record Showing Two-node Forward Wave at First Minor Resonant Speed

Record of Two-node First Minor Resonant Speed

Fig. 91 is a standard oscillogram taken on a wheel in which excessive dynamic unbalance was intentionally applied to obtain a 2-node resonant speed. The curve *T* is a 40-cycle timing wave. The curve *S* was registered by the coil stationary in space. The curve *R* is that registered by a revolving coil.

During each revolution the revolving coil passed through the influence of the stationary coil causing the disturbances noticed on the revolving coil record. Comparison of the spacing between these disturbances with the timing wave indicates the speed of rotation. It will be noted that while the revolving coil registers exactly two cycles per revolution the stationary coil registers three cycles per revolution. This indicates a 2-node forward wave which was developed in this special case.

From the ratio of these frequencies per revolution information is obtained of what is going on at the time the oscillogram is taken. A backward wave would have registered two cycles per revolution of the revolving coil and one cycle per revolution on the stationary coil. In this case caution must be exercised to note that the one cycle per revolution would develop at the same time as the two cycles per revolution on the revolving coil, since the ordinary autograph of a non-vibrating wheel might appear to register one per revolution at any speed, whereas a true backward wave would appear only at the instant of the vibration developing.

Minor Resonant Speeds

It is possible to excite and record minor resonant speeds for other nodal systems.

From a consideration of the equation of the 2-node minor resonant speed as well as the major resonant speed called critical speed, it can be shown for two nodes (and it also is true for other nodes) that some of the resonant conditions do not occur. The critical speed, if one exists, occurs at a speed given by equation (15)

$$N_s = \frac{f_s}{\sqrt{(\frac{1}{2}n)^2 - B}}$$

For 2 nodes $(\frac{1}{2}n)^2 = 1$ and the radical becomes $\sqrt{1-B}$. Now in the case of turbine wheels if $B > 1$, N_s is imaginary, namely, the 2-node backward-wave frequency line never intersects the zero line. There is, then, no critical speed for 2-node vibration. The danger from two nodes, if present, would be expected to occur at the minor resonant speed. The equations for first minor resonant speeds for any system are found as follows:

Referring to Fig. 92 it will be seen that the running frequency for a minor resonant speed is

$$f_r = N_s + \frac{1}{2}nN_s$$

Substituting in equation (5)

$$N_s + \frac{1}{2}nN_s = \sqrt{f_s^2 + BN_s^2}$$

Solving for N_s

$$N_s = \frac{f_s}{\sqrt{(1 + \frac{1}{2}n)^2 - B}} \qquad (16)$$

The equations for determining the first *sub-minor* resonant speed, indicated as the speed where the backward wave frequency line intersects the 1-cycle per revolution line below the zero frequency line is derived as follows:

$$\frac{1}{2}nN_s - N_s = \sqrt{f_s^2 + BN_s^2}$$

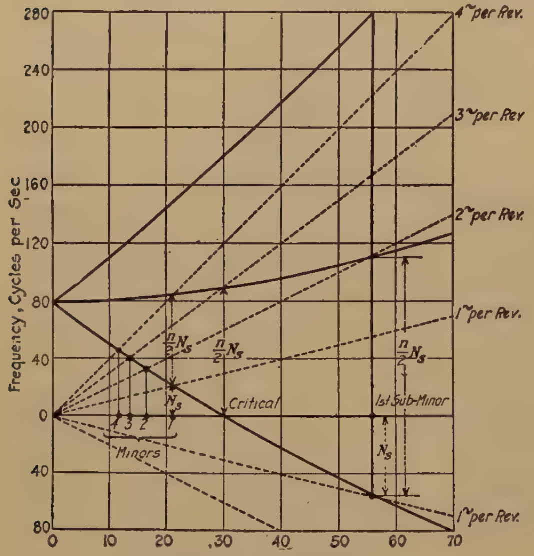

Fig. 92. Frequency-speed Diagram Showing Minor, Critical, and Sub-minor Resonant Speeds

Referring to Fig. 92,

$$\tfrac{1}{2}nN_s - N_s = \sqrt{f_s^2 + BN_s^2}$$

The first sub-minor resonant speed then equals

$$N_s = \frac{f_s}{\sqrt{(\tfrac{1}{2}n-1)^2 - B}} \qquad (17)$$

The second and third minor and sub-minor resonant speeds can be determined in a similar manner, the point of intersection in these cases being the 2-cycle and 3-cycle per revolution lines, respectively.

From the formulas in Table IV the various resonant speeds can be calculated when the standing frequency f_s and the speed coefficient B are known for the particular number of nodes n.

From the similarity of these formulas it will be noted that assuming the standing frequencies and speed coefficients to be constant, a speed which is critical for one nodal type is resonant as a first minor for the next smaller number of nodes and as a first sub-minor for the next larger number of nodes. Thus in order to appreciate this similarity, suppose that the standing frequencies and speed coefficients are the same. It will be seen that the 6-node critical speed is also resonant for a 4-node first minor and a 2-node second minor on the one hand, and also for an 8-node first sub-minor and a 10-node second sub-minor on the other hand.

From the fact that the speed coefficient B is always greater than unity it is easily shown that there are no 2-node critical or sub-minor resonances, nor any 4-node sub-minor resonances, etc., as indicated by the blank spaces in the table.

Fig. 93 is used for the rapid solution of all these formulas. The vertical scale represents the standing frequency f_s in cycles per second. The horizontal scale marked critical speed both in r.p.m. and r.p.s. is also used to determine the other resonant speeds. The diagonal lines, which are grouped for the different nodal systems, are also marked for various values of the speed coefficient B. The lowest group marked two cycles per revolution is made first for the 4-node critical speed, the two cycles per revolution meaning that two complete cycles would be recorded on the revolving coil in the wheel-testing machine. The three cycles per revolution group is for the 6-node critical speed, the four cycles per revolution for eight nodes, and so on. However, as already referred to, since the 2-node first minor resonance is represented by the same formula as the 4-node critical speed the lowest group is also used for determining the 2-node minor resonant speed. Similarly, the three cycles

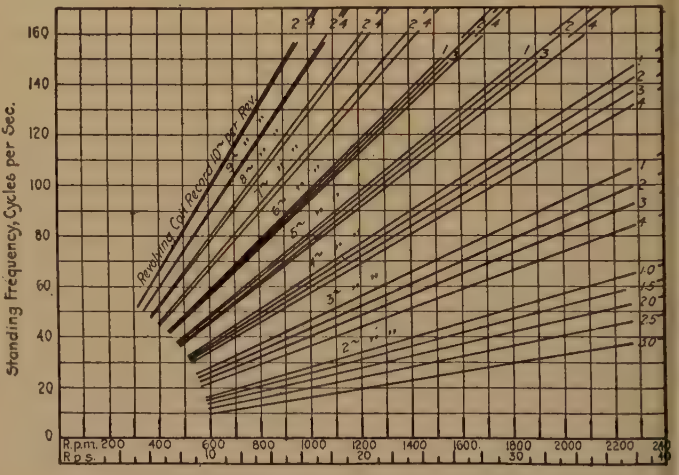

Fig. 93. The Critical-speed Chart. This is used also for the rapid determination of minor resonant speeds

per revolution group is used for the 4-node first minor and the four cycles per revolution group for the 6-node first minor, and so on. The group below any particular group of diagonal lines is used to determine the sub-minor critical speed for the same particular number of nodes.

For example, assuming a wheel with a 4-node standing frequency equal to 50 cycles per second, and with the speed coefficient 2, the major resonant or critical speed will then be at 35.5 r.p.s. For 6 nodes with standing frequency at 57.0 the critical speed would occur at 21.5 r.p.s. For 8 nodes at 75 and the speed coefficient of 2 the critical speed would be at 20 r.p.s.

The corresponding first minors will be found in the next higher groups than the critical and the first sub-minors in the next lower group. For example, consider another case where the 6-node standing frequency is 50 cycles per second with a speed coefficient of 2. The 6-node first minor resonant speed will then be 13.4 r.p.s., the 6-node critical speed would be 18.9 r.p.s., and the 6-node first sub-minor resonant speed would be 35.5 r.p.s.

TABLE IV

FORMULAS FOR RESONANT SPEEDS

		NODES				
		2	4	6	8	10
3rd Minor Resonance........	$N_{S_3} = \frac{f_S}{\sqrt{\left(3+\frac{n}{2}\right)^2-B}}$	$\frac{f_S}{\sqrt{16-B}}$	$\frac{f_S}{\sqrt{25-B}}$	$\frac{f_S}{\sqrt{36-B}}$	$\frac{f_S}{\sqrt{49-B}}$	$\frac{f_S}{\sqrt{64-B}}$
2nd Minor Resonance........	$N_{S_2} = \frac{f_S}{\sqrt{\left(2+\frac{n}{2}\right)^2-B}}$	$\frac{f_S}{\sqrt{9-B}}$	$\frac{f_S}{\sqrt{16-B}}$	$\frac{f_S}{\sqrt{25-B}}$	$\frac{f_S}{\sqrt{36-B}}$	$\frac{f_S}{\sqrt{49-B}}$
1st Minor Resonance........	$N_{S_1} = \frac{f_S}{\sqrt{\left(1+\frac{n}{2}\right)^2-B}}$	$\frac{f_S}{\sqrt{4-B}}$	$\frac{f_S}{\sqrt{9-B}}$	$\frac{f_S}{\sqrt{16-B}}$	$\frac{f_S}{\sqrt{25-B}}$	$\frac{f_S}{\sqrt{36-B}}$
Critical Speed...............	$N_S = \frac{f_S}{\sqrt{\left(\frac{n}{2}\right)^2-B}}$		$\frac{f_S}{\sqrt{4-B}}$	$\frac{f_S}{\sqrt{9-B}}$	$\frac{f_S}{\sqrt{16-B}}$	$\frac{f_S}{\sqrt{25-B}}$
1st Sub-Minor Resonance....	$N_{SA} = \frac{f_S}{\sqrt{\left(\frac{n}{2}-1\right)^2-B}}$			$\frac{f_S}{\sqrt{4-B}}$	$\frac{f_S}{\sqrt{9-B}}$	$\frac{f_S}{\sqrt{16-B}}$
2nd Sub-Minor Resonance....	$N_{SB} = \frac{f_S}{\sqrt{\left(\frac{n}{2}-2\right)^2-B}}$				$\frac{f_S}{\sqrt{4-B}}$	$\frac{f_S}{\sqrt{9-B}}$
3rd Sub-Minor Resonance....	$N_{SC} = \frac{f_S}{\sqrt{\left(\frac{n}{2}-3\right)^2-B}}$					$\frac{f_S}{\sqrt{4-B}}$

Interpretation of Films

Table V contains the information necessary to determine quickly the particular type of possible resonant speed occurring at the time of making the oscillograms during test in the wheel-testing machine. The number in the upper left-hand corner represents the number of cycles per revolution recorded on the revolving coil. In the lower right-hand corner are two numbers; the upper is that recorded on the stationary coil if a forward wave in the wheel is occurring, while the lower number is that on the same coil registered by a backward-traveling wave in the wheel. The backward wave in all minors always travels in a direction in space opposite to that of the wheel itself, while in all sub-minors it travels in space at a lower speed but in the same direction as the wheel. As an additional precaution, the standing frequency is computed from the running frequency and an estimated speed coefficient. Agreement with the measured standing frequency then forms a check on the particular type of resonant speed recorded and removes any ambiguity of the table.

Although little trouble is attributed to minor resonant speeds in general, the subject has been gone into here for the purpose of showing the reasoning used in locating a critical speed far above running speed when it is impossible safely to run the wheel so far above its operating speed. Minor resonant speeds are thus used to get the information necessary for the accurate determination of critical speeds when such speeds cannot safely be attained.

Tests of Wheels Already Installed and Operating

At an early stage of the investigation and as soon as sufficient evidence had been established as to the principal cause for turbine disk troubles, a program was worked out in order immediately to determine the condition of turbines already in operation. This work was taken up energetically, the machines were opened, and the natural periods of the wheels obtained.

For convenience in vibrating the wheels of turbines already installed, portable vibrating machines were used. The first device was operated electrically and was similar to that shown in Fig. 46.

A much more convenient device was later devised to be operated by compressed air. Fig. 94 shows this complete. The long connecting rod is provided with a clamping screw for temporary connection to the wheel shroud band. The opposite end of the rod is provided with a clevis, the lugs of which straddle a vertical lever. The lower end of the lever extends into a small block which is restrained by adjustable laminated springs. The upper end of this lever is connected by a crank to a ball-bearing eccentric shaft, which carries a ratchet-type wheel. Under some conditions the block is vibrated by the lever and at other times the block remains stationary, or practically so and forms a pivotal support for the lever as will be seen later.

The ratchet wheel serves as an air turbine and is driven by compressed air from a nozzle. Changes of speed are brought about by regulation of the air valve.

The driving shaft is carried in ball bearings. One end of the shaft has a worm, which meshes with a worm wheel, driving an electric generator forming part of an electric tachometer. A flexible rubber coupling is provided between the worm-wheel shaft and the generator. The generator is clamped in felt to absorb vibration. Current from the generator is supplied to a voltmeter which is calibrated in terms of r.p.m., and by means of which the speed of the driving motor, and hence the frequency of vibrations imparted to the turbine wheel, can be ascertained.

The operation of the vibrator is as follows: After supporting the device in such a manner as to provide for attaching the connecting rod to the shroud band of the turbine wheel, compressed air is admitted to the motor, causing rotation and actuating the vibrator or lever. At the start the tension of the leaf springs is purposely made comparatively light. The adjustment of the springs is made by moving the spring supporting block to and from the lever block. The lever vibrates about the pivotal connection to the connecting rod as an axis. Until a speed corresponding to a natural resonance of the turbine wheel is reached the connecting-rod pivot of the lever continues to act as a fulcrum. However, when a resonant speed is reached, an amplitude is built up in the bucket wheel allowing this pivotal point to vibrate back and forth. At the same time, the lower end of the lever quickly ceases to vibrate, and practically all the energy is transferred through the connecting rod.

TABLE V

FOR INTERPRETATION OF FILMS

Nodes	3rd. Minor	2nd. Minor	1st. Minor	Critical	1st. Sub Minor	2nd. Sub Minor	3rd. Sub Minor	Nodes
2	4 5 3	3 4 2	2 3 1					2
4	5 7 3	4 6 2	3 5 1	2 4 0				4
6	6 9 3	5 8 2	4 7 1	3 6 0	2 5 1			6
8	7 11 3	6 10 2	5 9 1	4 8 0	3 7 1	2 6 2		8
10	8 13 3	7 12 2	6 11 1	5 10 0	4 9 1	3 8 2	2 7 3	10

Key-Numbers are Cycles per Revolution

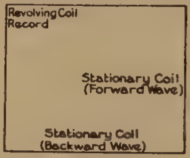
Revolving Coil Record
Stationary Coil (Forward Wave)
Stationary Coil (Backward Wave)

Example: A Combination of 3 Cycles per Revolution on the Revolving Coil and 5 on the Stationary Coil Represents a 4 Node 1st. Minor, Forward Wave.

The operator either by sense of touch or observation determines the number of nodal points practically at rest in the circumference of the wheel and this, together with the frequency of the applied force, is recorded.

It is often necessary, in order to build up an amplitude sufficiently large to obtain trustworthy observations, to increase the applied air pressure after having somewhat increased the spring tension. As the mass of the turbine wheel to be vibrated is great, and the energy of the vibrator is small, it is difficult to change the speed from one natural frequency of the wheel to another by merely changing the air supply to the motor, and therefore a method commonly employed is to release the spring tension on the block until such time as the turbine wheel comes to rest or practically so. The motor is then operated at a gradually increasing speed, and at the same time the tension is increased somewhat on the spring; the increase of speed is arrested automatically when the next higher natural frequency is reached. The former procedure is then gone through again and this process is repeated until all of the required frequencies have been determined.

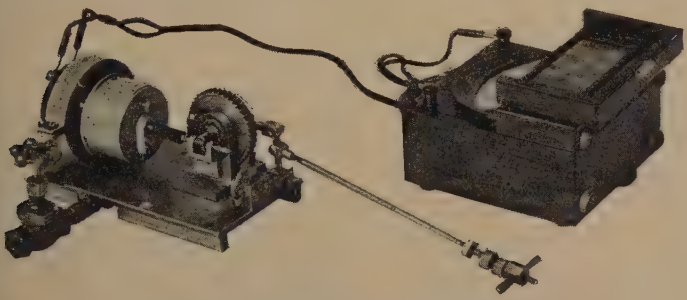

Fig. 94. Portable Compressed-air-driven Vibrator for Determining Standing Frequencies of Turbine Wheels
(Note the worm-gear speed reduction for electric tachometer.)

From the information thus obtained curves are made for each machine showing at what speed it might be possible for each individual wheel to give trouble. Over 1600 wheels were vibrated in this manner and reference to Table I will give an idea of the scope of this work.

Safe Design

To insure safe operation of turbine wheels, it is essential that all the wheels in a turbine rotor without exception shall be free from critical speeds within dangerous proximity to the operating speed of the rotor.

The chart of Fig. 93 is used for the rapid determination of the critical speed when the standing frequency for each particular nodal system is known together with a satisfactory speed coefficient *B*. After the various critical speeds have been determined in this manner, they are plotted on curves as shown in Fig. 95.

This diagram is for a 22-stage steam turbine. The horizontal scale represents revolutions per minute of the turbine rotor. The vertical scale represents wheels in the different stages of the rotor. In the diagram, the 13 largest wheels are the only ones indicated, the critical speeds corresponding to 4, 6 and 8 nodes being shown for each. These critical speeds are indicated in the diagram by circles, squares, and triangles respectively. It will be observed that some critical speeds occur close to the operating speed. Thus the wheels of stages 15, 16, and 17 all have critical speeds corresponding both to six and eight nodes occurring close to the operating speed, whereas stages 19, 20, 21, and 22 all have critical speeds corresponding to four nodes close to the operating speed. This diagram serves to indicate those stages whose critical speeds occur so close to running speed that, on account of the known variations of running speed, breadth of resonance, etc., the danger of stationary wave development cannot definitely be said not to exist. Figs. 96 and 97 are for machines especially designed to avoid wave development. It will be observed that there are no critical speeds in either case within 15 per cent of the operating speed. In Fig. 96 stages 16 and 17 have critical speeds below the operating speed, but Fig. 97 shows all critical speeds above the operating speed. The latter case is of course preferable where possible of attainment. In the case of stages 16 and 17 of Fig. 96, it was not possible to design wheels having 6 or 8 nodes above the operating speed, therefore care is necessary in the design to provide as large an interval as possible between the 4- and 6-node critical speeds.

Safe Limits

In determining the safe limits which should exist between the normal operating speed of the rotor and the speeds at which dangerous wave phenomena develop a number of considerations are involved. In the first place a certain broadness of resonance exists, throughout which vibration may develop. That is to say, wave phenomena do not occur with precise mathematical accuracy at exactly a particular speed, but may occur at speeds slightly above or slightly below the speed corresponding to the condition of maximum resonance. Special tests have shown that this broadness of resonance amounts to about two per cent above and below the critical speed.

Another factor, to be considered in determining safe limits between the operating speed and the calculated critical speed, is the uncertainty in the numerical speed coefficient *B*. This coefficient serves to determine the running frequency of the turbine wheel when the actual standing frequency is known. During the process of design, the errors which may occur in applying this coefficient to wheels similar to those that have been tested must also be allowed for. Another consideration is the possible variation of the line frequency on which the turbine is to be operated. Temperature variations must also be covered.

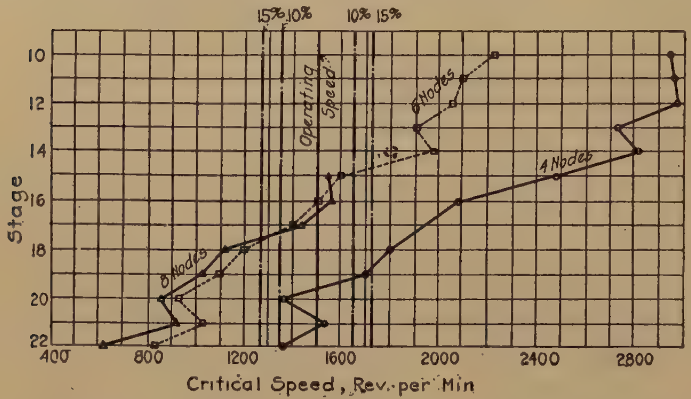

Fig. 95. Critical-speed Diagram for an Old-design 22-stage Turbine

(Stages 15, 16, 17, 19, 20, 21, 22 all have critical speeds separated from running speed by insufficient margins.)

For these effects 10 per cent above and below the operating speed is recommended for six and eight nodes, and 15 per cent for the 4-node condition. These limits have been rigidly adhered to for some time, with apparently sufficient justification. Furthermore, wheels are not passed for use that have 10-node, 12-node, etc, critical speeds near the operating speed. Such wheels are corrected by tuning. The same precautions are also taken for possible minor resonant speeds.

Tuning

Tuning is resorted to where necessary for the purpose of altering the natural frequencies and is carried out as follows:

In proportioning or in *tuning* a wheel to obtain the desired margins between the critical speeds of the wheel and the normal operating speed, the relations between the stiffness and the mass of the parts of the wheel must be made such as to give the desired natural frequencies of vibration in the wheel. In general it may be stated that in a vibrating system, such as a turbine disk, the frequencies of vibration increase with the stiffness of the wheel but decrease with the increase in mass of the wheel. This may be inferred from equation (1) for a particle

$$f_s=\frac{1}{2\pi}\sqrt{\frac{R_s}{m}}$$

where R_s equals stiffness and m equals the mass of the vibrating particle. In designing the wheel this relation is borne in mind, since nodal frequencies of different numbers of nodes correspond to bending actions or flexures extending into the body of the wheel toward its center to greater or less degrees. Depending on the number of nodes, changes in the wheel between stiffness and mass may be expected to affect to different degrees, frequencies corresponding to different numbers of nodes. In order, therefore, for the wheel to be free from dangerous critical speeds, a proper coördination between the stiffness and mass of different portions of the wheel should exist.

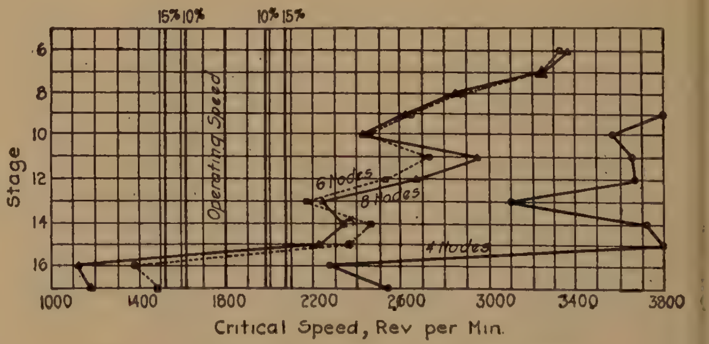

Fig. 96. Critical-speed Diagram for 17-stage Turbine

(This machine is designed to avoid development of vibration. All critical speeds fall outside the prescribed margins.)

Whenever there is reason to suppose that any wheel may have a critical speed within the limits set, the completely bucketed wheel is first vibrated off of the shaft and the probable critical speeds thereby determined. For the purpose of noting nodal segments during vibration, the wheel may be covered with a thin sheet of water. When the wheel is in vibration, the surface of the water exhibits rough or ripple areas conforming to vibration areas of the wheel. Water is preferred to sand for the purpose of getting immediate results. If a calculation made with a value of the speed coefficient determined for wheels of similar shape in the wheel-testing machine indicates a critical speed within the danger limits, the wheel is then placed upon its own shaft and vibrated again to determine more exactly the critical speeds as altered by the wheel fit on the shaft. Should the previous estimates be verified, then tuning is resorted to.

The tuning or reproportioning of the wheel may be done in a variety of ways depending upon the number of nodes and the frequency which it is desired to change. The previous experience and recorded data are found exceedingly helpful in facilitating this work.

Suppose, for example, the case of a 22nd stage wheel with buckets 28 in. long and a disk diameter of 7½ ft., which upon being vibrated is found to have the 4-node critical speed approximately 8 per cent above the operating speed, and the critical speeds corresponding to six and eight nodes well outside the lower 10 per cent limit for these critical speeds. In this case it is necessary to raise the 4-node frequency to 15 per cent or more above the operating speed. This is done by removing the necessary amount of weight from the buckets. Temporarily attaching known weights to the shroud band of the wheel approximately indicates the effect of bucket weight on the frequencies of the wheel. From these data the necessary amount of weight to be removed from the buckets is determined. Of course it is necessary to remove the buckets from the wheel in order to machine off metal which is taken from the backs of the buckets.

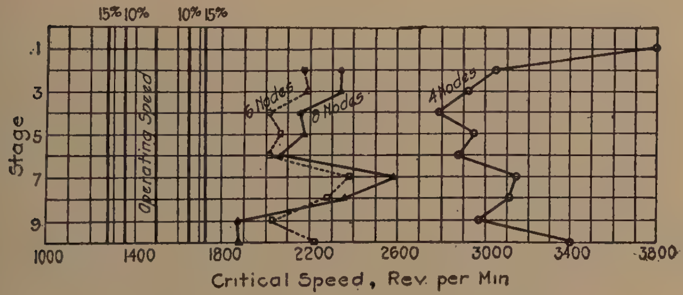

Fig. 97. **Critical-speed Diagram for 10-stage Turbine**

(This machine is designed to avoid development of vibration. All critical speeds are above the prescribed margins.)

Removal of weight from the outer or convex portion of the buckets is illustrated in Fig. 98 as indicated by the dotted lines. This remedy however is very rarely resorted to, as attempts are always made to insure a 4-node critical speed occurring well above the 15 per cent limit.

Removing weight from the buckets in this manner results in a reduction of the mass without any appreciable effect on the stiffness, resulting in raising the frequency of the complete wheel.

As another illustration, consider a wheel with buckets 11½ in. long and with a disk diameter of 6 ft., but let it be supposed that the vibration tests show the existence of the 6-node critical speed about 3 per cent above the operating speed and the 8-node critical speed about 4 per cent below the operating speed, the 4-node critical speed occurring about 25 per cent above the operating speed. In this case, the 6-node and 8-node critical speeds may be lowered by removal of material from the wheel at a suitable point, but this must be done in such a way that the 4-node critical speed will not at the same time be lowered so far as to come within the danger limit of 15 per cent. This means that the 6-node critical speed must be brought to a point at least 10 per cent below the operating speed, the 8-node critical speed lowered from 4 per cent to 10 per cent below the running speed, and all of these without lowering the 4-node critical speed by more than 10 per cent. In a case like this, great care must be taken to cut the wheel in the location which will most affect the critical speed which it is desired to change. Thus in the one under consideration, alterations in the web of the wheel next to the rim circumference have the greatest effect on the 8-node and 6-node frequency, while in the zone nearest the center of the wheel the removal of the material from the web has its greatest effect on the 4-node frequency.

For adjusting the 6- and 8-node frequency the wheel is then placed on the boring mill and slightly machined in the zone extending from 6 to 8 in. inwardly from the rim. The wheel is then vibrated and the change in frequency noted. The operations are repeated until the desired frequencies are obtained. It is not passed however until it has received a running test in the wheel-testing machine or has shown by tests on its own shaft that the desired results have been obtained.

Fig. 99 at *A* is a profile of the turbine wheel. Dotted lines indicate where metal has been removed from the outside portion of the web of the wheel. The removal of metal from this region affects mostly the frequencies corresponding to six or eight nodes but has little effect upon the frequency corresponding to four nodes. Fig. 99 at *B* shows by dotted lines the location having most effect on the 4-node frequency.

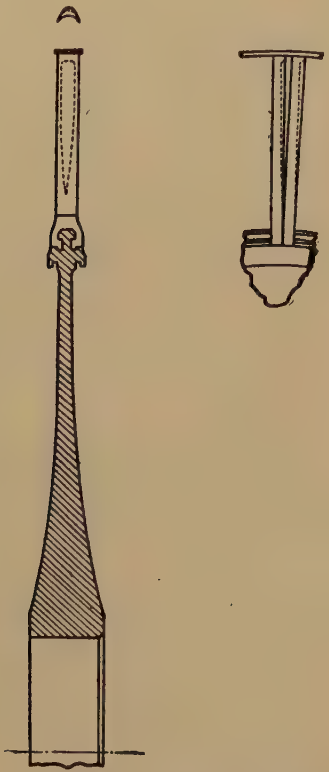

Fig. 98. Methods of Tuning

(Frequency may be raised by removing weight from the buckets as shown.)

Summary of Procedure for the Production of a Turbine Wheel

The principles and theory of bucket-wheel vibration and the methods of testing have been explained and described. In conclusion it remains to summarize the protective measures utilized in the ordinary process of production in order to assure the safety of turbine wheels.

The first step is to design the bucket in accordance with the thermodynamic requirements, select the dovetail suited to the bucket and thus fix upon the design of wheel rim.

The second step is to select the general dimensions and contour of the wheel with a view to vibration characteristics. For this, reference is made to records of wheels of like bucket design and diameter. There are two complete catalogs showing the complete vibration characteristics of all wheels so far tested. In one catalog the wheels are listed according to dimension and this is used for design purposes. In the other the wheels are catalogued by machines and this is useful in tracing the record of any particular turbine or wheel.

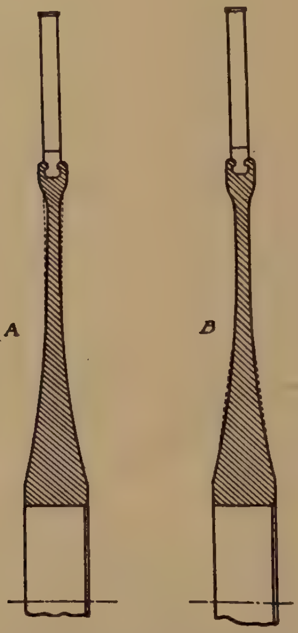

Fig. 99. Methods of Tuning

(Removal of weight from the outer web, as shown at *A*, affects mainly the 6- and 8-node frequencies. Removal of weight from the inner web, as shown at *B*, affects mainly the 4-node frequency.)

The third step is the calculation of the stresses due to centrifugal force and the completion of the details in a satisfactory manner.

The fourth step is a review of the resulting design on two bases. The stresses must be satisfactory and the wheel design must suit the space and clearance requirements of the turbine assembly. Either one of these check inspections may serve to condemn the design and require a new start from the beginning.

The fifth step is the selection and assignment of a forging. It should be understood that every forging is examined for its strength properties by means of coupons and for its uniformity by a magnetic survey of its entire structure. A complete record of every forging is kept by serial number, and the assignment of a forging is a separate step in the process. Any deviation in the shop, from the drawing, however slight, that does not result in the destruction of the forging, is placed on record by a new drawing.

The sixth step is the standing vibration survey of the finished wheel to make sure that it does not deviate more than an allowable amount from the original expectations. If all the resonant speeds, including both the critical and the various minor resonant speeds do not have the required margins from running speed, tuning is resorted to. Generally one or two trials are sufficient to obtain by tuning the required vibration characteristics but occasionally a wheel has to be altered five or six times. This process of course necessitates a revision of the drawing and a corresponding alteration of all the records involved.

In some cases the standing vibration test confirms the predictions from the catalogs of similar wheels for which satisfactory speed coefficients have been determined in the wheel-testing machine. Such wheels may be accepted as having satisfactory margins on the basis of the standing vibration test alone. But in the majority of all cases each wheel receives a complete running test in a wheel-testing machine.

The seventh step is the complete running vibration test in the wheel-testing machine. From 30 to 60 oscillograph films are taken showing exactly all phases of the wheel's behavior under running conditions. These films are all examined and those of value are indexed and filed. About 18,000 such records have been taken, and, of this great number, about one-third are preserved and available for quick reference at the present time.

The final result is a wheel which is either satisfactory and thoroughly protected from the possibility of resonant vibration, or else the wheel is rejected and a new design started through the necessary seven steps toward a final acceptance.

It will be readily appreciated that this thoroughness of examination and verification of predicted properties is at the basis of the remarkable freedom from vibrational troubles exhibited in the behavior of recently built turbines.

1500-volt Direct-current Electric Railway Installation of the Kobe-Himeji Railway Co., Kobe, Japan

By M. Takagi
Chief Engineer, Kobe-Himeji Electric Railway Co.

This article is of noteworthy interest because it describes the first electrification in Japan to utilize 1500-volt interurban cars, as distinct from locomotive drawn trains. The installation included seventy-two 750/1500-volt motors, eighteen sets of pneumatic-cam control equipments and as many air brake equipments, together with the necessary cars, substation, and line material. The author's satisfaction with the 1500-volt direct-current electrification is very evident, and is particularly pleasing to us because he credits the article "High-voltage Direct-current Railway Installations in the United States and Canada," by W. D. Bearce, General Electric Review, April, 1920, as having been of much assistance to Japanese engineers.—Editor.

In Japan, high-voltage electrification was first started in 1915 by the Imperial Government Railways with 1200 volts direct current between Tokio and Yokohama, a distance of 20 miles. Following the uniformly satisfactory operation of the 1200-volt service between Tokio and Yokohama, the Imperial Government Railways began work on the electrification of the main line of the Tokaido Division employing 1500 volts direct current.

In 1921 the Chichibu Railway Company electrified 29.6 miles of its line, and in 1923 the Aume Railway Company also electrified its 14-mile line, both with 1200 volts direct current. In 1923 the Osaka Railway Company started work on its 19.3 miles, and the Yoro Railway Company on its 35.8 miles with 1500 volts direct current. Our Kobe-Himeji Electric Railway Company also completed its new 24.4-mile line in August, 1923, also with 1500 volts direct current, which construction will briefly be described in this article.

M. TAKAGI

The entire route in sight is between Kobe and Himeji which are 35.5 miles apart, of which 24.4 miles between Akashi and Himeji are completed. The line between Kobe and Akashi is expected to be completed rather shortly. The entire route is shown in Fig. 1.

Although Akashi and Himeji are rather small cities, both located west of Kobe, the line runs close to the most beautiful and famous inland seacoast and attracts a large number of passengers including also seekers of the historical remains in that vicinity. It has become a genuine asset to the people along the coast who have long been in want of handy means of communication. The view along the route includes four bridges and two tunnels. The main civil work, wherever necessary, was executed by reinforced concrete.

The rolling stock consists of 15 motor passenger cars, 3 motor freight cars, and 10 freight wagons. Each passenger car (Fig. 2) has an overall length of 45 feet 8 inches and outside

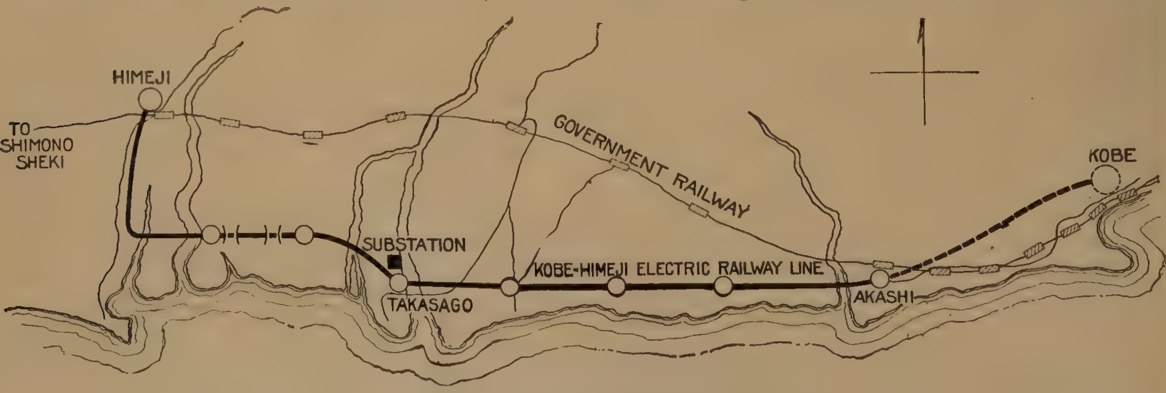

Fig. 1. Map of the Kobe Himeji Electric Railway

width of 8 feet 6 inches with seating capacity for 44 and weighs about 58,000 lb. when empty. Each of the 18 motor cars is equipped with four GE263-A, 65-h.p., 750/1500-volt motors; multiple-unit PC control equipment; straight air brakes with emergency features; CP-29, 27 cu. ft. per min. compressor; and car lighting equipment.

The entire line is served by one substation, an outside view of which is shown in Fig. 4.

The power supply is obtained from the Sanyo Chuo Hydro Electric Company and the Sanyo Water Power Company at 22,000 volts, 60 cycles, 3 phase.

The overhead construction is of the cross-suspension and single-catenary suspension type as shown in Fig. 3. The trolley wire is of BS No. 0000 grooved copper, the messenger being $\frac{7}{16}$ in. steel stranded wire.

The pole span is 150 ft. on tangent, and 120 ft. as well as 90 ft. on curves. The hanger spacing is 15 ft. throughout. The poles employed are mostly of structural angle iron, but in some sections wooden poles of white cedar are used.

The feeder is a 500,000 cir. mil. stranded copper cable, supplemented by another of like size near the substation.

The track gauge is standard (4 ft. 8½ in.), double track with 60-lb. rails, bonded with BS No. 0000 compressed terminal bonds. The ties are of Japanese chestnut but those used for joints and crossings are of red-wood.

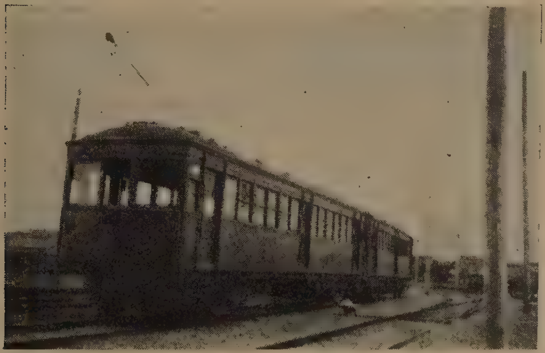

Fig. 2. Multiple-unit Passenger Train on the K.H.E. Ry. All the car bodies are of local make

The automatic signal equipments are of local make. At each stop electro-mechanical interlocking devices are now being installed.

The traction service is 54 round trips daily, of which 45 are local services, each requiring 65 minutes one way, making 23 stops; and 9 express services, each requiring 45 minutes, making 6 stops.

The power consumption is estimated at 2.2 kw-hr. per car-mile at the direct-current feeder panel.

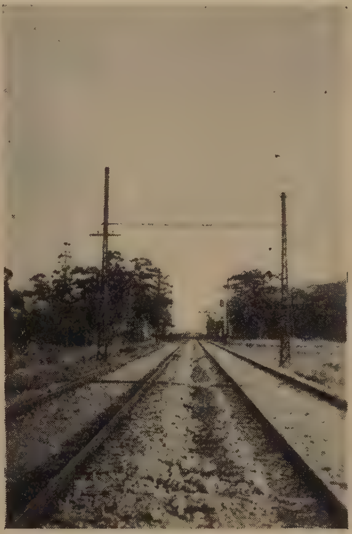

Fig. 3. A Tangent Section of the Line

In Japan the Kobe-Himeji system may be said to be the pioneer to adopt PC control equipments for 1500 volts direct-current. On account of their simple, dependable, and satisfactory automatic features, the training of a motor man is very easy. A non-informed amateur is so easily taught in a short time to become a perfect motorman that he is held entirely responsible for the transportation of the public.

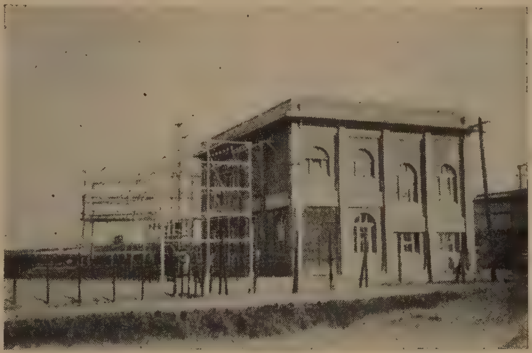

Fig. 4. Substation Located at Takasago. Its equipment includes two 1500-kw., 60-cycle, 750-volt synchronous converters permanently connected in series, and a high-speed circuit breaker connected between the negative bus of the converter set and ground

For car lighting, the GE-RVG motor-generator sets were adopted because they are practically unaffected by the voltage drop of the trolley wire. The passengers can thus enjoy a congenial trip in the evening.

The author is entirely satisfied with the 1500-volt system as adopted, the good service of which has been made possible by the entire dependability of the equipment. He does not hesitate to advocate and prophesy the larger use of this 1500-volt direct-current railway system wherever the mileage is found suitable for that voltage.

Studies of Electric Discharges in Gases at Low Pressures

PART II

TYPICAL EXPERIMENTAL DATA ILLUSTRATING THE USE OF PLANE COLLECTORS

By Dr. Irving Langmuir and Harold Mott-Smith, Jr.
Research Laboratory, General Electric Company

This series of articles reports an investigation in which new methods of using collecting electrodes were applied to the determination of the complicated discharge phenomena that take place in an atmosphere of low gas pressure, such as in the mercury arc rectifier. In our last issue, Part I dealt with the theory of plane, cylindrical, and spherical collectors in retarding and accelerating fields. The present installment reports various experimental data obtained with plane electrodes, and includes a discussion of the visual observation of sheaths.—Editor.

The electrode H in the mercury arc tube shown in Fig. 3 consisted of a square nickel plate 1.90 cm. on a side which was bent into a cylindrical surface to conform to the inner surface of the glass tube (3.2 cm. inside diameter). The lower part of the apparatus was immersed in the water of a thermostat at 60 deg. C. and care was taken to maintain the remainder of the tube at a temperature above 60 deg. C. to avoid condensation of mercury vapor. The pressure of mercury vapor was therefore 33 bars. The current-voltage curve given in Fig. 4 was obtained while a current of 6.0 amp. was flowing to the anode A and the sum of the electron currents flowing to H and B was kept constant at 2.0 amp. With this nearly plane electrode the flat portions of the curve corresponding to the positive ion and electron saturation currents are particularly marked. As the potential of the collector[7] was changed from -80 to -20 (measured from the anode) the current i_H changed only from -2.87 to -2.44 ma.

In this range the current is a positive ion current which is limited by the rate at which ions reach the edge of the sheath.

Between -20 and -12 volts the current increases rapidly owing to the electrons taken up because of their proper velocities. The current finally becomes saturated again when the collector is at a positive potential with respect to the space so that it gathers all the electrons which reach the sheath. At a still higher voltage ($E_H=-5$) ionization by collision within the sheath becomes sufficient to neutralize the electron space charge so that the current can increase indefinitely. At this point a strong local glow sets in near the surface of the electrode, usually in the form of a diffuse ball-shaped glow.

At a potential $E_H=-17.8$ volts with respect to the anode, the current to the collector becomes zero, which merely means that it collects equal numbers of electrons and ions. From the shape of the curve between B and D, it is clear that the collector began to collect electrons near B and that if it had not been for these electrons the current would follow a curve such as BC. An analysis of the curve ABC will be made later. We may take the differences between the observed currents according to curve BD and those extrapolated along BC as representing the true electron currents i_e. The positive ion currents i_p as given by BC are very nearly equal to -2.5 ma., so the value of i_e is approximately $i_H+2.5$.

The values of i_e thus found may be plotted on semi-logarithmic paper against the collector potential E_H. In Fig. 1 a similar curve is obtained by plotting the logarithm of i_e against E_H, the upper of the two curves being taken from the data of Fig. 4 which we have just been discussing.

---

[7] For convenience we shall adopt the convention that the sign of a current is positive when positive current flows from the electrode into the space.

Over a range in the values of i_e in which they increase over 1000-fold, the points lie (within the experimental error) along a straight line whose slope is 0.549 volt^{-1}. It is more convenient to deal with the slope which we should have if we had plotted natural logarithms of i_e. We shall thus take the slope to be 2.303×0.549, or 1.26 volt^{-1}. By equation (6) this slope should be equal to $e/(kT)$. The value of e/k is 11,600 deg. per volt, so that the temperature T_e corresponding to the electron velocities is 9200 deg. K. The average kinetic energy of the electrons

$$\left(\frac{3}{2}\frac{kT}{e}\right)$$

expressed in equivalent voltage is 1.19 volts.

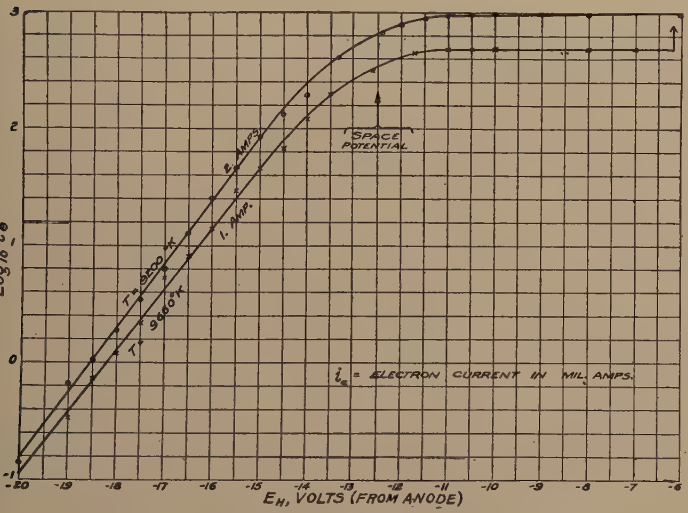

Fig. 1. Semi-logarithmic Plot of Current-voltage Curve for Collector H (*Repeated from Part I*)

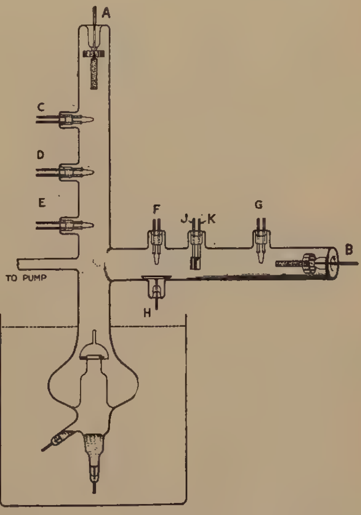

Fig. 3. Mercury Vapor Tube with Various Types of Collectors

The lower curve in Fig. 1 is made from data taken under exactly the same conditions as those for the upper curve, except that the sum of the currents to B and H was held at 1 amp. instead of 2. A change of two-fold in the current density in the arc thus has no appreciable effect on the electron-temperatures.

The straight line part of the upper curve in Fig. 1 extends only up to about $E_H = -15$ volts, and the curve then gradually becomes less steep, until at about -11 volts it becomes horizontal and straight again. From the theory which we have developed we should have expected the transition between the two straight portions to be sharp, a kink occurring when the collector is at the space potential. The case considered is one with an unusually long transition region.

The following causes tend to make the transition gradual:

(*1*) *Removal of Electrons by the Collector*

When the collector takes an electron current comparable with the current through the arc ($i_H + i_B$ being kept constant), the intensity of the arc between the collector H and the anode B decreases and the supply of positive ions which reach the neighborhood of H is decreased. This naturally causes a disturbance in the arc near H which may manifest itself by a decrease in the random electron current density I_e and also by a change in the potential distribution along the tube which may decrease the potential difference between the anode and the space near H, when the electron current to H increases. These effects cause the slope of the line to decrease when the current to the collector becomes appreciable in comparison with the current to the anode. In the upper curve of Fig. 1 the current to the collector reached a value of 1 amp., while the anode current was 2 amp. The curve only began to decrease appreciably in slope at about -14.5 volts where the current to H became about 7 per cent of the anode current.

(2) Variation of Current with Accelerating Fields due to change in sheath area or to orbital motion

We have already discussed how the current to cylindrical or spherical collectors varies with the accelerating potential because of changes in sheath area or orbital effects.

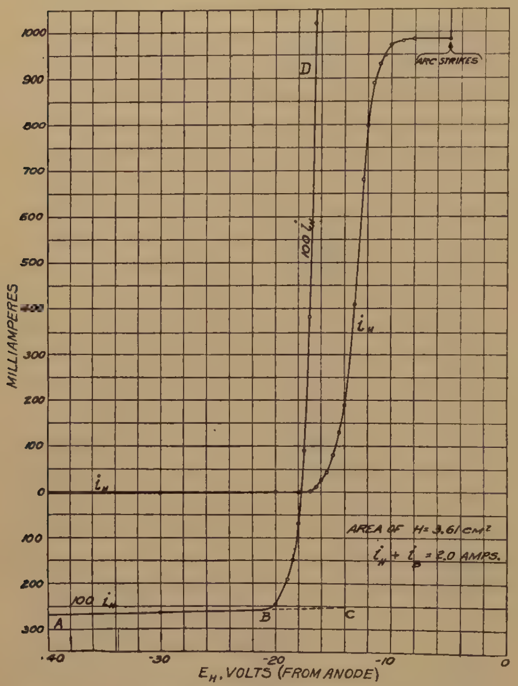

Fig. 4. A Typical Current-voltage Curve of Collector H

The resulting change in slope, although it occurs only when the collector is above the space potential, produces a transition curve which may be hard to distinguish from that discussed in the foregoing paragraphs. With plane collectors, although orbital effects are absent, there are edge corrections (to be analyzed below) which produce a gradual approach to the horizontal portion of the curve.

(3) Electron Reflection from Collector

If electrons are reflected or secondary electrons are emitted, these cause the current collected *with retarding fields* to be less than those calculated by equation (1). The reflection coefficient presumably varies with the velocities of the impinging electrons. With retarding fields, however, the velocity distribution and the average energy (2 kT) of the electrons striking the collector is governed by Maxwell's Law and is independent of the potential on the collector. Therefore a reflection of electrons from a collector does not prevent the semi-logarithmic plot of the current-voltage curve from being straight, nor does it alter the slope, but results merely in a parallel displacement. As soon as the collector is made positive with respect to the space, the velocity of the impinging electrons increases so the reflection coefficient may vary, but the reflected or secondary electrons produced are in general drawn back to the collector, so that the effect of the reflection is neutralized. The result is to steepen the semi-logarithmic plot at potentials slightly above the space potential.

Examination of semi-logarithmic plots, such as those in Fig. 1, allows an estimate of the space-potential around the collector to be made, but to do this the three factors mentioned should be kept in mind.

The curves illustrated in Fig. 1 thus indicate that the space potential near electrode H was -12.5 ± 1 volts with respect to the anode B.

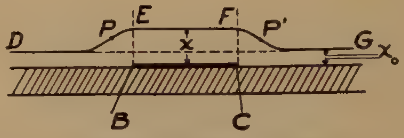

Fig. 5. Diagram of Positive Ion Sheath on a Plane Collector

The data from which the lower part (ABD) of the curves in Fig. 4 was plotted are given in the first and third columns of Table I. In the second column is the potential V of the collector with respect to the space near it, which is equal to $E_H + 12.5$.

For a plane collector of infinite extent the positive ion current should be independent of the potential. We see from Table I that the current increases slightly with the negative potential between 30 and 80 volts. This is due to an edge effect which should be taken into account for accurate determinations of the positive ion current density I_p.

Theory of Edge Corrections for Square and Circular Collectors

Consider a square collector with side equal to b, or a circular collector of diameter d, and let A_e be the effective area of the collector taking into account the edge corrections. There are two cases to consider: (1) where the collector is surrounded by the ionized gas or (2) where the collector is placed upon or flush with a non-conducting surface such as glass or mica. In the first case the surface of the sheath is approximately that of an oblate spheroid, while in the second case the sheath surface is like that represented by the line D E F G in Fig. 5.

TABLE I

Plane Positive Ion Collector H. Run 49-b. 2-amp. arc in tube 3.2 cm. diam. containing Hg vapor at 33 bars pressure. Square Collector 1.9 cm. on a side flush with surface of tube. $I_p = 0.71$ ma. cm.$^{-2}$

1	2	3	4	5	6	7
E_H	V	i_H ma.	ν	i_p ma.	i_e ma.	x cm.
−80.0	−67.5	−2.87	670.0	−2.874		0.060
−50.0	−37.5	−2.75	295.0	−2.744		0.040
−30.0	−17.5	−2.64	104.0	−2.643		0.024
−20.0	− 7.5	−2.44	34.0	−2.581	+0.14	0.014
−19.0	− 6.5	−1.90	28.1	−2.574	0.67	0.012
−18.5	− 6.0	−1.50	25.4	−2.570	1.07	0.012
−18.0	− 5.5	−0.68	22.8	−2.566	1.89	0.011
(−17.8)	− 5.3	(.00)	21.6	−2.564	2.56	0.011
−17.5	− 5.0	+0.91	20.0	−2.561	3.47	0.010
−17.0	− 4.5	+3.8	17.5	−2.557	6.36	0.010
(12.5)	0.0	(654.)	0.0	−2.499	656.	0.000

Let x_0 be the thickness of the positive ion sheath that exists over the glass surface (because of the negative charge on the glass) and let x be the sheath thickness over the central part of the collector. Ions which enter the sheath in the transition region between the sheath of thickness x_0 and that of thickness x will have velocity components parallel to the surface of the collector since they tend to move along the normal to the surface of the sheath. Thus all ions which enter the sheath between points P and P′ will reach the collector. As a reasonable approximation we may assume that the effect of this displacement of P from E is equivalent to an increase in the radius of a circular collector, or the semi-side of a square collector, by an amount equal to $\gamma(x-x_0)$ where γ is a numerical coefficient which cannot differ greatly from unity. We may thus place for a square collector

$$A_e = p\,[b+2\,\gamma\,(x-x_0)]^2 \qquad (49)$$

where $p=1$ if only one side of the collector is exposed, and $p=2$ if both sides are exposed.

For a circular collector

$$A_e = \frac{\pi}{4}\,p\,[d + 2\gamma\,(x-x_0)]^2 \qquad (50)$$

The values of x and x_0 may be calculated from equation (10). It is, however, more convenient to eliminate A_e from equations (49) and (50) by means of the relation

$$i = A_e I, \qquad (51)$$

and substitute into the resulting equation the value of x from equation (10). It is then found that $\sqrt{i}$ is a linear function of $\sqrt{\nu}$ and that the slope S of the straight line obtained by plotting $\sqrt{i}$ (i being in amperes) against $\sqrt{\nu}$ is given for square collectors by

$$S = 0.00306\,\gamma\,\sqrt{p}\,(m_e/m)^{1/4}. \qquad (52)$$

For circular collectors this equation needs to be modified only by altering the numerical factor to 0.00272. For mercury ions where $\sqrt{m/m_e} = 605$, equation (52) becomes

$$S = 1.24 \times 10^{-4}\gamma\,\sqrt{p}. \qquad (53)$$

It is interesting that the slope of this line comes out to be independent of the size of the electrode and of the intensity of ionization of the gas.

In the case of a collector lying on a nonconducting surface the method of determining the current density I will be seen from the example furnished by the data of Table I. The square-roots of the current i in amperes (1/1000 of the figures given in the third column) are plotted against the square-roots of ν given in the fourth column. The first three points, corresponding to a wide range of voltage, are found to lie accurately on a straight line of slope

$$S = 1.40 \times 10^{-4} \qquad (54)$$

Comparing this with equation (53) we find $\gamma = 1.14$ in accordance with our original assumption that this factor should have a value not far from unity.

From the straight line plot the values of $\sqrt{i}$ corresponding to each value of $\sqrt{\nu}$ obtainable from the fourth column may be read off and from these the values of i are found which are given in the fifth column, and are there denoted by i_p because they represent the positive ion component of the current. These values were used in plotting the dotted part BC of the curve in Fig. 4. It is seen that the calculated currents i_p for the first three points agree within the experimental error with the observed currents in the third column. The differences between i and i_p, which we may denote by i_e and which are given in the sixth column, represent the electron components of the current which flows against the retarding potential on the collector. These are the values of i_e which are plotted in the upper curve of Fig. 1.

When the collector is at such a potential that the current is zero (-17.8 volts in Table I) the potential must be the same as that of the glass walls, and therefore the sheath on the collector has the same thickness x as that on the walls x_0. The value of i_p corresponding to this voltage (-2.564 ma.) therefore gives the positive ion current corrected for edge effects. Dividing this by the area of the collector (3.61 cm^2) gives the positive ion current density

$$I_p = 0.71 \text{ ma. cm}^{-2}.$$

The last column of Table I gives the values of the sheath thickness x, calculated from the foregoing value of I_p by equation (10) which reduces to

$$x = 0.00233\sqrt{\nu}.$$

With a collector *surrounded* by ionized gas ($p=2$) the procedure for calculating I_p is essentially similar since equation (53) applies also to this case. The value of i_p used to calculate I_p is determined from the intercept of the curve of $\sqrt{i}$ against $\sqrt{\nu}$ on the $\sqrt{i}$ axis, that is, the value of i_p is chosen which corresponds to $V=0$. An illustration of data obtained with a disk-shaped collector surrounded by gas will be given in connection with another experiment.

The equations that have been derived are also applicable to the *electron* currents obtained with a plane collector. When the collector lies upon a non-conducting surface it follows from symmetry considerations that the edge correction becomes zero when the thickness of the electron sheath on the collector is the same as that of the positive ion sheath on the adjacent non-conducting surfaces. With the collector for positive ions that we have been considering, it was not possible to observe directly the ion current at a time when the sheath on the collector was of the same thickness as that on the adjacent surface, because the ion current was masked by electrons which moved against the retarding field. Therefore it was necessary to resort to a calculation of the ion current. But in the case of the positive collector the positive ions that reach it are wholly negligible as compared to the electrons, and to eliminate edge corrections it is therefore only necessary to observe the electron current when the collector is at a space potential which will give an electron sheath of the same thickness as that of the ion sheath on the adjacent surface.

From equation (10) we see that the condition that an electron sheath shall have the same thickness as the positive ion sheath x_0 is that ν for the electron collector shall be

$$\nu' = \frac{\nu_0 I_e}{I_p}\sqrt{\frac{m_e}{m_p}} \tag{55}$$

where ν_0 is the value of ν for a negatively charged collector at which the total current to it is zero. Because the current-voltage curve for the electron collector is comparatively flat in the region given by ν', very approximate values of I_e and I_p are usually sufficient. Thus in all the experiments with the collector H it was found that the positive potential equivalent to ν' ranged from 60 to 70 per cent of the negative potential V_0 corresponding to ν_0.

An analysis of typical data taken with collector H is contained in Table II.

The current-voltage data are taken from the run which is plotted in Fig. 4. The values of ν are calculated by equation (11) using $T=9200$ found from the curve of Fig. 1. The values of $\sqrt{\nu}$ in the third column were plotted against the square roots of i_H in the fourth column (expressed in amperes). The points corresponding to voltages (V) from 2.5 to 7.5 lay accurately along a straight line, but the points at lower voltages diverged considerably. The currents corresponding to the straight line for the various values of $\sqrt{\nu}$ are given in the fifth column. It is seen that the lower four observed values of i_H agree excellently with the calculated values while the first points show increasingly great divergences as we pass to lower voltages, so that when the collector is at the space potential it collects only about 72 per cent of the electrons impinging on it. This is probably the result of electron reflection, experiments of other kinds[8] having shown reflection coefficients of approximately this magnitude. The fact that the currents agree with the straight line relation for collector potentials of 2.5 volts or more above that of the space indicates that most of the reflected electrons leave the surface with energies less than about 2.5 volts.

---

[8] Langmuir and Jones, *Science 59*, 380 (1924).

TABLE II

Plane Electron Collector H (Run No. 49b). Same Conditions as for Table I except Collector is Positive. Slope $S = 0.0047$; $\gamma = 1.53$; $I_e = 270$ ma. cm.$^{-2}$. ν Calculated from $T = 9200$.

1 E_H	2 V	3 $\sqrt{\nu}$	4 i_H ma.	5 $i_{cal.}$	6 x
−12.4	+0.1	0.55	680	948	0.002
−12.0	0.5	1.22	800	954	0.004
−11.5	1.0	1.84	890	960	0.005
−11.0	1.5	2.32	930	964	0.007
−10.5	2.0	2.75	950	968	0.008
−10.0	2.5	3.12	970	971	0.009
	(3.3)	(3.68)		(976)	0.0108
− 9.0	3.5	3.84	980	978	0.011
− 8.0	4.5	4.50	985	984	0.013
− 5.0	7.5	6.20	1000	1000	0.018

The slope of the straight line was $S = 0.0047$, and by comparing this value with equation (52) we find

$$\gamma = 1.53,$$

a value somewhat larger than obtained for the collection of positive ions, but still of the order of magnitude of unity.

Taking an approximate preliminary value of I_e and using the values $I_p = 0.71$ and $\nu_0 = 21.6$ from Table I, we find from equation (55) a value of ν' from which we can obtain by interpolation from Table II an accurate value of I_e. We thus find $\nu' = 13.6$ and $i_H = 97.6$ ma. for the potential $V = 3.3$ which should be the potential for which the edge corrections disappear. This gives for the electron current density $I_e = 27.0$ ma/cm^2.

The electron sheath thickness x, calculated by equation (10) from this value of I_e, is given in the last column. It is seen, in fact, that for the voltage $V' = +3.3$ the electron sheath has the same thickness ($x = 0.0108$ cm.) as that of the positive ion sheath for the voltage $V_0 = -5.3$ for which the total current was zero. The ratio V': $(-V_0)$ is 62 per cent. In general, to determine I_e with a plane collector it is not necessary to plot $\sqrt{i}$ against $\sqrt{\nu}$ as we have done here, for the current corresponding to ν' (976 ma. in Table II) can be obtained directly by interpolation as soon as V' is determined, according to equation (55) or more conveniently by assuming V' to be 65 per cent of $(-V_0)$.

If we make the reasonable assumption that the positive ions have average energies less than those of the electrons, and if the space charge of the electrons were neutralized by an equal number of positive ions per unit of volume, we can readily see that the currents carried by the electrons should exceed those carried by the ions by a ratio greater than 605:1 (the square root of the ratio of the masses of the mercury ion and the electron). Actually, however, the ratio I_e:I_p from the data of Tables I and II comes out to be 380:1. In connection with the general discussion of the data obtained with various kinds of collectors, it will be shown that the small value of this ratio is probably due to the presence of negative ions in the ionized gas.

The data of Tables I and II and Fig. 1 and 4 have been selected as typical of those obtained with collector H. About 40 such sets of data (or "runs") were obtained with this electrode, the current i_B being varied from 0.1 to 8.0 amp., and the pressure of mercury from 1.0 to 34.0 bars. The effects of transverse and longitudinal magnetic fields (up to about 150 gauss) were also studied. A longitudinal field has relatively little effect on the characteristics of collector H, but a transverse field at sufficiently low pressures of mercury vapor deflects the arc to one side, so that it travels along the glass surface, the electrons, by successive reflections from the sheath that forms on the glass, being enabled to travel along the tube in spite of the transverse field.

Under these varied conditions the straight-line relation between $\sqrt{i}$ and $\sqrt{\nu}$ for negative potentials on the collector was found always to hold, but the value of γ calculated from the slope varied somewhat, though in a manner that bore no obvious relation to any of the known variables. The average value of γ was

$$\gamma = 1.00 \pm 0.22$$

where the 0.22 is the "probable error of a single observation."

The semi-logarithmic plots, like those of Fig. 1, were in most cases satisfactorily straight over a range covering a 1000-fold increase in i. A few of the curves, however, showed deviations from straight lines greater than the probable errors in the measurements, and these probably indicate deviations from a Maxwellian distribution of velocities. But in nearly all cases all the points within a 1:1000 range lay within 1 volt of a straight line. In a good many cases the deviations were of such a kind as to make all the points lie exactly on two straight lines meeting at an intermediate point. For example, Run No. 34b (see Table III), which showed the most marked kink of this kind, gave 16 evenly spaced points which all came within 0.2 volt of the broken straight line, the average deviation being less than 0.08 volt. The average deviation from the best single straight line was 0.30 volt. The total voltage range covered by the straight portion of the curve was 16 volts. The slope of the single straight line corresponded to $T_e = 27{,}500$ deg., while the broken line gave $T_e = 23{,}000$ deg. for the lower portion and 30,200 deg. for the upper portion, the kink occurring at about -11 volts with respect to the space potential.

TABLE III

Summary of Typical Data Obtained with Collector H

1	2	3	4	5	6	7	8	9	10
Run No.	Bulb Temp. Deg. C.	Vapor Pressure, Bars	i_B Amp.	E_{BC}	E_{SB}	T_e	I_e	I_p	I_e/I_p
20-a	32.0	4.3	3.95	41.0				2.72	
20-b	34.5	5.3	5.0	39.1				3.77	
34-b	15.5	1.05	0.5		−7.0	27500	78.4	0.17	450
35-a	15.5	1.05	1.0	37.0	−8.2	29000	88.6	0.25	360
35-b	15.5	1.05	2.0		−7.0	26600	183.0	0.44	415
36-a	15.5	1.05	4.0		−6.0	25200	388.0	1.11	350
36-b	15.5	1.05	5.9		−7.0	21600	635.0	1.67	381
37-a	15.5	1.05	8.0	35.0	−6.0	19500	775.0	2.29	338
44	30.0	3.7	0.1	33.0	−9.0	16000	17.2	0.059	443
45	30.0	3.7	0.2	36.0	−10.0	16700	16.9	0.041	410
46	30.0	3.7	0.5	40.0	−8.0	20600	42.1	0.086	493
47	30.0	3.7	1.0	39.0	−7.0	21000	97.0	0.205	473
48-a	60.0	33.0	0.2	40.0	−19.0	8400	24.2	0.065	375
48-b	60.0	33.0	0.5	38.0	−15.0	8300	68.0	0.172	394
49-a[9]	60.0	33.0	1.0	38.0	−13.5	9660	133.0	0.338	394
49-b[9]	60.0	33.0	2.0	37.0	−12.5	9200	272.0	0.710	380

Average 405 ± 25

[9] The values of i_e for Runs No. 49-a and 49-b are plotted in Fig. 1. In order to prevent overlapping of the curves, the curve for Run No. 49-a (lower curve) is displaced one volt to the right.

Deviations of this character, however, seemed to bear no definite relation to the known variables and are therefore probably to be looked upon as a type of experimental error due to some uncontrolled factor. The probable errors of the values of T_e are therefore about 10 per cent.

A summary of typical data obtained with collector H without magnetic fields is contained in Table III. The second column gives the temperature of the water bath in which the lower part of the tube was immersed, and the third column gives the corresponding vapor pressure of the mercury. The current to the anode *B* is given in the fourth column, while the next column gives E_{BC}, the potential of the anode B with respect to the cathode C. The sixth column gives the space potential in the neighborhood of electrode H referred to that of the anode B. The temperature T_e in the seventh column is determined from the best single straight line that can be drawn as a semi-logarithmic plot of the type of Fig. 1. The electron and positive ion current densities I_e and I_p in the eighth and ninth columns are expressed in ma. per cm^2.

It will be noted that the ratio $I_e : I_p$ in the tenth column is fairly nearly constant, having the average value 405 ± 25.

The current densities I_e and I_p increase roughly in proportion to the arc current i_B. For very low currents, such as that in Run 44, the ionization near H, resulting from diffusion of electrons from the 6-amp. arc maintained in the vertical arm containing anode A, outweighed that produced by the current i_B, so that I_e and I_p were about the same as for larger values of i_B.

The electron temperatures T_e decrease very markedly as the mercury vapor pressure is raised, but are nearly independent of the arc current, showing, if anything, a tendency to decrease as the arc current is raised. The average values are

Pressure	T_e
1.05 bars	25,000 deg.
3.7 "	18,500 "
33.0 "	8,900 "

High Negative Voltages on Collector H

A few runs were made to study the behavior of a positive ion collector at negative voltages as high as 1340 volts (direct current), while a 2-amp. arc flowed through the tube and the mercury vapor pressure was 8.0 bars (40 deg. C.). When the potential was first raised to this value there were occasional brilliant flashes of light (arcing-back) on the surface of the collector, and upon subsequent examination it was found that tree-like branching figures had been etched into the metal. However, after a few such flashes they ceased and the current-voltage data, which had been previously somewhat erratic above about 500 volts, became perfectly steady up to 1330 volts, and no further signs of breakdown occurred. Table IV gives some of the typical data obtained under these conditions. The values of $\sqrt{i}$ were plotted against $\sqrt{\nu}$ in the manner described in connection with Table I. The points came very close to a straight line of slope $S = 1.39 \times 10^{-4}$, which gives $\gamma = 1.12$, nearly the same as the value (1.14) obtained from Table I. The fourth column gives the values that the currents would have if the points came exactly on the straight line. It is seen that the agreement between i_H and $i_{cal.}$ is excellent, although with these high potentials the sheath became 4 mm. thick.

TABLE IV

Collector H at High Negative Voltages. Mercury Vapor Pressure 8.0 bars. $I_B = 4.0$. Slope $S = 1.39 \times 10^{-4}$. $\gamma = 1.12$. $I_p = 1.05$ ma. cm.$^{-2}$. T_p assumed to be 5000 deg. in calculating ν.

1 V	2 i_H	3 $\sqrt{\nu}$	4 $i_{cal.}$	5 x cm.
− 30	3.95	14.7	3.91	0.028
− 115	4.4	37.6	4.32	0.072
− 295	4.9	74.1	5.01	0.142
− 470	5.6	105.0	5.66	0.202
− 650	6.4	132.8	6.26	0.254
− 815	6.9	158.0	6.82	0.302
− 990	7.4	181.0	7.36	0.347
−1160	7.6	207.0	7.99	0.396

Thus the increase in the current i_H with increasing voltage is wholly accounted for as an edge correction in accordance with the theory we have developed. Even at potentials as high as 1300 volts, the *current density* of the collected current is independent of the voltage. This must mean that only a negligible proportion of electrons is emitted as a result of the intense positive ion bombardment of the collector. It may seem remarkable that at such high voltage the cathode does not act like a self-sustaining cathode of a glow discharge. It must be remembered, however, that at pressures as low as 8 bars such discharges do not occur in pure mercury vapor. The breakdown which was at first observed at 1300 volts is of a totally different nature and involves extremely high local current densities. It is probably more in the nature of a cold-cathode effect in which electrons are pulled out of the metal by intense local fields, in accordance with a theory proposed by Schottky.

Visual Observation of Sheaths

In the experiments with the tube of Fig. 3 it was frequently observed, when high negative voltages were used on collectors or when the arc current was low, that the sheath became visible as a dark space around the collector. The electrodes of this tube, however, did not lend themselves to measurements of the sheath thickness. In a subsequent experiment, with a tube containing spherical electrodes, measurements were made which showed that the observed thickness agreed well with that calculated by the space charge equation. These will be discussed again in connection with a study of the data obtained with spherical collectors.

A special tube, which is shown in Fig. 6, was then constructed in such a way that the sheaths could be observed without the necessity of looking through a layer of glowing gas, which greatly hindered observation and measurement. In this tube the arc is made to pass into a bulb about 7.5 cm. diameter, so that it becomes diffused throughout the bulb. Two electrodes, B and G, are placed in the bulb, B being a cylindrical wire which can be observed end-on through a plain glass window W, and G being a flat metal disk in a plane perpendicular to the axis of the wire. At present we shall consider only some of the measurements of the thickness of the sheaths observed on the collector G, and their relations to the currents and voltages.

The experimental data given in Tables V, VI, VII, and VIII were obtained with the tube of Fig. 6 while the entire bulb containing the conical molybdenum auxiliary anode D was maintained at 12 or 13 deg. C., in order to fix the vapor pressure of the mercury in the upper bulb which contained the collector G. A current of about 5 amp. to the anode D was maintained throughout the experiments. By using a large choke coil with an inductance of several henries in series with the anode A, it was found possible to work with steady currents i_A to this anode as small as 0.003 amp., but current up to several amperes could be obtained if desired. With all these currents the interior of the bulb was filled with a very uniform glow, except that at low currents there was a distinct dark sheath covering all the glass surfaces as well as the electrodes. With large currents the intensities of ionization in the upper bulb were so great that the dark sheaths on the electrodes and on the glass were too thin to measure accurately. With currents below 0.05 amp. the light intensity was not sufficient to favor accurate measurements of sheath thickness with a cathetometer, but with the naked eye the sheaths could be seen and measured within 0.2 or 0.3 mm. even down to currents i_A = 0.003 amp.

TABLE V

Visual Observations of Sheath Thickness on Plane Collector. Run No. 108. Bulb at 12 deg. C. Hg pressure 0.75 bars. Current $i_A = 0.15$ amp. $E_{AC} = 26.8$ volts. $S = 1.6 \times 10^{-4}$; $\gamma = 1.03$; $I_p = 0.065$ ma. cm.$^{-2}$; $T_e = 39{,}400$ deg.

1 E_{GA}	2 V	3 $\sqrt{v}$	4 i_G ma.	5 x_{obs} mm.	6 $x_{cal.}$ mm.
−90	−89	31.5	−0.450	2.1	2.42
−50	−49	20.6	−0.379	1.4	1.58
−30	−29	14.4	−0.340	0.8	1.11
−21	−20	11.2	0.000	0.7	0.86
Sheath on glass window......				0.7	0.86

TABLE VI

Cathetometer Measurements of Sheath Thickness on Plane Collector. Run No. 114. Bulb at 13 deg. C. Hg pressure 0.81 bars. Current $i_A = 0.10$ amp. $E_{AC} = 27.9$ volts. $S = 1.36 \times 10^{-4}$; $\gamma = 0.88$; $I_p = 0.045$ ma. cm.$^{-2}$; $T_e = 38{,}000$ deg.

1 E_{GA}	2 V	3 $\sqrt{v}$	4 i_G ma.	5 $x_{obs.}$ mm.	6 $x_{cal.}$ mm.
−300	−295	74.5	−0.481	6.40	6.89
−200	−195	55.5	−0.412	5.10	5.13
−150	−145	44.7	−0.368	4.27	4.13
−100	− 95	33.2	−0.322	3.00	3.07
− 80	− 75	28.5	−0.300	2.58	2.64
− 60	− 55	22.6	−0.280	2.10	2.09
− 50	− 45	19.6	−0.262	1.82	1.81
− 40	− 35	16.4	−0.246	1.33	1.52
− 30	− 25	12.8	−0.230	1.12	1.18
− 25	− 20	11.0	−0.179	0.98	1.02
− 20	− 15	9.2	+0.195	0.91	0.85

In general, whenever the collector was at potentials of 25 volts or more, negative with respect to the space, the positive ion sheaths seemed perfectly dark and had apparently perfectly sharp edges. As the potential was raised toward the space potential and as electrons thus began to be collected in spite of the retarding field, the sheath became less sharply defined and some light was clearly produced within it. The presence of the dark sheath could be detected until the electrode was within 2 or 3 volts of the space potential, but measurements under these conditions were almost useless because the edge was not definite.

TABLE VII

Cathetometer Measurements of Sheath Thickness on Plane Collector. Run No. 117. Bulb at 13 deg. C. Hg pressure 0.81 bars. Current $i_A = 0.40$ amp. $E_{AC} = 27.5$ volts. $S = 1.77 \times 10^{-4}$; $\gamma = 1.14$; $I_p = 0.119$ ma. cm.$^{-2}$; $T_e = 29{,}100$ deg.

1 E_{GA}	2 V	3 $\sqrt{v}$	4 i_G ma.	5 $x_{obs.}$ mm.	6 $x_{cal.}$ mm.
−400	−393	92.4	−1.208	5.24	5.27
−300	−293	74.2	−1.090	4.12	4.24
− 80	− 73	27.6	−0.708	1.54	1.57
− 60	− 53	21.9	−0.662	1.19	1.25
− 50	− 43	19.0	−0.633	1.05	1.08
− 30	− 23	12.2	−0.570	0.77	0.70

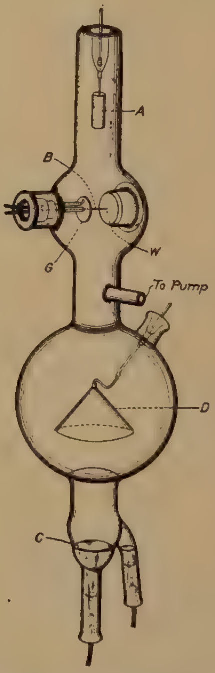

Fig. 6. Mercury Vapor Tube for Observing Sheath Diameters and Thicknesses

When the collector was made 2 to 5 volts *positive* with respect to the space, a much less distinct dark space could be seen which increased in thickness as the voltage was made more positive. The indistinctness of this electron sheath did not appear to be due to indefiniteness in the boundary, but rather to the lack of contrast between the light intensities within and without the sheath. It was also frequently observed, although only with difficulty, that just outside this dark sheath there was a faint increase in light intensity which was never observed in the case of positive ion sheaths.

Experiments now in progress show that when two positively charged plane collectors are placed opposite one another at a distance comparable with the mean free path of the positive ions, the positive ions ejected from the sheath of one collector have the effect of breaking down the electron sheath of the other. The trapping of the positive ions by their reflection from the opposing sheaths has the effect of breaking down the anode drop which otherwise occurs with high anode current densities. This is the explanation of the effects observed with small hollow anodes in mercury arc tubes[10].

TABLE VIII

Visual Observation of Sheath Thickness on Glass Window with Low Intensities of Ionization. Bulb at 13 deg. C.; Hg pressure 0.81 bar

Run No.	i_A	E_{AC}	I_p ma./cm.^{2}	$x_{obs.}$ mm.	ν	V Volts	T_e
104-a	0.013	28.0	0.0063	4.1	275	35.6	48,400
104-b	0.010	27.1	0.0050	4.0	208	29.0	47,000
105-a	0.006	26.2	0.0026	5.5	204	28.5	45,000
105-b	0.003	26.0	0.0016	7.5	234	31.6	60,000

When the collector potential was raised to a definite value (which in different runs varied from 9 to 12 volts above space), a bright film or sheath appeared quite suddenly on the surface of the collector within the dark sheath already referred to. Upon raising the potential this bright sheath increased rapidly in thickness. This sheath seems to result from ionization within the electron sheath by the electrons when they acquire energies a few volts in excess of the ionizing potential.

At the low pressures employed in these experiments, the number of ions formed in this way is not sufficient to have any appreciable effect on the space charge within the sheath, for the positive ions are promptly ejected by the field and the number formed is a very minute fraction of the number of electrons flowing. But when the sheath thickness and the voltage increase, the number of ions increases until finally, when the number of ions formed becomes about equal to 1/605th of the number of electrons flowing to the collector, the electron sheath breaks down and the current (with sufficiently low external resistance) increases indefinitely.

In Tables V to VIII, i_A is the sum of the currents to A and to G; E_{AC} is the potential of anode A with respect to the cathode C; E_G is the potential of G with respect to the anode A; V is the potential of G with respect to the surrounding space, the space potential having been determined from the kink of the semi-logarithmic plot of i_e against E_G.

The third columns of Tables V, VI, and VII contain $\sqrt{\nu}$ which has been calculated by equation (11) as usual on the assumption that $T_p = 5000$ deg. Although T_p undoubtedly varies with the conditions, this value is believed to be sufficiently accurate, considering that it only comes into equation (11) as a correction term involving $\sqrt{T_p}$.

The square roots of the currents i_G in the fourth columns were plotted against $\sqrt{\nu}$, and in each case the points lay nearly on a straight line of the slope given by S, until at values of V greater than about -30, electrons began to be collected. From S the values of γ were calculated by equation (53), placing $p=2$, and changing the coefficient to 1.10, since the collector G is circular and is exposed on both sides to the ionized gas.

To calculate the positive ion random current I_p, the current i_G was first obtained, corrected for edge effects by extrapolating to

---

[10] Guenther-Schulze, *Zeit. fuer Physik*, has suggested that the lowering of the anode drop in such cases is due to the effect of radiation reflected back into the gas from the walls of the hollow anode. Such an explanation is found to be contrary to many experimental facts.

$\nu=0$ on the straight line plot just referred to. This corrected current was then divided by the effective area of collector G, which was taken to be 4.0 cm.^{2}. This value was arrived at as follows. The diameter of the disk *G* was 1.90 cm. so that its surface was 2.84 cm.^{2} for each face. Observations of the sheaths on the front and back faces showed, however, quite uniformly that the sheath on the back was about 1.5 times thicker than that on the front. This was due no doubt to the too close proximity to the glass surfaces of the bulb and the tubing covering the leads from electrodes B and G, which surfaces robbed the ionized gas of positive ions. From the space charge equation (10) it can be seen that the current density on the back was only 0.44 of that on the front face. Thus the effective surface of the whole collector should be $2.84 \times 1.44 = 4.09$. Considering the direct screening effect of glass tubing in covering up a portion of the back face it was considered that the round figure 4.0 cm.^{2} was the most probable for the effective surface.

The electron temperatures T_e given in Tables V to VII were obtained from semi-log plots which gave very good straight lines. It will be noted that the temperatures at these low vapor pressures are unusually high and that they decrease considerably as the arc current is raised to 0.4 amp. The temperature data in the last column of Table VIII were obtained with a cylindrical collector B 1.3 mm. diameter, and at these very low arc currents it was found that the semi-log plots were not very straight, so that the temperatures in this table are very rough, the probable error being estimated at ±8000 deg. The values of I_p in Table VIII were also derived from the cylindrical collector B, no measurements of currents to G having been taken in these runs.

The observed sheath thicknesses, $x_{obs.}$ in Tables V and VIII, were made with the unaided eye holding a millimeter scale in front of the tube. The calculated sheath thicknesses, $x_{cal.}$ (in mm.) in the last columns of Tables V to VII, were obtained from the current densities I_p given by equation (10) which took the form

$$x = 0.621\sqrt{\nu / I'} \text{ mm.},$$

where I' is the value of I_p expressed in microamperes per cm.^{2}.

The agreement between the calculated and observed sheath thicknesses seems to lie within the experimental error, even with voltages ranging from $V=15$ to 393. Not only does the observed sheath vary with the voltage according to the theory, but it varies in the correct manner with the intensity of ionization. Thus I_p in Table VII is 2.64 times as great as in Table VI, and the sheath thickness at $V=80$ volts is in the ratio 1:1.67 which is close to the theoretical value 1:1.63 (1.63 being the square root of 2.64).

The sheath thickness 0.7 mm. observed on the plane glass window, according to Table V, was the same as that observed on the collector G when its potential was adjusted so that the current i_G became zero. The existence of these sheaths under these conditions is the most direct proof that insulated surfaces, whether conducting or not, acquire potentials as much as 20 volts negative with respect to the gas.

The data of Table VIII show that with very low arc currents, the sheaths on the glass surfaces become very thick, as much as 7.5 mm. being observed. Again the results are in accord with the theory. From the observed values of x and the observed current density I_p the value of ν (sixth column) can be calculated by equation (10). From this, taking $T_p = 5000$ deg., the values of V (seventh column) were calculated. These then represent the potentials of the glass surface with respect to the ionized gas. These values are higher than those usually found but not more so than should correspond to the high values of T_e observed in these runs (eighth column). In general the negative potential acquired by an insulated collector should be proportional to the electron temperature T_e.

(*To be continued*)

House Service Generators; Their Types and Field of Application

By W. R. Herod

Construction Engineering Department, General Electric Company

An economical and reliable supply of energy for station auxiliaries under all operating conditions is essential in the modern generating plant, whether the station be that of a large public utility or one supplying power to an industrial plant. With the advent of the house service generator came notable advances in auxiliary economies, and the various methods of utilizing such units now receive careful attention. The author briefly outlines various types of house service generator drives and the fields of service to which they are usually applied. It should be realized, however, that local conditions influence the selection primarily, and that changing conditions in a plant may make advantageous the changing of the method of house service generator drive from time to time. The chart included in the article summarizes the usual house service generator drives and their conditions of operation.—Editor.

Introduction

With the development of the power industry, and the corresponding concentration of generating capacity in large stations, together with the advent of higher prices for coal, thoughts were more forcibly directed toward the improvement of efficiency in power plant design and operation. As a consequence, higher steam pressures and temperatures began to be employed, resulting in increased economy of power production and lower costs per kilowatt-hour of electric energy. But in these installations the higher investments for auxiliary drive became quite an important item, especially for the small auxiliary turbines and other steam-driven units, which could not in economy of operation take full advantage of the higher steam pressures and super heats. Likewise, more critical attention was directed toward the fallacy of the old proposition that inefficient non-condensing auxiliaries were of no consequence in that the heat in the exhaust was delivered to the feed water. Such an idea had been extremely misleading in so far as indicating economical methods of producing power, and now more efficient heat balance is obtained in a variety of ways with a tendency toward extraction heating with its attendant economies.

The higher investment costs and operating difficulties which at first were encountered with piping subjected to these severer temperatures and pressures necessitated more careful consideration. Also, the complications arising from a multiplicity of minor connections with drips, drains, etc., caused increased cost and difficulties of design. Hence, any reduction in these items would be directly realized in a more simple layout with consequent saving.

Electric Drive for Auxiliaries

The obvious alternative to these evils was the use of electrically-driven auxiliaries, with corresponding reductions in the cost and difficulties with piping and the elimination of the small auxiliary turbines. Likewise, this would result in simplified station design. But here the question of reliability entered fundamentally into the scheme. It must be remembered that in steam power stations the auxiliaries may be divided into two main classes. The first of these includes the auxiliaries, such as the circulating and condensate pumps, etc., which if they failed would ordinarily cause loss of load and great inconvenience but probably no material damage to equipment. The second class includes the boiler feed pumps, etc., which by failure would not only cause loss of load but might cause serious damage to equipment and even loss of life. Hence, continuity of operation of the auxiliaries is essential.

Motor-driven auxiliaries were accordingly handicapped for some time:

(1) By a mistaken impression as to the unreliability of the driving motors.

(2) By doubt as to the reliability of the source of supply of electrical energy to these auxiliaries.

The first of these handicaps was almost immediately dispelled, as the reliability of motor drive was easily demonstrated; and to answer the second, the house service generator was employed, this unit being free from disturbances on the main bus (which might be caused by short circuit or other interruption) and furnishing an independent source of electrical supply for the auxiliaries. In some stations, especially with interconnected systems, the probability of failure of electrical supply has been considered

HOUSE SERVICE GENERATOR CHART SHOWING VARIOUS CONDITIONS OF OPERATION

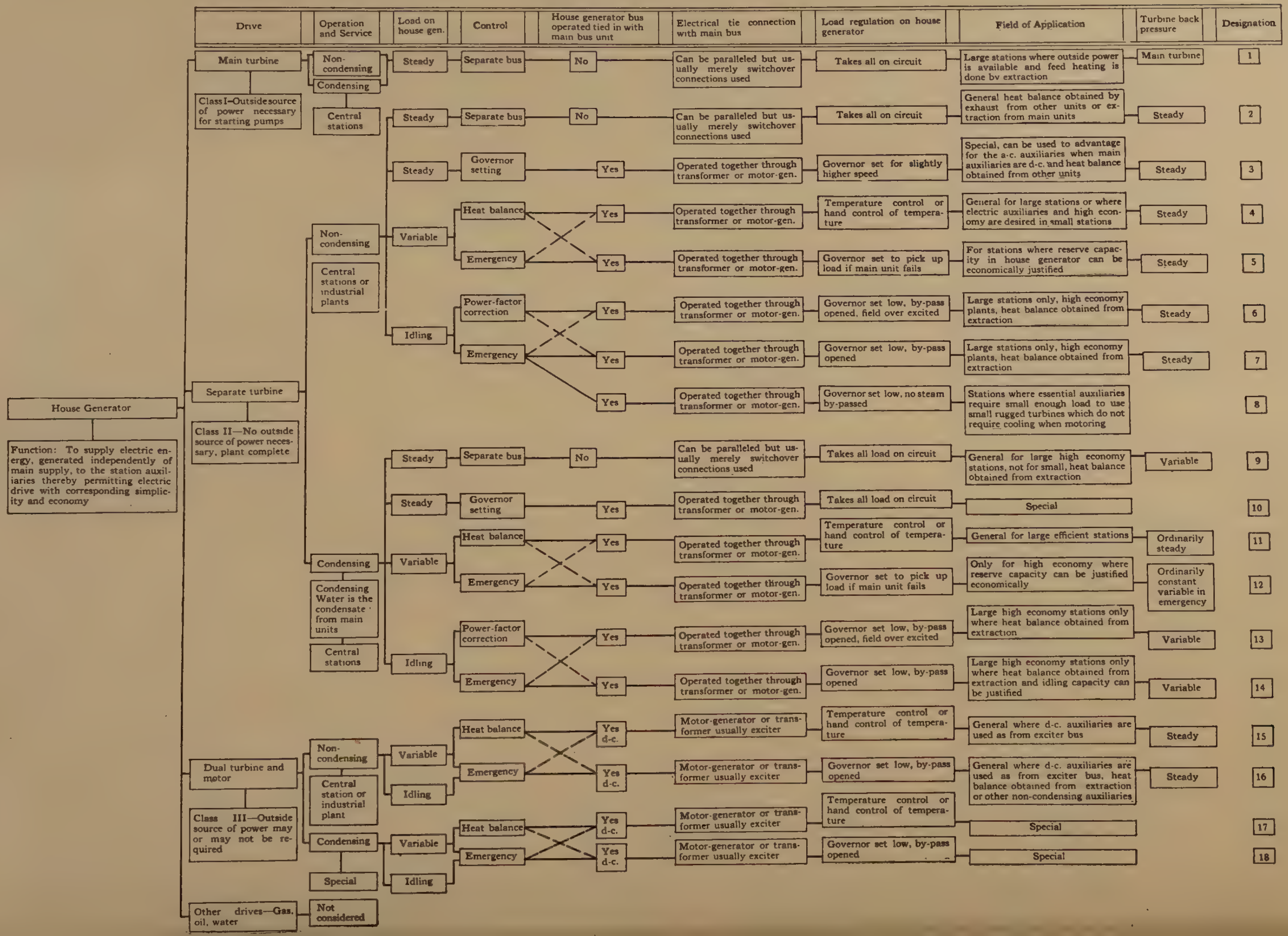

House Generator

Function: To supply electric energy, generated independently of main supply, to the station auxiliaries thereby permitting electric drive with corresponding simplicity and economy

Drive	Operation and Service	Load on house gen.	Control	House generator bus operated tied in with main bus unit	Electrical tie connection with main bus	Load regulation on house generator	Field of Application	Turbine back pressure	Designation
Main turbine Class I—Outside source of power necessary for starting pumps	Non-condensing Condensing Central stations	Steady	Separate bus	No	Can be paralleled but usually merely switchover connections used	Takes all on circuit	Large stations where outside power is available and feed heating is done by extraction	Main turbine	1
Separate turbine Class II—No outside source of power necessary, plant complete	Non-condensing Central stations or industrial plants	Steady	Separate bus	No	Can be paralleled but usually merely switchover connections used	Takes all on circuit	General heat balance obtained by exhaust from other units or extraction from main units	Steady	2
		Steady	Governor setting	Yes	Operated together through transformer or motor-gen.	Governor set for slightly higher speed	Special, can be used to advantage for the a-c. auxiliaries when main auxiliaries are d-c. and heat balance obtained from other units	Steady	3
		Variable	Heat balance	Yes	Operated together through transformer or motor-gen.	Temperature control or hand control of temperature	General for large stations or where electric auxiliaries and high economy are desired in small stations	Steady	4
			Emergency	Yes	Operated together through transformer or motor-gen.	Governor set to pick up load if main unit fails	For stations where reserve capacity in house generator can be economically justified	Steady	5
		Idling	Power-factor correction	Yes	Operated together through transformer or motor-gen.	Governor set low, by-pass opened, field over excited	Large stations only, high economy plants, heat balance obtained from extraction	Steady	6
			Emergency	Yes	Operated together through transformer or motor-gen.	Governor set low, by-pass opened	Large stations only, high economy plants, heat balance obtained from extraction	Steady	7
				Yes	Operated together through transformer or motor-gen.	Governor set low, no steam by-passed	Stations where essential auxiliaries require small enough load to use small rugged turbines which do not require cooling when motoring		8
	Condensing Condensing Water is the condensate from main units Central stations	Steady	Separate bus	No	Can be paralleled but usually merely switchover connections used	Takes all load on circuit	General for large high economy stations, not for small, heat balance obtained from extraction	Variable	9
		Steady	Governor setting	Yes	Operated together through transformer or motor-gen.	Takes all load on circuit	Special		10
		Variable	Heat balance	Yes	Operated together through transformer or motor-gen.	Temperature control or hand control of temperature	General for large efficient stations	Ordinarily steady	11
			Emergency	Yes	Operated together through transformer or motor-gen.	Governor set to pick up load if main unit fails	Only for high economy where reserve capacity can be justified economically	Ordinarily constant variable in emergency	12
		Idling	Power-factor correction	Yes	Operated together through transformer or motor-gen.	Governor set low, by-pass opened, field over excited	Large high economy stations only where heat balance obtained from extraction	Variable	13
			Emergency	Yes	Operated together through transformer or motor-gen.	Governor set low, by-pass opened	Large high economy stations only where heat balance obtained from extraction and idling capacity can be justified	Variable	14
Dual turbine and motor Class III—Outside source of power may or may not be required	Non-condensing Central station or industrial plant	Variable Idling	Heat balance	Yes d-c.	Motor-generator or transformer usually exciter	Temperature control or hand control of temperature	General where d-c. auxiliaries are used as from exciter bus	Steady	15
			Emergency	Yes d-c.	Motor-generator or transformer usually exciter	Governor set low, by-pass opened	General where d-c. auxiliaries are used as from exciter bus, heat balance obtained from extraction or other non-condensing auxiliaries	Steady	16
	Condensing Special	Variable Idling	Heat balance	Yes d-c.	Motor-generator or transformer usually exciter	Temperature control or hand control of temperature	Special		17
			Emergency	Yes d-c.	Motor-generator or transformer usually exciter	Governor set low, by-pass opened	Special		18
Other drives—Gas, oil, water	Not considered								

sufficiently remote to dispense with all auxiliary generators, but in the greater number of larger stations the house service generator has been installed, where electric auxiliaries have been used.

House Service Generator Drive

There are three main classifications of house service generators:

(1) Those driven by the main turbine shaft, which is extended for this purpose.

(2) Those driven by a separate steam turbine.

(3) Those units which have dual or duplex drive, being connected to both a turbine and a motor.

The usual features of these types of installation are graphically presented in the chart on the opposite page.

Other types of auxiliary generated power, such as by gas engine, oil engine, etc., are of such limited application in steam power stations as not to be considered here.

House Service Generator Driven by Main Unit

The first method classified represents an especially efficient type of installation, where advantage can be taken of the favorable water rate of the main unit in the generation of auxiliary power and still retain the advantages of independent electrical supply to the auxiliaries. In this case the difficulties of a multiplicity of bearings might be considered somewhat of a handicap; however, the advantages of such an arrangement in the economical generation of power have more than warranted such development and the modern tendency is apparently in this direction, with suitable heat balance being obtained by extraction from the main turbines. An outside source of power, either in the form of a separate turbine generator or a connection to another station, is necessary in such an installation to start the essential auxiliaries and to carry at first the circulating pumps, etc., in order to avoid starting the turbines non-condensing with correspondingly high temperatures in the exhaust elements and undesirable expansion in the condenser.

In general, from economical considerations, the chief field of service for this type of equipment is in connection with large units and hence in the central station. Usually for such installations, due to the fixed relation between the generated voltages of the main generator and the house service generator, and likewise due to both units being driven by the same steam element, the house service generator is not operated in parallel with the main bus but feeds a separate bus from which certain auxiliaries are driven. However, these auxiliaries usually may be transferred through transformers to the main bus by suitable switch-over connections as has been provided, for example, in the new Peoria Station of the Illinois Electric Power Company.[1] On the other hand, parallel operation of such a house service generator, at least temporarily, with the main bus can be accommodated as provided in the proposed Weymouth Station of the Boston Edison Company.[2] Such systems of house service generator drive are becoming very popular and, in addition to furnishing an independent source of electrical supply to the auxiliaries, they offer the same thermodynamical advantages as systems having auxiliaries driven from the main bus. Accordingly, multi-stage bleeding and even reheat can be applied in such cases, resulting in one of the most favorable single-vapor cycles economically available. In the right-hand column of the chart this condition is designated as *No. 1*.

Separate Turbine Drive for House Service Generators

The second main classification, with the house service generator driven by a separate turbine, embraces the applications of the ordinary house service turbine. Such a unit has the distinct advantage of giving the electrically-driven auxiliaries an independent source of power within the station. Thermodynamically, it does not present quite such favorable possibilities as the cycles based upon generators driven from the main unit for, due to the smaller size of the unit, the water rate on the house service turbine for similar steam conditions is not ordinarily as favorable as that on the main unit. However, considerations as to size, starting conditions, and the possibility of lower feed water temperatures at low loads due to the reduction in pressure of the extracted steam for low loads on the main turbines may more than offset this feature, and in fact may in cases make the thermodynamic characteristics of the separately driven house service generator as favorable as those obtained with the house service generator driven from the main unit. The chief field of service for the separate house service turbine at the present time appears to be in central stations. However, it is quite probable that in the future, with the popularity of motor-driven auxiliaries increasing, the field will be extended into industrial plants with a corresponding abandonment of the non-condensing steam auxiliaries now used. It is also probable that the larger central stations may work away from such units by going to the generator driven from the main turbines, since such systems present thermodynamically better possibilities.

---

[1] *Power*, April 22, 1924.

[2] *Journal A.I.E.E.*, August, 1923.

Non-condensing House Service Turbines

Probably the greatest number of installations of separate turbine generators for house service are for non-condensing operation. These have a field of service which embraces both the central station and the industrial plant, though most of the present installations are in central stations.

In certain cases, such as that designated as *No. 3*, a more or less steady load is maintained on the house service generator even when equipped for and operating in parallel with the main bus through suitable transformers or motor-generators. In such cases, the governor is set for slightly higher speed so that the house service turbine carries the connected auxiliary load or any desired portion of it. Such a system, though somewhat special, is applicable where the major portion of the auxiliaries are otherwise driven, and only certain auxiliaries are carried on the house service unit, the steam being used for feed heating, but no minute regulation of heat balance being required in so far as the house service unit is concerned.

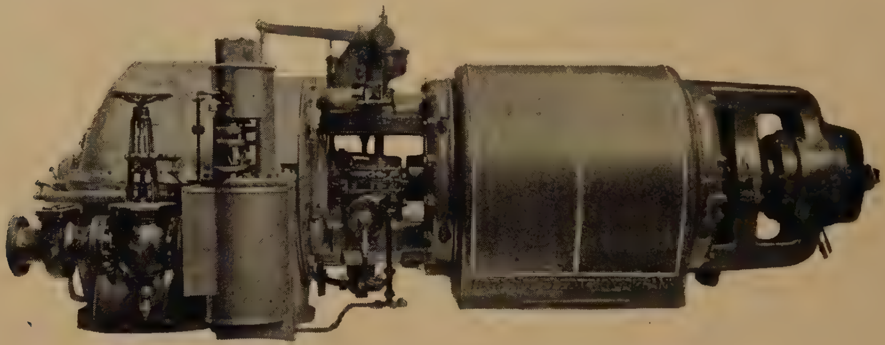

Fig. 1. 1000-kw., 60-cycle Turbine as Used for House Service Purposes

For such units, there are several elements which control the operation. They may feed a separate bus from which certain auxiliaries are driven, and in this way contribute partially to the heat balance, but with the regulation of heating requirements taken care of otherwise. This condition is represented by designation *No. 2* on the chart, in which case the load is substantially steady and no paralleling of house service and main generators during ordinary operation is necessary.

An example of such an installation is in the Hell Gate Station of the United Electric Light and Power Company, where the heat balance is controlled by bleeding steam from the main units.[3] For such conditions the investment must cover both the extraction heaters and piping in addition to the house turbine, but the advantages of reliability and freedom from the regulation of parallel generators may more than offset this, especially in large stations where this is only a small portion of the investment.

One of the most economical methods of operating a non-condensing house service turbine is under variable load, as covered by condition *No. 4* on the chart, thereby obtaining heat balance with the house service turbine as well as an independent source of power for the auxiliaries. In such cases the bus fed by the house turbine is tied in with the main bus by transformers or motor-generators, and the load on the unit varied either automatically or in such a way as to pass the correct amount of steam for heat balance purposes. The remaining portion of the auxiliary load is supplied from the main units. An example of such an installation is the Cahokia Station of the Union Electric Light and Power Company of St. Louis[4]. Of course other sources of steam for feed heating may likewise be available for the control of heat balance, but the regulation of the heating in this case is taken care of on the house service unit. Usually in such installations, should the main bus be down, the house service turbine will pick up the auxiliary load imposed even at some slight drop in frequency. By the provision of some reserve capacity in the house unit practically all the auxiliary load may be carried in such an emergency, whereas, during ordinary times the operation is for heat balance purposes. Thus, conditions *No. 4* and *No. 5* have accordingly been interlinked as indicating probable combined services to which the same unit may be subjected. This has also been indicated in certain of the other examples as will be noted on the chart.

---

[3] *Trans. A.S.M.E.*, Vol. 43, 1921.
[4] *Power*, April 1, 1924.

In stations where heat balance may be obtained in other ways but a separate house service unit is desired from other considerations, the idling unit has been installed. Such a unit may combine emergency capacity with a certain amount of power-factor correction for the auxiliary load, which is obtained by over exciting the field, the unit only picking up a load in case of interruption of service on the main bus to which it is connected through suitable transformers. An installation of this type was made in the Northeast Station of the Kansas City Power and Light Company.[5] Such conditions, represented by *No. 6* and *No. 7* on the chart, require a by-pass to insure a cooling flow of steam through the turbine, though for certain small units or single-stage machines of rugged design the by-pass can be omitted as in condition *No. 8*.

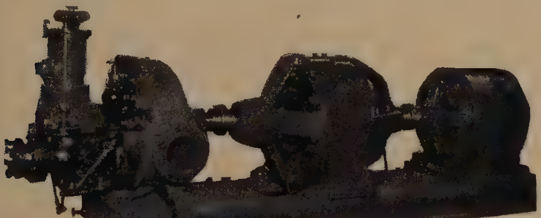

Fig. 2. 100-kw., Dual-driven Exciter Set, Consisting of Turbine, Exciter, and Induction Motor

In practically all cases where the house service generator is operated in parallel with the main bus, suitable relay protection is necessary to prevent the house service unit from feeding the main bus in the event of a short circuit on the station. This can be accomplished by reverse power relays with proper settings and permits the auxiliary bus to be automatically cut off from any serious fault on the main system should such a contingency arise.

Condensing House Service Turbines

In large central stations the proportion of auxiliary load to the main load is ordinarily such that sufficient condensate from the main units is available to condense the steam from the house service turbines at a pressure less than atmosphere, and accordingly greater economy in B.t.u. per kw-hr. output of the station can thereby be obtained. Obviously, it is most economical to expand whatever steam is used for heating purposes, either in the main unit or in the house service turbine, to as low a point as possible and consistent with the temperature requirements. Accordingly, the condensing house service turbine thermodynamically represents a favorable economy, especially for such installations in conjunction with economizers, where it is not necessary to heat the feed to more than 140 to 200 deg. F. before introducing it into the economizers. In some installations of this type small barometric condensers are used as at Connors Creek and Colfax, in which case the feed water is heated by direct contact with the steam. In other installations the exhaust from the house service turbines is piped to low-pressure heaters or surface condensers as is done in the case of the Marysville Plant of the Detroit Edison Company.

The loading conditions on the condensing house units are substantially similar to those with non-condensing operation, as will be noted on the chart. For example, conditions *No. 9* and *No. 10* represent economical installations where the auxiliaries or a certain portion of them are carried by the house service turbine as a more or less steady load, the vacuum on the turbine varying with the conditions on the main units and the detail regulation of heat balance being obtained in other ways. In such cases, for example, condition *No. 10*, the governor is set for over speed and the load on the house service unit is regulated by setting the throttle valve. Provision for such a condition of operation was made in the Marysville Plant of the Detroit Edison Company.[6]

Of special economy is the variably loaded condensing house service turbine, such as condition *No. 11*, and if reserve capacity is provided in it, condition *No. 12*, wherein the load is varied either automatically or by hand in such a way as to regulate the heat balance of the plant usually by maintaining a set feed water temperature, which may be as low as 140 deg. F. or as high as 212 deg. F., depending upon the conditions. For the higher temperatures the unit is practically a non-condensing machine. Thermostatic control is sometimes used for this service and when the house service unit is tied in through an induction-motor synchronous-generator set to the main bus, where the slip of the induction motor may be set for any desired value, great advantages in the regulation of heat balance, by the transfer of load from the house service unit to main unit and vice versa, can be obtained. In general, when the feed temperature is thus held constant, the vacuum on the house service generator is substantially steady. Examples of such installations are found in the Colfax Station of the Duquesne Light Company and in the Connors Creek Plant of the Detroit Edison Company.[7]

---

[5] *Power*, August 14 and 28, 1923.
[6] *Power*, May 29, 1923.

A more or less special application of the condensing house service unit is its operation motoring, where reserve capacity for emergency service is obtained to insure continuity of auxiliary drive. Here a certain amount of power-factor correction on the auxiliary load may be obtained by over exciting the field. In such an installation heat balance is obtained in other ways, by extraction heating for example, and the proportion of steam to the less efficient auxiliary unit reduced to a minimum for ordinary operation, the quantity being merely that amount passed through the unit for cooling purposes. In such a case the vacuum when motoring is ordinarily higher than where the unit picks up load, resulting in a variable condition in so far as the house turbine back pressure is concerned depending upon the load. Installations of this type are covered by conditions *No. 13* and *No. 14* on the chart, an example being the unit for Toho Denryoku, Japan.

Dual Drive

The use of dual turbine and motor drive for auxiliaries has presented some attractive features and has been used in certain power stations where reliability of auxiliary drive for the circulating pumps, etc., has been given special consideration, with the division of load between motor and turbine determined by heat balance requirements. Such an installation requires no house service turbine and an example is found in the Delaware Station of the Philadelphia Electric Company.[8]

The use of dual drive for an auxiliary generator, however, instead of dual drive for the auxiliary itself, as covered in Classification III, offers the opportunity of eliminating the multiplicity of smaller turbines and still give satisfactory assurance of continuity of auxiliary supply. Such installations, usually for exciter drive, have been proposed for various stations and present some very attractive features, though their application is usually limited to small units. A triple unit of this type may be operated in such a fashion as to control heat balance or it may represent merely emergency capacity depending upon the conditions in the station. An exciter with combination motor and turbine drive of this type would be covered by conditions *No. 15* and *No. 16* on the chart. An example of this type of installation is in the Colfax Station of the Duquesne Light Company.[9]

Conclusion

It is accordingly seen that many possibilities are presented by the house service generator, some of the more usual of which have been briefly described together with their application. The choice of system and method of operation for any particular station is obviously dependent upon the particular conditions, but the general field of application, as indicated by present practice, is frequently a useful guide for contemplated installations.

---

[7] *Trans. A.S.M.E.*, Vol. 43, 1921.

[8] *Trans. A.S.M.E.*, Vol. 43, 1921.

[9] *Power*, April 21, 1921.

An Example of Metallic-arc Welding in Bridge Repair

An operation of interest to the engineering profession in general and to structural engineers in particular recently took place when certain bridge members, which had been eaten away by extensive corrosion, were reinforced and built up by electric welding. The bridge is located at Pittsburgh over the Allegheny River, connecting Herrs Island with the North Shore, and is a 240-ft. through truss, pin and linkspan, built about 31 years ago.

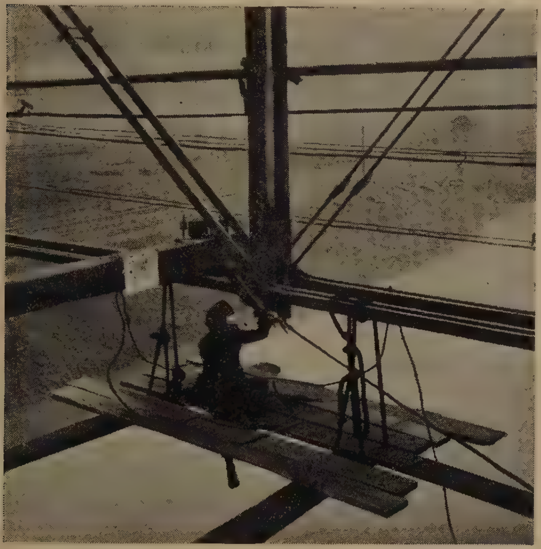

Fig. 1. Electric Arc Welder at Work on One of the Defective Bridge Members

The floor of the bridge was carried on timber stringers supported on cross timbers bolted to the web of the floor beams. While the upper portions of the structure are still in a good state of preservation, the parts which were inaccessible to painting and which were kept constantly moist by the proximity of the timber were so greatly reduced in section as to be perforated and, in many places, almost severed. The webs of the floor beams and bottoms of the vertical posts suffered particularly, being reduced from ⅜ of an inch in thickness to $\frac{1}{32}$ in. over a large area.

It was decided to renew the entire floor by cutting away the floor beams and sidewalk brackets from their connection to the vertical posts. This operation presented no very unusual difficulties. The strengthening of the columns, however, was a more serious problem. These were compression members built of Z-shaped bars and web plate, and directly above and below the pin the bearing plates were found to be perforated and reduced in section over 60 per cent.

The reinforcing of these defective members was accomplished by electric arc welding with metallic electrodes. A General Electric 200-amp. motor-generator welding set furnished the necessary current. The method adopted by the Pittsburgh Welding Corporation, under the supervision of the engineering department of the city of Pittsburgh, was first to clean the surface of the original metal thoroughly and then to weld strips of steel, 1 by ½ in. section, extending from the bottom of the column to a point well beyond the corroded portion. These vertical bars were then tied together at close intervals with crossbars of the same section. After each point was completed, the strength of the weld was tested by subjecting the bars to a number of blows with an eight-pound maul. The results of physical tests showed practically no deterioration of the original metal when welded by this process.

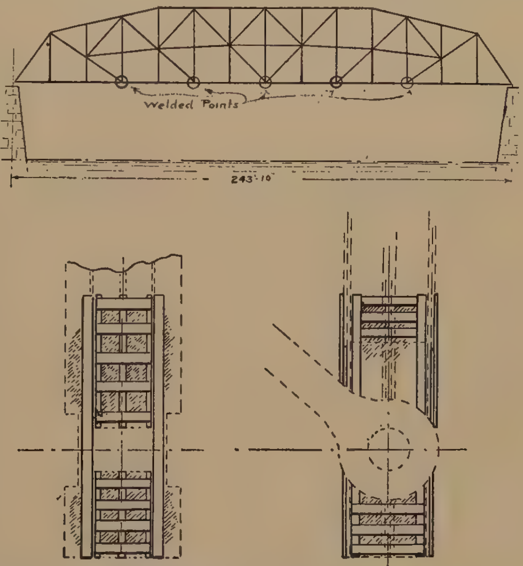

Fig. 2. The upper sketch shows the points where the bridge members became weak due to corrosion and where electric arc welding successfully repaired the damage. The lower sketches are of the vertical posts and show the reinforcing bars welded in place. The shaded area represents the corroded surface

The Effect of a Horn on the Pitch of a Loud Speaking Telephone

AN INTERPRETATION OF CERTAIN FORMULAS DEVELOPED BY LORD RAYLEIGH

By E. W. Kellogg
Research Laboratory, General Electric Company

Many people have tried experiments with telephone receivers and horns and have observed the marked difference in quality as well as intensity which results from attaching a horn to the receiver and the further difference when the same receiver is used as a head telephone. One would naturally expect differences in intensity due to these changes, but it may not be obvious why the quality should change as it does. A mere change in intensity will cause an apparent change in sound quality owing to the masking of high tones by low tones, the masking being more pronounced at high intensity. But if the intensity at the ear be kept constant by regulating the strength of the current supplied to the receiver, and if the receiver is not in any case overworked, there still remains a decided difference in quality under the three conditions mentioned.

These effects are in accordance with the general theory developed in Rayleigh's "Theory of Sound," and the purpose of the present article is simply one of interpretation and application. It has been contended by some that a horn is simply a resonator tuned for several frequencies. Resonance is an important factor in the action of all except very large or very wide angle horns, but apart from resonance a suitably designed horn has a marked effect in helping to bring out the lower tones.—Editor.

If we listen to voice or music from a telephone receiver held tight against the ear, and then slowly take the telephone away, we notice that not only does the general loudness decrease but the voice becomes thin and squeaky, or the music becomes tinkly. The change in quality begins with the first air leak between the receiver and the ear, and progresses till the receiver is a foot or so away, after which the change is principally one of intensity.

It will be convenient to use the term "high pitched" to describe the quality of the telephone held away from the ear in contrast to the much lower pitch obtained when it is held to the ear. In this sense, "high pitched" means tending to accentuate the high-pitched or high-frequency sounds in the voice or music, and "low pitched" means giving greater prominence to the low tones. The tendency of a telephone or loud speaker to give undue prominence to certain sounds is best shown by a curve of sound pressure as a function of frequency. The instrument is supplied with a sine-wave alternating current of variable frequency, the voltage[1] being kept constant, and the sound intensities are measured and plotted as the ordinates of a curve with frequency as abscissas as shown in Fig. 1. This curve is sometimes called the "frequency-response curve." The ideal frequency response would be a straight horizontal line as shown in Fig. 2, and would mean that the instrument was equally efficient at all frequencies in the working range. In the case of a head telephone we are concerned with the sound intensities or variations of air pressure in the cavity between the diaphragm and the ear drum, while in the case of a loud speaker we are interested in the sound pressures produced at some distance from the instrument. Let us find how the frequency-response curves compare in the two cases. The following symbols will be used.

B = effective area of diaphragm in sq. cm.
D = extreme deflection of diaphragm during vibration, cm.
x = instantaneous diaphragm deflection, cm.
v = instantaneous diaphragm velocity, cm. per sec.
f = frequency of vibration, cycles per sec.
$\omega = 2\pi f$.
t = time in seconds.
A = maximum rate of diaphragm displacement, cc. per sec.
s = condensation or proportional change in volume of a given quantity of air.
e = bulk modulus of elasticity. For air $e = 1.4$ (atmospheric pressure) $= 1.4 \times 10^6$ dynes per sq. cm. average.
p = pressure in sound wave, $= es$, dynes per sq. cm.
ρ = density of air, grams per cc.
a = velocity of sound propagation $= \sqrt{\frac{e}{\rho}}$ cm. per sec.
u = velocity of air movement in sound wave.
λ = wavelength $= \frac{a}{f}$ cm.

---

[1] Either voltage or current might be held constant, depending on the information sought. A plan commonly followed is to use a series resistance about equal to the average impedance of the loud speaker winding, and to maintain a constant voltage across the combination. Under these conditions, the curve obtained represents approximately the performance of the instrument when supplied through an amplifying tube with a constant alternating-current voltage applied to the grid.

In the case of the telephone held against the ear, if the cavity has a total volume V, and the diaphragm advances a distance D, the change in the volume of the cavity will be BD and the condensation will be $s=\frac{BD}{V}$, giving a pressure rise

$$p=es=e\frac{BD}{V}. \qquad (1)$$

This will be substantially the same (assuming there is no leak) whether the diaphragm advances quickly or slowly, or in other words, the pressure on the ear drum is proportional to the diaphragm deflection and independent of the frequency. A diaphragm which is very light and stiff, so that its resonance occurs at a frequency higher than any in the working range, would have the property of giving substantially the same maximum deflection for all frequencies, provided the actuating force is the same. Throughout the remainder of our discussion we shall assume for the sake of simplicity that the actuating force is the same for all frequencies. If the magnetic system is designed to minimize high-frequency losses, and the winding is supplied with constant current, the force on the diaphragm will be nearly constant over a wide range of frequency. We may then think of Fig. 2 as representing the frequency response, with constant current, of a receiver held to the ear and having a very light stiff diaphragm.

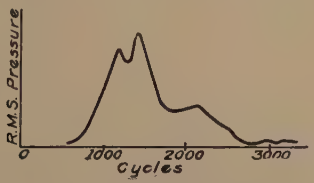

Fig. 1. Typical Frequency-response Characteristic of Loud Speaker

What would be the frequency response of the same receiver if held 30 cm. from the point at which the pressures are measured? The receiver being small in comparison with all but the shortest wavelengths with which we are concerned, the equations developed by Rayleigh[2] for radiation from a point source are applicable. If the diaphragm deflection is expressed by

$$x=D\sin\omega t,$$

its velocity will be

$$v=\frac{dx}{dt}=\omega D\cos\omega t$$

and the rate of displacement in cubic centimeters per second is

$$Bv=B\omega D\cos\omega t=A\cos\omega t.$$

The equations given by Rayleigh in the paragraphs mentioned, together with the relation $p=es=a^2\rho s$, enable us to express the pressure at a distance r, assuming the rate of displacement at the source to be $A\cos\omega t$

$$p=-\frac{A\rho f}{2r}\sin\omega\left(t-\frac{r}{a}\right) \qquad (2)$$

or since $A=\omega BD=2\pi fBD$

$$p=-\frac{\pi BD\rho f^2}{r}\sin\omega\left(t-\frac{r}{a}\right). \qquad (3)$$

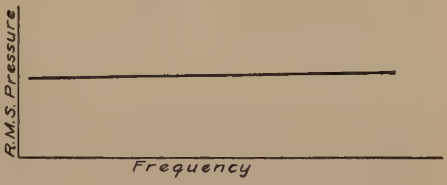

Fig. 2. Ideal Frequency-response Characteristic

The maximum pressure above or below mean atmospheric corresponds to

$$\sin\omega\left(t-\frac{r}{a}\right)=+1 \text{ or } -1,$$

so we may write

$$P_{max}=\frac{\pi BD\rho f^2}{r} \qquad (4)$$

and since B and ρ are considered constant, the pressure variations are proportional to $\frac{D}{r}f^2$. We found that a receiver whose diaphragm had the same amplitude of motion for all frequencies (D constant) gave the flat frequency response shown in Fig. 2 when held to the ear. The same receiver in free space would produce, at a distance r, sound pressures which vary as the square of the frequency; and its frequency-response curve would be like that shown in Fig. 3. It is not surprising that under these conditions the telephone sounds high pitched.

There are other factors which cause a change in quality when a receiver is taken away from the ear. The diaphragm motion is somewhat damped when the receiver is against the ear, and if there is a resonance it becomes more marked when the receiver is removed. A mere change of intensity makes the quality seem to change, the lower tones becoming more prominent when the intensity is high.[3]

---

[2] "Theory of Sound," Vol. II, Paragraphs 279 and 280.

It may be of interest to calculate from the foregoing formulas what the sound pressures might be in a typical case.

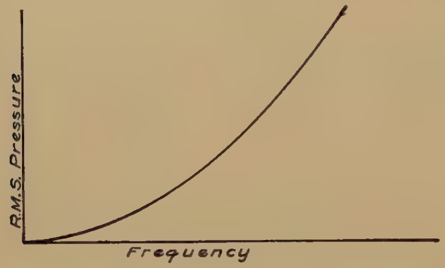

Fig. 3. Sound Pressures at a Distance in Free Space Produced by a Receiver Having Constant Diaphragm Amplitude

With the telephone held to the ear, if

$B = 10$ sq. cm.,
$D = 0.001$ cm.,
$V = 2$ cc.,
$e = 1.4 \times 10^6$ dynes per sq. cm.;

$$P_{max} = e\frac{BD}{V} = 1.4 \times 10^6 \times \frac{0.01}{2} = 7000$$

dynes per sq. cm.

With the telephone in free space, the pressure variations at $r = 30$ cm. from the telephone would be

$$P_{max} = \frac{\pi BD\rho f^2}{r} = \frac{\pi \times 0.01 \times 0.00129 f^2}{30}$$

$$= \frac{1.35}{10^6} f^2$$

$= 0.0135$ dynes per sq. cm. at 100 cycles
$= 1.35$ dynes per sq. cm. at 1000 cycles.

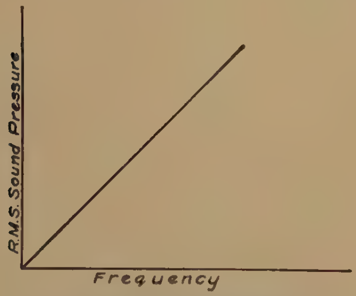

Fig. 4. Sound Pressures Produced in a Tube by a Receiver Having Constant Diaphragm Amplitude

Since the limit of audibility at a frequency of 100 cycles is a pressure of the order of one-tenth dyne per square centimeter,[3] the 100-cycle tone would be inaudible to most ears at the distance assumed.

If the same telephone receiver is connected to a pipe of cross-section c, the air velocity in the pipe close to the receiver[4] will be $\frac{1}{c}A \cos \omega t$, or $\omega\frac{BD}{c} \cos \omega t$. If there were neither wall friction nor reflections,[5] the velocity at a distance r from the receiver would be

$$u = \omega\frac{BD}{c} \cos \omega \left(t - \frac{r}{a}\right)$$

and the pressure (above mean atmospheric) would be

$$p = a\rho u = a\rho\omega\frac{BD}{c} \cos \omega \left(t - \frac{r}{a}\right) \quad (5)$$

and

$$P_{max} = a\rho\omega\frac{BD}{c}. \quad (6)$$

It will be noticed that P changes in phase but not in magnitude along the tube, and that for a given value of diaphragm amplitude D, the pressure varies directly as ω or as the frequency. The receiver which we have been considering would when connected to a pipe give a frequency response like that shown in Fig. 4. This is seen to be more favorable to low tones than is the response illustrated in Fig. 3 (receiver in free space) but less so than that in Fig. 2 (receiver held to the ear). The pressures developed are also intermediate. For example, if $B = 10$ sq. cm., $D = 0.001$ cm., as in the previous examples, and if the pipe cross-section is $c = 2.5$ sq. cm., and taking

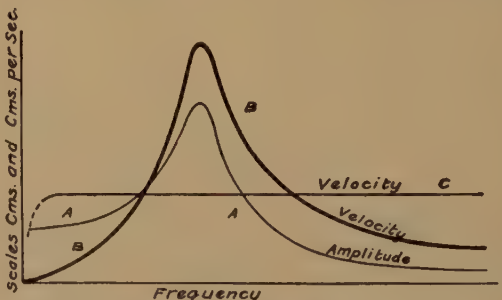

Fig. 5. Characteristics of Resonant and Perfectly Damped Diaphragms

---

[3] "Physical Measurements of Audition and Their Bearing on the Theory of Hearing," H. Fletcher, *Journal Franklin Inst.*, September, 1923; *Bell System Technical Journal*, October, 1923; also "Auditory Masking of One Pure Tone by Another," R. L. Wegel and C. E. Lane, *Physical Review*, February, 1924.

[4] This ignores the cushioning effect of an air chamber in front of the diaphragm, but in the practical case is approximately true for all but very short waves.

[5] The equations for plane waves, Rayleigh, "Theory of Sound," Vol. II, paragraph 245, are applicable to a frictionless straight tube.

$a=3.292\times10^4$ cm. per sec., and $\rho=1.29\times10^{-3}$ grams per cc.,

$$P_{max}=\frac{a\rho 2\pi fBD}{c}$$

$$=\frac{3.292\times10^4\times1.29\times10^{-3}\times2\pi f\times10\times0.001}{2.5}$$

$$=1.07f=107 \text{ dynes per sq. cm. at } 100 \text{ cycles}$$

$$=1070 \text{ dynes per sq. cm. at } 1000 \text{ cycles.}$$

The diaphragm characteristics assumed in drawing the curves in Figs. 2, 3, and 4 are not representative of ordinary receivers, and such a diaphragm would not in general be employed for a loud speaker. Fig. 5 shows the amplitude D and velocity v as a function of frequency f for a common type of diaphragm, the electrical driving force being assumed to be the same at all frequencies. With the diaphragm amplitude given, we could calculate the frequency response for the three conditions of Figs. 2, 3, and 4, but the complex shape of the diaphragm characteristic curve, Fig. 5, would make the effects of changing from ear to tube or to free space less clear, so we shall assume that we could work with a receiver which would on the average give about the same balance between low- and high-frequency response as the common resonant diaphragm, but without the resonance. This would be true of a strongly damped diaphragm whose vibration amplitudes were such as to give the same *velocity* at all frequencies. The velocity of such a diaphragm is shown by curve C of Fig. 5. Figs. 6, 7, and 8 show the response curves for a damped diaphragm, against the ear, in free space, and connected to a tube, respectively. The frequency response with the tube is flat. The air in the tube itself constitutes a damping load, so it is not out of the question to approximate the characteristic of Fig. 8 with an ordinary diaphragm.

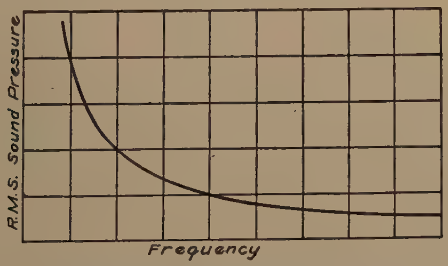

Fig. 6. Sound Pressures Produced in Confined Cavity by Diaphragm Having Same Average Velocity at All Frequencies

Attempts have been made to design horns which would load the diaphragm in much the same way as a straight tube, and thus to obtain a nearly flat frequency response.[6] The present discussion, however, will deal only with simple conical horns.

Everyone who has experimented with home-made loud speakers has noticed the marked drop in pitch as well as the increase in loudness when the horn is applied to the receiver. We might naturally expect that confining the sound waves to a slowly expanding cone would give a frequency response intermediate in shape between that obtained when the waves diverge very rapidly in free space and when they do not diverge at all as in a pipe. And yet, from another point of view, it is not clear why the frequency response with a conical horn should be different in *shape* (although the intensity would be greater at all frequencies) from that of the same receiver without a horn. In the latter case air flows in and out of the small hole in the receiver cap at a rate $A\cos\omega t$ or $\omega BD\cos\omega t$ and the waves set up expand in all directions or into a solid angle of 4π steradians. If we had n conical or pyramidal horns, each including a solid angle $\frac{4\pi}{n}$, with their vertices all together, and

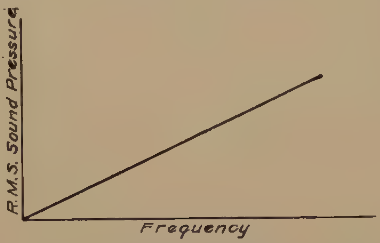

Fig. 7. Sound Pressures Produced at a Distance in Free Space by Diaphragm Having the Same Average Velocity at All Frequencies

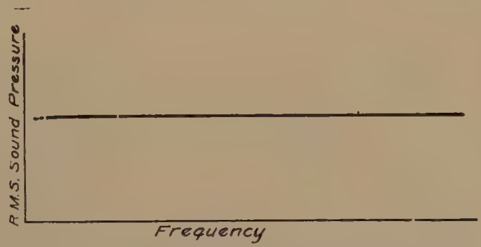

Fig. 8. Sound Pressures Produced in a Non-resonant Tube by Diaphragm Having the Same Average Velocity at All Frequencies

pumped air in and out of the vertex of each horn at the rate $\frac{1}{n}A\cos\omega t$ cubic centimeters per second, the effect (neglecting friction) would be the same as though the separating walls were not there. Hence the pressure in any of the horns, at a given distance from the center, would be the same as that produced at the same distance by the receiver without a horn, and the frequency-response curve would be the same. Removing all of the other horns would cause reflections to take place at the large end of the remaining horn unless the walls are extended far enough so that the final opening is several wavelengths across, in which case reflection is negligible. Then we should have left a single conical horn, and if measured at any point within the horn or in front of it in the beam of sound, the frequency-response curve would be the same as that for a point source in space at the same distance.

---

[6] "Function and Design of Horns for Loud Speakers," by C. R. Hanna and J. Slepian, A.I.E.E., 1924.

But we observe a drop in pitch when a horn of ordinary proportions is applied to a receiver, nor is the effect purely psychological due to the increased intensity. The important difference is that with the practical horn the source is not applied at the vertex. The effect of this difference may be shown from Rayleigh's equations, Vol. II, Paragraph 279, for radiation of spherical waves from a point (or small) source. If the rate of displacement at the source is $A\cos\omega t$ the total flow across a spherical surface r centimeters from the source is

$$4\pi r^2 u = A\left\{\cos\omega\left(t-\frac{r}{a}\right)-\frac{2\pi r}{\lambda}\sin\omega\left(t-\frac{r}{a}\right)\right\} \quad (7)$$

If we consider a fraction of the space surrounding the source to be separated from the remainder by a conical surface with its vertex at the center, and including a solid angle $\frac{4\pi}{n}$, it would receive an nth part of the flow $A\cos\omega t$ at the center and also would include an nth part of the spherical surface mentioned, whence for the waves within the cone

$$\frac{4\pi r^2 u}{n} = \frac{A}{n}\left\{\cos\omega\left(t-\frac{r}{a}\right)-\frac{2\pi r}{\lambda}\sin\omega\left(t-\frac{r}{a}\right)\right\}$$

Or if we redefine A as the maximum rate of flow into and out of the vertex of the cone of solid angle W, we may write

$$Wr^2 u = A\left\{\cos\omega\left(t-\frac{r}{a}\right)-\frac{2\pi r}{\lambda}\sin\omega\left(t-\frac{r}{a}\right)\right\} \quad (8)$$

Fig. 9 shows for frequencies of 500 cycles, 1000 cycles, and 2000 cycles, the total flow at various distances from the center expressed as a ratio to the flow at the center. Stating it differently, if we take the vector of $A\cos\omega t$ as unity, Fig. 9 shows the magnitude of the sum of the vectors of

$$A\cos\omega\left(t-\frac{r}{a}\right) \text{ and } -A\frac{2\pi r}{\lambda}\sin\omega\left(t-\frac{r}{a}\right).$$

We see that the total flow increases with distance, becoming at larger distances directly proportional. This corresponds to the familiar law that the energy density in the wave front varies inversely as the square of the distance. Since the energy density is proportional to the square of the amplitude, the amplitude (and velocity of air motion) varies inversely as the distance. But the product of the velocity multiplied by the wave front area (which increases with the square of the distance) varies directly as the distance, except near the source where there is a departure from this relation.

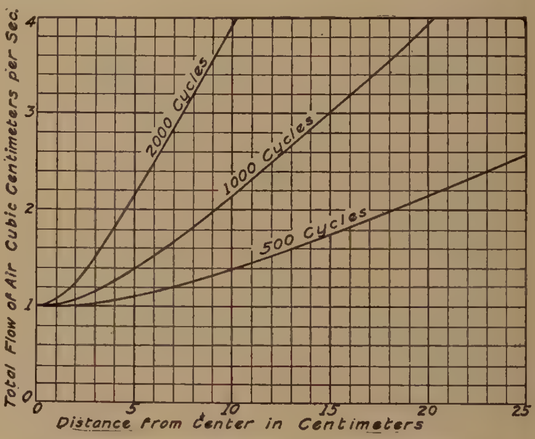

Fig. 9. Total Air Movement at Various Distances from Source of Sound

From Fig. 9 we can see the effect of cutting off the tip of the cone. For example, suppose we cut the cone at ten centimeters from the vertex, and by applying a receiver cause a flow into and out of the opening equal to that which previously flowed past this surface when the source $A\cos\omega t$ was supplied at the vertex. We see from the curves that at ten centimeters from the vertex we should have to pump air at the rate of 3.95 $A\cos\omega t$ cubic centimeters per second to give the equivalent of $A\cos\omega t$ cubic centimeters per second, introduced at the vertex if the frequency is 2000 cycles, or conversely if the receiver diaphragm vibrates to give a displacement of $A \cos \omega t$ cubic centimeters per second when applied at ten centimeters from the vertex, it would be equivalent to only $\frac{A \cos \omega t}{3.95}$ at the vertex. Similarly at 1000 cycles, the equivalent source at the center would be $\frac{A \cos \omega t}{2.15}$ and at 500 cycles $\frac{A \cos \omega t}{1.38}$. Thus the effect of cutting off ten centimeters of the cone (the receiver diaphragm displacement remaining the same) is to reduce the intensity of the 2000-cycle radiation in the ratio 1 to 3.95, that of the 1000-cycle tone in the ratio 1 to 2.15, while the 500-cycle tone is much less affected. What the frequency-response curve would be may best be shown by combining equation (2) for pressure at a given distance with equation (8) for total flow. Equation (2) gives the pressure at a distance r, resulting from a source $A \cos \omega t$ radiating waves in all directions or into a solid angle 4π. If the radiation is confined to a solid angle W instead of 4π, the intensity within the cone will be greater in the ratio $\frac{4\pi}{W}$ whence for this case equation (2) must be changed to

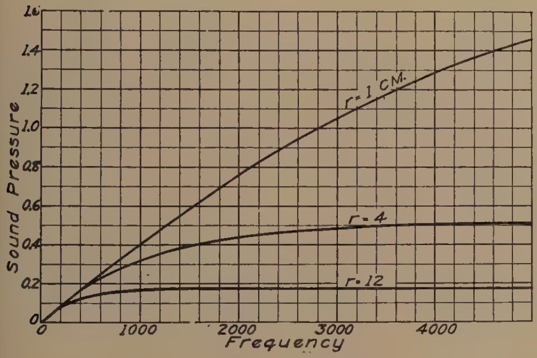

Fig. 10. Effect of Applying Sound Sources at Various Distances from Vertex of a Conical Horn

$$p = -\frac{4\pi}{W}\,\frac{A\rho f}{2R}\sin\omega\left(t-\frac{R}{a}\right) \qquad (9)$$

in which R is the distance from the center.

Now if instead of supplying air at the rate $A \cos \omega t$ at the vertex, we cut off the cone at r centimeters from the vertex and cause sufficient air movement at this point to give the equivalent of $A \cos \omega t$ at the vertex, the rate of displacement at the opening will by equation (8) have to be

$$Wr^2u = A\left\{\cos\omega\left(t-\frac{r}{a}\right)-\frac{2\pi r}{\lambda}\sin\omega\left(t-\frac{r}{a}\right)\right\} \qquad (8)$$

We are interested in the relation of the pressure at a considerable distance R, to the motion of the diaphragm of the receiver at the small opening of the cone, and since relative phase is not important we may simplify matters by comparing the maximum pressure at R with the maximum rate of displacement at r. From equation (9)

$$P_{max} = \frac{4\pi}{W}\,\frac{A\rho f}{2R} \qquad (10)$$

and since the two terms in the parenthesis in equation (8) are in quadrature

$$Wr^2u_{max} = A\sqrt{1+\left(\frac{2\pi r}{\lambda}\right)^2} \qquad (11)$$

$=\omega BD$ when expressed in terms of diaphragm amplitude and effective area.

From equations (10) and (11)

$$P_{max} = \frac{\frac{4\pi}{W}\,\frac{A\rho f}{2R}}{A\sqrt{1+\left(\frac{2\pi r}{\lambda}\right)^2}}\,\omega BD$$

$$= \frac{2\pi\rho f}{WR\sqrt{1+\left(\frac{2\pi r}{\lambda}\right)^2}}\,\omega BD.$$

Taking $R=100$ cm. and $W=0.2$, Fig. 10, shows the values of the factor

$$\frac{2\pi\rho f}{WR\sqrt{1+\left(\frac{2\pi r}{\lambda}\right)^2}}$$

for $r=1$, $r=4$, and $r=12$ cm. It will be seen that shifting the receiver from 1 cm. from the vertex to 12 cm. from the vertex has changed the instrument from one of very high pitch to one with more nearly flat frequency response. The fact that the curve for $r=12$ falls below that for $r=4$ or $e=1$ should not be taken to mean that the flatter frequency response is necessarily secured at the cost of reduced sound output. In practice larger values of r are associated with smaller values of W, or the narrower the angle of the cone the longer the tip we cut off, so as to keep the size of the opening about the same. In the limiting case this gives us a cylindrical tube. Fig. 11 shows the curves of Fig. 10 replotted in such a way as to show the same output at very high frequencies, for the three values of r. These curves show the shape of the frequency response of receivers with conical horns attached assuming that the diaphragm velocity is the same at all frequencies, as would be true with adequately damped diaphragms.

In the foregoing we have attempted to show the effect of a conical horn on pitch. It remains to show how it affects the general intensity of the sound radiated. That the intensity within the cone or within the beam of sound should be increased by confining the radiation to a small solid angle seems obvious; but, that the total amount of sound in the room will be increased by confining the sound to a small angle for a short distance and then releasing it at the large end of the cone, is not so clear. But if we find that placing a horn on a receiver increases the total energy radiated (rather than simply focusing it) the case will be more convincing. In "Theory of Sound," Vol. II, paragraph 280, Rayleigh gives an equation for energy radiated into a cone. Using our symbols the equation is

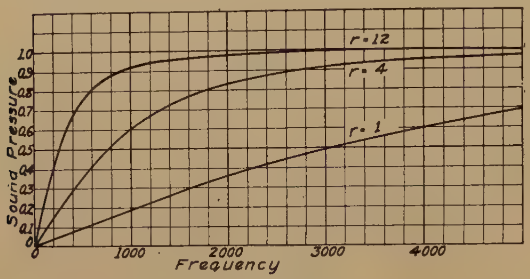

Fig. 11. Curves of Fig. 10 Replotted on Basis of Equal Sound Pressures for Very High Frequencies

$$\text{Power radiated} = \frac{2\pi^2 \rho f^2 A^2}{aW} \text{ ergs per sec.} \quad (12)$$

from which we see that the power radiated varies inversely as the solid angle W, the displacement at the source being assumed to remain constant. This assumption is in general justified in the problem we are discussing, since the inertia and elastic forces of the diaphragm are usually large compared with air reactions on the diaphragm, except at resonance, when the air load may cut down the amplitude considerably.

We have so far assumed that the walls of the horn could be extended far enough to prevent appreciable reflections. The ordinary horn falls far short of this, permitting strong reflections of the longer waves. This in general means less radiation of low tones than would be the case if the cone were extended far enough to prevent appreciable reflections, but there is a compensating factor so far as the general pitch level of the instrument is concerned. It is the longer waves that are most strongly reflected, since in comparison with these the diameter of the bell is small and reflections at the bell mean that the horn will resonate to certain frequencies. Those frequencies for which the horn is resonant are radiated much more strongly than would be the case if there were no reflections. Fig. 12 shows in a qualitative way the effect of reflections on the frequency-response characteristic. The longer the horn, the lower the frequency at which the first resonance occurs and the nearer together the resonances on the frequency scale. The larger the bell the less pronounced will be the resonances, or the nearer the frequency-response curve will approximate that for a non-reflecting horn. The resonances are undesirable, especially for an instrument intended to reproduce speech and vocal music rather than instrumental music, but they partly offset the loss of radiation of low tones which reflections would otherwise cause. Most of the sounds which a loud speaker is called upon to reproduce are so complex that one or more of the resonance frequencies are present a large part of the time, and the bringing out of even a small fraction of the lower tones present is sufficient to give the impression of increased volume of sound and lower pitch level.

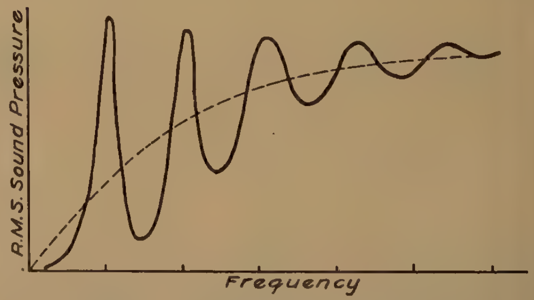

Fig. 12. Effect of Horn Resonance on Frequency-response of Loud Speaker

Radicalism That Means Real Progress

By C. M. Ripley

Publicity Department, General Electric Company

In geography we used to think the world was flat, and now we know it's round.

In astronomy they were positive that the sun moved around the earth, now we know positively that the earth moves around the sun. The first man, however, to say that the earth moved around the sun was threatened with the tortures of the inquisition, and made to "recant."

In physiology we used to think the blood was stationary in the body like the juice of an orange. When Harvey came out with the statement that the blood circulates in the body, they wanted to run him out of the medical profession as an impostor.

In architecture the weight of the framework of buildings always used to be carried by the walls but now in all of the steel skeleton structures, it is the weight of the walls which is carried by the framework. Those who were down in New York know that the walls of the Woolworth Building were started at some point above the 10th floor and carried up, while the steel skeleton below was clearly visible, thus proving that the framework now carries the weight of the walls in that type of building.

Railroad car wheels used to revolve on the axle, now they are fixed on the axle. The flange used to be on the rail, whereas now it is on the wheel.

All rubber tires used to be solid, now most of them are hollow; books used to be one long piece of paper called a scroll and now they are made up of many separate short pieces of paper called pages. In writing we used to use a quill, with the ink on the outside, now we use rubber with the ink on the inside.

All airships used to be lighter than air, now nine out of ten are heavier than air. For centuries the eye of the needle was at one end and the point was at the other, and we could not have a sewing machine until they put the eye and the point both at the same end. The armature of all motors and generators used to be on the inside of the field but now in many types of machines the armatures are on the outside of the field.

But don't think that these improvements—these revolutionary changes—have been carried out without opposition. According to the *Dearborn Independent*, the first telegraph wires were cut; the first railroad tracks were torn up; the first sewing machine was smashed; and the first man to sell anthracite in Philadelphia was run out of the State of Pennsylvania as an impostor.

In 1832, a group of men in Lancaster, Ohio, wrote to the school board, requesting the use of the schoolhouse. They wanted to hold a meeting in order to promote a railroad in their vicinity. As an example of the opposition which progressive minds must always meet, you will be interested in the letter sent this group of men by the school board, as follows:

"You are at liberty to use the schoolhouse to hold meetings for all proper purposes. But railroads and telegraphs are impossible and rank infidelity. If God had intended his intelligent creatures should travel at the frightful speed of 16 miles an hour by steam, he would clearly have foretold it in the holy prophets. It is a device of Satan to lead immortal souls down to Hell."

The old time mariners laughed at Robert Fulton when he steamed out of New York in the *Clermont*; Copernicus and Galileo were persecuted for their views on astronomy; and Pasteur was threatened with expulsion from the medical profession and advised to stick to the well-known principles of medicine and forget his wild theory of germ life.

Now and then we meet some courageous individual who thinks he has some new way of doing something. Let us remember the great changes which have taken place in past generations and in recent years. Then we will be tolerant of his views:

Yes—the world is changing; the radical engineering thought of today is the progressive thought of tomorrow; and one interesting thing about it is that engineers and scientists are in the forefront in revolutionizing ideas and demonstrating why people should adopt the new devices and different modes of work and living conditions, which they have made possible with inventions and discoveries.

In Memoriam

Wilfred Campbell was born in Manchester, England, in 1884, and served an apprenticeship with the Lancashire and Yorkshire Railway for seven years. During the latter part of his apprenticeship he was selected as one of two to attend the Manchester Municipal School of Technology where he received several prizes of distinction for his ability in design. Later he was employed as a draftsman by the Northeastern Railway Company.

In 1907 he came to America, and for a year was assistant to the master mechanic at the Arnold Print Works, North Adams, Mass. In 1908 he was employed by the General Electric Company as a draftsman in the Direct-current Department. During the war he was associated with Mr. C. E. Eveleth, now manager of the Schenectady Works, and Dr. Irving Langmuir of the Research Laboratory, in connection with the design of submarine detectors by the General Electric Company for the United States Government.

WILFRED CAMPBELL

Since 1919 Mr. Campbell has been an engineer in the Turbine Engineering Department of the General Electric Company where he has had charge of the investigation of turbine vibrations of all sorts. In recognition of his outstanding contributions to turbine design, he recently received an award from the Charles A. Coffin Foundation.

The results of this exceptionally valuable research were presented by Mr. Campbell at the recent spring meeting of the American Society of Mechanical Engineers. This paper is being reprinted in full in the Review and the concluding installment appears in this issue.

Mr. Campbell's untimely death occurred at Schenectady on July 7th, after an attack of acute appendicitis. The loss to the turbine art will be appreciated by all who are familiar with his work. The breadth of his scientific knowledge is well illustrated by this paper, although it was only one of many interests. His ready ingenuity was supported by a keen intuition which was invaluable to an engineer of his type. His genial good nature and unfailing optimism endeared him to all his associates. His integrity and fearlessness won the confidence of turbine operators all over the land to an unusual degree. His intense interest in all modern inventions gave him confidence that no problem was beyond solution.

Francis C. Pratt, vice-president of the General Electric Company, in charge of engineering, in commenting on Mr. Campbell's death, made the following statement:

"Mr. Campbell's sudden death is a great shock to his many friends and associates in this Company. At the time of his death he was the engineer in charge of investigations of turbine wheel vibrations. When he undertook this important work in 1919, it was thought by some engineers that the limits in the size of individual turbine units had been reached. Mr. Campbell had a rare genius for analyzing and solving abstruse problems of a mechanical nature and did not share these adverse opinions regarding the limitations in the size of steam turbines. He discovered the cause of the trouble with large turbine wheels and buckets, devised remarkably ingenious methods of detecting and measuring the phenomena connected with them and provided means for overcoming them. He has made a fine and lasting contribution to the industry and his work will be long remembered by engineers who design and who operate steam turbines."

LIBRARY SECTION

Condensed references to some of the more important articles in the technical press, as selected by the G-E Main Library, will be listed in this section each month. New books of interest to the industry will also be listed. In special cases, where copy of an article is wanted which cannot be obtained through regular channels or local libraries, we will suggest other sources on application.

Arc Welding

Fluxing Problems in Welding of Mild Steel with the Metallic Arc. Ogden, H.
Am. Weld. Soc. Jour., May, 1924; v. 3, pp. 40-43.

Car Lighting

Present Practice in Motor Bus Lighting and Suggestions for Improvement. Porter, L. C. and Roy, A. C.
Illum. Engng. Soc. Trans., May, 1924; v. 19, pp. 456-474.

Circuit Breakers

Self-Contained Extra-High-Tension Switch Gear.
Engng., May 16, 1924; v. 117, p. 650.
(Illustrated description of circuit breaker equipment shown at the British Empire Exhibition by Ferguson, Pailin, Ltd.)

Circuit Breakers—Testing

Circuit Breaker Tests at Bessemer, Ala., on 300-Ampere, 110,000-Volt Breakers. Hilliard, J. D.
A.I.E.E. Jour., May, 1924; v. 43, pp. 430-435.
(Results of tests on Alabama Power Company equipment.)

High-Voltage Oil Circuit Breaker Tests, Alabama Power Company System. MacNeill, J. B.
A.I.E.E. Jour., May, 1924; v. 43, pp. 436-441.

Coal, Pulverized

Unit System for Pulverized Coal. Martin, S. C.
Power Pl. Engng., May 1, 1924; v. 28, pp. 471-472.
(Describes such a system, and gives results of tests.)

Condensers, Steam

Tendencies in Surface Condenser Practice.
Power Pl. Engng., May 15, 1924; v. 28, pp. 530-533.

Electric Cables

High-Voltage Cables.
Elec. Wld., May 24, 1924; v. 83, pp. 1087-1091.
(Report of the National Electric Light Association Underground Systems Committee.)

Electric Current Rectifiers

Alternating Current Rectification by Thermionic Valves. Melling, C. T.
Met.-Vick. Gaz., Apr., 1924; v. 8, pp. 79-82.

Electric Distribution

Swedish Water Power and the Farmer.
Elec. Wld., May 17, 1924; v. 83, pp. 993-998.
(Illustrated account of Swedish methods of supplying electrical energy to the rural districts.)

Electric Drive—Mining

Electrical Engineers Discuss Ways in Which Savings in Power Cut Mining Costs.
Coal Age, May 22, 1924; v. 25, pp. 754-760.
(Abstracts of a number of papers read at a recent meeting of the American Mining Congress. Suggests several economies that may be effected in the applications of electricity to mining.)

Electric Drive—Power Plant Auxiliaries

Control of Auxiliary-Drive Motors. Harvey, A. L.
Power, May 13, 1924; v. 59, pp. 761-762.

Motors and Control for Stoker Drive. Kelly, Ralph.
Elec. Jour., May, 1924; v. 21, pp. 221-224.

Electric Drive—Steel Mills

Power Consumed in Rolling Steel. Fox, Gordon.
Iron Tr., May 29, 1924; v. 74, pp. 1431-1433.
(Abstract of paper read before the American Iron and Steel Institute.)

New Three-High Plate Mill at the Clydebridge Works of Messrs. David Colville & Sons, Ltd.
English Elec. Jour., Apr., 1924; v. 2, pp. 311-319.
(Illustrated description of English Electric Company electric drive equipment in an English steel mill.)

Electric Drive—Ventilating Machinery

Selecting the Best Type of Motor for Driving a Mine Fan at Variable Speed. Chadbourne, B. W.
Coal Age, May 15, 1924; v. 25, pp. 722-725.
(Gives curves and data for calculating the type of equipment best suited for various needs.)

Electric Furnaces

Electric Furnaces for the Heat Treatment of Razor Blades.
Engng., May 30, 1924; v. 117, pp. 713-714.
(Illustrated description of a Wild-Barfield furnace in a British cutlery plant.)

Electrode-Regulating Motors for Electric Steel Furnaces. Kerpely, K. (In German.)
Giess. Zeit., Apr. 15, 1924; v. 21, pp. 153-157.
(Considers the characteristics of the motors generally used, and discusses the mathematical theory of such motors.)

Electric Heating

Electric Heating in the Esparto Union High School. Strauch, A.
Jour. Elec., May 1, 1924; v. 52, pp. 321-323.
(Illustrated description of the system in an Esparto, California, school. Includes data on power consumption and costs.)

Electric Heating, Industrial

Making Industrial Electric Heating Pay. Scott, Wirt S.
Elec. Wld., May 10, 1924; v. 83, pp. 971-972.
(Analyzes the growth of the central station business created by the industrial heating load.)

Electric Lighting—Power Plants

Illumination of Power Houses and Substations. Samuels, M. M.
Elec. Lt. & Pr., May, 1924; v. 2, pp. 155-157.

Electric Meters

Fundamentals of Meter Service. Fryer, R. C. and Gregory, L. J.
Elec. Wld., May 17, 1924; v. 83, pp. 1003-1006.

Transmission of Meter Readings by the Impulse Method. Smith, B. H.
Elec. Jour., May, 1924; v. 21, pp. 219-221.

Electric Meters—Testing

Meter Testing Equipments. Wilson, A. H.
Met.-Vick. Gaz., Apr., 1924; v. 8, pp. 75-79.

Electric Transmission Lines

Power Transmission Lines.—I. Taylor, William T.
Elec. Rev., May 16, 1924; v. 94, pp. 780-782.
(Serial article on theory of design.)

Electrical Machinery, Explosion-proof

Flameproof Mining Switchgear. Bannister, A.
Met.-Vick. Gaz., Feb. 1924; v. 8, pp. 36-40.
(Illustrated description of Metropolitan-Vickers apparatus.)

Electrical Machinery—Parallel Operation

Oscillation and Resonance in Systems of Parallel Connected Synchronous Machines. Putman, H. V.
Franklin Inst. Jour., May, 1924; v. 197, pp. 603-621.
(Theoretical. Serial.)

Electrical Machinery—Temperature

Experimental Study of Ventilation of Turbo Alternators. Fechheimer, Carl J.
A.I.E.E. Jour., May, 1924; v. 43, pp. 416-423.

Evaporators

Adapting Evaporators to Heat Balance—I. Chapin, Ernest H.
Power Pl. Engng., May 15, 1924; v. 28, pp. 534-536.
(On evaporators for steam power plant work. Serial.)

Evaporators Furnish Distilled Make-Up Water.
Power Pl. Engng., May 1, 1924; v. 28, pp. 485-488.
(Illustrated description of various types of evaporators.)

Factory Lighting

Unit Costs of Industrial Lighting. Tuck, Davis H.
Illum. Engng. Soc. Trans., May, 1924; v. 19, pp. 411-423.

Fire Protection

Fire Extinguisher Using Dry CO_2 Gas. Jones, C. L.
Elec. Wld., May 31, 1924; v. 83, p. 1138.
(Short description of an extinguisher that is claimed to be especially effective in combating fires in electrical machinery.)

Heat Transmission

Fluid Friction and Heat Transference. Morely, Thomas B.
Engr., May 30, 1924; v. 137, pp. 596-597.
(Presents a chart for use in calculation of such phenomena.)

Hydro-electric Development

Davis Bridge Development of the New England Power Company.
Power, May 13, 1924; v. 59, pp. 776-779.
(On the hydraulic features.)

Insulators

Application of High-Tension Insulators. Fleming, T. B.
Elec. Jour., May, 1924; v. 21, pp. 217-218.

Magnetism

Ferromagnetism and Its Dependence Upon Chemical, Thermal and Mechanical Conditions. McKeehan, L. W.
Franklin Inst. Jour., May, 1924; v. 197, pp. 583-601.
(Theoretical. Serial.)

Nozzles

Third Report of the Steam Nozzles Research Committee.
Engng., May 23, 1924; v. 117, pp. 681-685.
(Report of a committee of the Institution of Mechanical Engineers. See also abstract of discussion, p. 657; and editorial, pp. 673-674.)

Oil Fuel Burners

Individual Forced Draft Fuel Oil Burners. Charlton, A. M.
Am. Soc. Nav. Engrs. Jour., May, 1924; v. 36, pp. 208-230.
(Illustrated description.)

Power Costs

Relative Cost of Water and Steam Power.
Power, May 20, 1924; v. 59, pp. 827-828.
(Gives comparative cost figures.)

Power Plants, Electric

Design Features of Trenton Channel—I. Thompson, Paul W.
Elec. Wld., May 31, 1924; v. 83, pp. 1119-1128.
(Describes the engineering and construction details of a new Detroit Edison plant at Trenton, Mich. A second installment will deal with the electrical features.)

Hudson Avenue—Brooklyn Edison's Super-Station.
Power, May 13, 1924; v. 59, pp. 750-758.
(Illustrated description, with detailed list of principal mechanical equipment. Also described in *Power Plant Engineering*, May 15, 1924, pp. 549-553.)

Power Plants, Electric

Operating Features at Delaware.
Power Pl. Engng., May 15, 1924; v. 28, pp. 537-542.
(Describes equipment and control in the Delaware Station of the Philadelphia Electric Company.)

Prime Movers at Cahokia. Packe, L. N.
Elec. Lt. & Pr., May, 1924; v. 2, pp. 134-137, 173.
(Serial.)

Protective Apparatus

Overload Protection by "Z" Connected Relays or Trip Coils.
Elec. Rev., May 23, 1924; v. 94, pp. 828-829.

Protection of Supply Networks. Wilson, W.
Elec'n., May 23, 1924; v. 92, pp. 624-627.
("Some critical notes on the McColl system.")

Radio Communication

Further Progress Made with Voice Transmission from Underground Workings to Surface. Jakosky, J. J.
Coal Age, May 29, 1924; v. 25, pp. 801-804.
(A discussion of various tests so far made on radio communication between points on the surface of the earth and in underground mines.)

Radio Engineering

Faithful Reproduction by Broadcast. Eckersley, P. P.
Wireless Wld. & Radio Rev., May 29, 1924; v. 14, pp. 250-254.
(A paper read before the Radio Society of Great Britain. Treats of the engineering features of radio broadcasting. Serial.)

Steam Turbines

Maintaining Impulse-Turbine Efficiency by Checking the Condition Curve. Walden, Robert R.
Power, May 20, 1924; v. 59, pp. 823-825.

Stokers

Computing Guaranteed Stoker Efficiency. Gauss, H. F.
Power, May 27, 1924; v. 59, pp. 858-860.

Street Lighting

Asymmetric Illumination Distribution for Ornamental Street Lighting. Wood, L. A. S.
Elec. Wld., May 17, 1924; v. 83, pp. 999-1003.
(Describes the Sheridan Road installation, Chicago.)

Making Street-Lighting Business More Desirable. Perry, Allen M.
Elec. Wld., May 10, 1924; v. 83, pp. 958-964.
(Discusses the value of adequate street lighting. Graphs showing rates are given.)

Substations, Automatic

Automatic Electric Stations for Steel Mills. Lichtenberg, Chester.
Iron & St. Engr., May, 1924; v. 1, pp. 252-256.

Synchronizing

Arrangement of Connecting Induction and Synchronous Generators to Three-Phase Systems. Wurmbach, E. (In German.)
E.T.Z., Apr. 24, 1924; v. 45, pp. 397-398.
(Brief description of a synchronizing scheme which is claimed to be very simple and inexpensive.)

Transverters

Electrical Engineering Exhibits.
Engr., May 16, 1924; v. 137, pp. 533-536.
(An article on the English Electric Company's display at the British Empire Exhibition, but devoted almost entirely to an illustrated account of that company's "transverter" exhibit.)

NEW BOOKS

Alternating Currents. Ed. 5, rev. and enl. Alfred Hay. 420 pp., 1923, N. Y., Harper & Bros.

Electricity and Magnetism. Ed. 4. Sydney G. Starling. 612 pp., 1924, N. Y., Longmans, Green & Co.

Factory Management. Henry Post Dutton. 329 pp., 1924, N. Y., Macmillan Co.

Fundamentals of Radio. James L. Thomas. 207 pp., 1923, N. Y., D. Van Nostrand Co.

Instructions for Installation and Care of Thermo-Electric Pyrometers. 68 pp., 1924, Phila., Brown Instrument Co.

Introduction to Wireless Telegraphy and Telephony. J. A. Fleming. 112 pp., 1923, N. Y., Isaac Pitman & Sons.

Line Charts for Engineers. W. N. Rose. 95 pp., 1923, N. Y., E. P. Dutton & Co.

Management Engineering. P. F. Walker. 359 pp., 1924, N. Y., McGraw-Hill Book Co., Inc.

Marine Boiler Management and Construction. Ed. 6. C. E. Strommeyer. 398 pp., 1924, N. Y., Longmans, Green & Co.

Principles of Electric Motors and Control. Gordon Fox. 499 pp., 1924, N. Y., McGraw-Hill Book Co., Inc.

Principles of Electroplating and Electroforming. William Blum and George B. Hogaboom. 356 pp., 1924, N. Y., McGraw-Hill Book Co., Inc.

Pulverized Fuel, Colloidal Fuel, Fuel Economy and Smokeless Combustion. Leonard C. Harvey. 466 pp., 1924, Lond., Macdonald & Evans.

Tulley's Handbook; Steam and Electrical. Ed. 7, rev. and enl. Henry C. Tulley. 3 vols., 1924, N. Y., McGraw-Hill Book Co., Inc.

Wiring for Light and Power. Ed. 4. Terrell Croft. 551 pp., 1924, N. Y., McGraw-Hill Book Co., Inc.

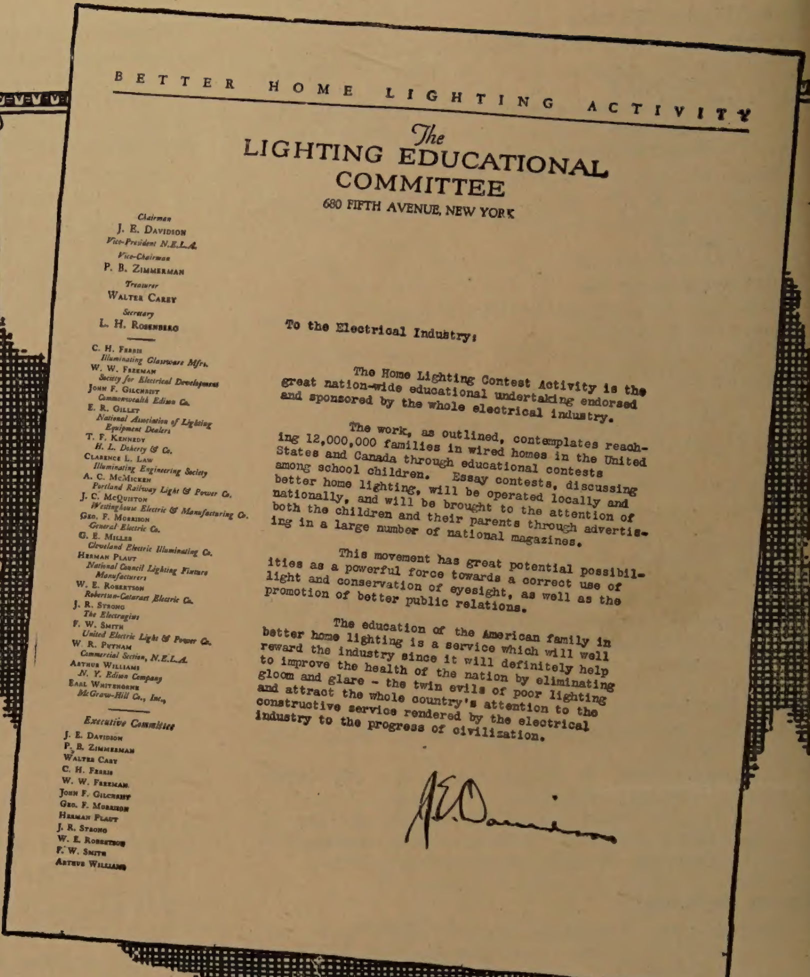

HAS YOUR TOWN STARTED A Home Lighting Contest?

BETTER HOME LIGHTING ACTIVITY

The
LIGHTING EDUCATIONAL
COMMITTEE
680 FIFTH AVENUE, NEW YORK

Chairman
J. E. Davidson
Vice-President N.E.L.A.
Vice-Chairman
P. B. Zimmerman
Treasurer
Walter Carey
Secretary
L. H. Rosenberg

C. H. Ferris
Illuminating Glassware Mfrs.
W. W. Freeman
Society for Electrical Development
John F. Gilchrist
Commonwealth Edison Co.
E. R. Gillet
National Association of Lighting Equipment Dealers
T. F. Kennedy
H. L. Doherty & Co.
Clarence L. Law
Illuminating Engineering Society
A. C. McMicken
Portland Railway Light & Power Co.
J. C. McQuiston
Westinghouse Electric & Manufacturing Co.
Geo. F. Morrison
General Electric Co.
G. E. Miller
Cleveland Electric Illuminating Co.
Herman Plaut
National Council Lighting Fixture Manufacturers
W. E. Robertson
Robertson-Cataract Electric Co.
J. R. Strong
The Electragist
F. W. Smith
United Electric Light & Power Co.
W. R. Putnam
Commercial Section, N.E.L.A.
Arthur Williams
N. Y. Edison Company
Earl Whitehorne
McGraw-Hill Co., Inc.

Executive Committee
J. E. Davidson
P. B. Zimmerman
Walter Cary
C. H. Ferris
W. W. Freeman
John F. Gilchrist
Geo. F. Morrison
Herman Plaut
J. R. Strong
W. E. Robertson
F. W. Smith
Arthur Williams

To the Electrical Industry:

The Home Lighting Contest Activity is the great nation-wide educational undertaking endorsed and sponsored by the whole electrical industry.

The work, as outlined, contemplates reaching 12,000,000 families in wired homes in the United States and Canada through educational contests among school children. Essay contests, discussing better home lighting, will be operated locally and nationally, and will be brought to the attention of both the children and their parents through advertising in a large number of national magazines.

This movement has great potential possibilities as a powerful force towards a correct use of light and conservation of eyesight, as well as the promotion of better public relations.

The education of the American family in better home lighting is a service which will well reward the industry since it will definitely help to improve the health of the nation by eliminating gloom and glare - the twin evils of poor lighting and attract the whole country's attention to the constructive service rendered by the electrical industry to the progress of civilization.

J. E. Davison

The Home Lighting Contest is the great educational movement approved and endorsed by the whole electrical industry. It is designed to bring into each wired home a complete knowledge of the benefits to be obtained from good home lighting.

The main feature of The Home Lighting Contest is the essay competition among 24,000,000 school children of the country. Local and national prizes will be awarded to the winning children. The First National Prize is the $15,000 model electrical home of 1924.

To get the full benefit of this activity, start now to organize your local contest. Arrange to have this model electrical home built for display in your town.

Start the activity in your town now—write for your Plan Book. No city is too large—no town too small to join in this great activity.

There is an experienced Regional Director near you who will help you organize and plan successfully.

HOME LIGHTING CONTEST

The
LIGHTING EDUCATIONAL COMMITTEE
680 Fifth Avenue • • • New York, N.Y.